

**Cloning and characterization of Enaptin, a novel
giant actin-binding protein connecting the
nucleus to the actin cytoskeleton**

INAUGURAL-DISSERTATION
zur
Erlangung des Doktorgrades
der Mathematisch-Naturwissenschaftlichen Fakultät
der Universität zu Köln



vorgelegt von

Sabu Abraham

aus

Thiruvaniyoor, Kerala, Indien

Köln, 2004

Referees/Berichterstatter: Prof. Dr. Angelika A. Noegel
Prof. Dr. Jens Brüning

Date of oral examination: 08.07.2004

Tag der mündlichen Prüfung

The present research work was carried out under the supervision of Prof. Dr. Angelika A. Noegel, in the Institute of Biochemistry I, Medical Faculty, University of Cologne, Cologne, Germany from August 2001 to July 2004.

Diese Arbeit wurde von August 2001 bis Juli 2004 am Biochemischen Institut I der Medizinischen Fakultät der Universität zu Köln unter der Leitung von Prof. Dr. Angelika A. Noegel durchgeführt.

To my beloved Pappa and Mummy

Acknowledgements

First of all, I would like to thank Prof. Dr. Angelika A Noegel for giving me an opportunity to work in her department and to do my PhD studies under her guidance. Her valuable guidance, creative suggestions, constructive criticism and constant encouragement during the course of work inspired and enabled me to complete this project. I would like to express here my deep sense of gratitude to her.

I cannot find words to say thanks to our group leader Dr. Iakowos Karakesisoglou for his constant encouragement and discussions during the course of this study. His 'story for a lesson' approach always lifted my spirit up. It was wonderful to work with him. Thank you Akis.

I would also like to thank Dr. Elena Korenbaum for guiding me in the first year of my study. Her valuable guidance enabled me to initiate the project. Thank you Elena.

I also owe my thanks to Dr. Francisco Rivero, Dr. Budi Tunggal, Dr. Ludwig Eichinger, and Dr. Andreas Hasse for their cooperation and help as and when required.

Its hard to find words to say thanks to Kumar, my colleague and 'partner' for the Enaptin project. I would also like to thank Thorsten Libotte, my 'bench mate' for his valuable friendship. Thanks also to Hafi, Thorsten Olski and Yen for their friendship and discussions during the life in Lab10.

I pay my sincere thanks to Martina for her technical assistance as and when required and helping me for the initial paper works.

I am thankful to Bettina Lauss, our secretary, for all the excellent assistance in the paper works. I would also like to thank Berthold for teaching me the cell culture techniques, Maria for providing me the paraffin sections, and Rolf and Rosi for technical advices.

Now its the turn to say thanks to all my other colleagues and friends in the lab and in Köln for all the parties and laughter. Your friendships made life more meaningful. Thank you very much guys.

Last but not the least, I would like to thank my loving parents and brother for being there for me.

Sabu Abraham

Table of Contents

1	Introduction	1-12
1.1	The Cytoskeleton	1
1.2	The Actin Cytoskeleton	2
1.3	Actin binding proteins	3
1.4	Actin-binding proteins of a-actinin superfamily	4
1.5	Diseases related to actin-binding proteins	7
1.6	The Nuclear Lamina	8
1.7	Nuclear envelope	8
1.8	The nuclear lamina and inherited disease	9
1.9	Role of Actin-binding proteins in nuclear positioning	11
1.10	Aim of the study	12
2	Materials and methods	13-42
2.1	Materials	13
2.2	Instruments	14
2.3	Enzymes, inhibitors and antibodies	15
2.3.1	Enzymes for molecular biology	15
2.3.2	Antibodies	16
2.3.3	Inhibitors	16
2.3.4	Antibiotics	17
2.4	Reagents	17
2.5	Kits	18
2.6	Bacterial host strains	19
2.6.1	Media for E. coli culture	19
2.7	Eukaryotic cells	19
2.7.1	Media for cell culture	20
2.8	Vectors	20
2.9	Oligonucleotides	20
2.9.1	Oligonucleotides used for amplifying the full length cDNA of Enaptin	21
2.9.2	Knockout target vector primers	21
2.9.3	Primers for making GFP-dominant negative constructs for Enaptin	22
2.9.4	Primers for GST-specII fusion protein	22

2.9.5	Primers for probes for northern blotting	22
2.9.6	Primers for C-terminal syne-1 probe for multiple tissue expression array	22
2.10	Construction of vectors	22
2.10.1	Cloning of cDNA fragments	22
2.10.2	Generation of C-terminal Enaptin-GFP fusions	22
2.10.3	Cloning of GST-SpecII	23
2.10.4	Probes for northern blot analysis	23
2.11	Buffers and other solutions	24
2.12	Computer programs	24
2.13	Molecular biological methods	24
2.13.1	Plasmid-DNA isolation from E. coli by alkaline lysis miniprep	24
2.13.2	Plasmid-DNA isolation with a kit from Macherey-Nagel	25
2.13.3	DNA agarose gel electrophoresis	25
2.13.4	Isolation of total RNA from mouse tissue with TRIzol reagent	25
2.13.5	RNA agarose gel electrophoresis and northern blotting	26
2.13.6	Labeling of DNA probes	26
2.13.7	Generation of Riboprobes	27
2.13.8	Elution of DNA fragments from agarose gels	27
2.13.9	Measurement of DNA and RNA concentrations	27
2.13.10	Restriction digestion of DNA	28
2.13.11	Dephosphorylation of 5'-ends of linearized vectors	28
2.13.12	Creation of blunt ends	28
2.13.13	Ligation of vector- and DNA-fragments	28
2.13.14	Polymerase chain reaction (PCR)	28
2.13.15	Transformation of E. coli cells with plasmid DNA	29
2.14	Protein methods and immunofluorescence	29
2.14.1	Extraction of protein homogenate from mouse tissues and cell cultures	29
2.14.2	SDS-polyacrylamide-gel electrophoresis (SDS-PAGE)	30
2.14.3	Gradient gel electrophoresis	31
2.14.4	Western blotting	31
2.14.5	Immunofluorescence	33
2.14.6	Small-scale GST fusion protein expression	33
2.14.7	Purification of GST-fusion proteins	34
2.14.8	Affinity purification of polyclonal antibodies by blot method	34

2.14.9	Affinity purification by the CNBr method	34
2.14.10	Immunohistochemical staining of formalin-fixed paraffin-embedded sections	35
2.14.11	Microscopy	36
2.15	Disruption of the cytoskeleton using various drugs	36
2.16	Digitonin experiment	36
2.17	Gene targeting protocols	36
2.17.1	Target vector construction	36
2.17.2	Probe generation	37
2.17.3	Embryonic stem cell culture	37
2.17.4	MEF cell culture and Mitomycin treatment	38
2.17.8	ES cell culture	38
2.17.9	ES cell transfection	39
2.17.10	Antibiotic selection and picking of ES cell clones	39
2.17.11	Splitting and freezing ES cells	39
2.17.12	Genomic DNA isolation	40
2.17.13	Southern blotting	40
2.17.14	Labeling of DNA probes and hybridisation	41
3	Results	43-80
3.1	Sequence analysis of Enaptin	43
3.1.1	cDNA cloning of the longest isoform of Enaptin	43
3.1.2	Organisation of the Enaptin gene	45
3.1.3	Domain analysis of Enaptin	45
3.1.4	Isoforms of Enaptin	51
3.2	Examination of Enaptin's tissue distribution by northern blot analysis	52
3.2.1	Tissue distribution of Enaptin	52
3.2.2	Northern blot analysis of Enaptin	54
3.3	Western blot analysis of Enaptin	55
3.3.1	Western blots with an ABD Enaptin antibody of different tissue lysates	55
3.3.1	Expression and purification of GST-SpecII	56
3.3.2	Generation and purification of the Enaptin polyclonal antibody	57
3.4	Subcellular localization of Enaptin using the SpecII antibody	59
3.5	Enaptin is a component of the outer nuclear membrane	60
3.6	Nuclear membrane localization of Enaptin is not affected by drugs disrupting	

	microfilament and microtubule cytoskeleton	61
3.7	Tissue expression of Enaptin	63
3.7.1	Expression of Enaptin in muscle	63
3.7.2	Expression of Enaptin in cerebrum, cerebellum and hippocampus	65
3.7.3	Expression of Enaptin in the skin	66
3.7.4	Expression of Enaptin in a 16-day-old mouse embryo	67
3.8	Generation of GFP-fusion proteins containing the C-terminus of Enaptin	68
3.8.1	C-terminal Enaptin GFP fusions localize to the nuclear membrane	69
3.9	Lamin dependent localization of Enaptin	72
3.9.1	Localization of Enaptin in Lamin A/C knockout cells	72
3.9.2	Dominant negative interference of Enaptin using a Xenopus lamin B construct	72
3.9.3	Nuclear localisation of Enaptin in fibroblasts from laminopathy patients	73
3.10	Distribution of Enaptin during myoblast differentiation	74
3.11	Generation of an Enaptin mouse mutant	76
3.11.1	Analysis of the structure of the mouse Enaptin gene	76
3.11.2	Construction of the targeting vector (Enaptin KO)	78
3.11.3	ES cell transfection	79
3.11.4	Screening of recombinant clones	80
4	Discussion	81-90
4.1	Enaptin is a giant protein of the α -actinin superfamily	81
4.2	Enaptin is a nuclear membrane protein	82
4.3	Expression and tissue distribution of Enaptin and its isoforms	85
4.4	Lamin dependent localization of Enaptin	86
4.5	Enaptin and Laminopathies	88
4.6	Possible functions of Enaptin	88
5	Summary	91-92
6	Bibliography	93-102
7	Abbreviations	103
	Erklärung	-
	Curriculum Vitae / Lebenslauf	-

Introduction

1 Introduction

1.1 The Cytoskeleton

Cells have to organise themselves in space and interact mechanically with their environment. They have to be correctly shaped, physically robust, properly structured internally and should retain their ability to move or change their shape. For all these cellular processes, cells depend on a remarkable system of filaments called the cytoskeleton. Three major cytoskeletal filamentous networks are present in eukaryotic cells, the actin microfilaments, intermediate filaments and microtubules. Microfilaments are fibers typically 7-9 nm of diameter whereas microtubules have a diameter of 24 nm. Intermediate filaments have a diameter of 10 nm which is in between the other two filaments and hence the name. Together all these filamentous networks provide, not only a dynamic skeleton for the cells, but they are also involved in organelle transport, organelle and cell-fate-determinant positioning, cell polarity development, mitosis, cytokinesis, secretion and the formation of cell extensions, and the maintenance of cell integrity.

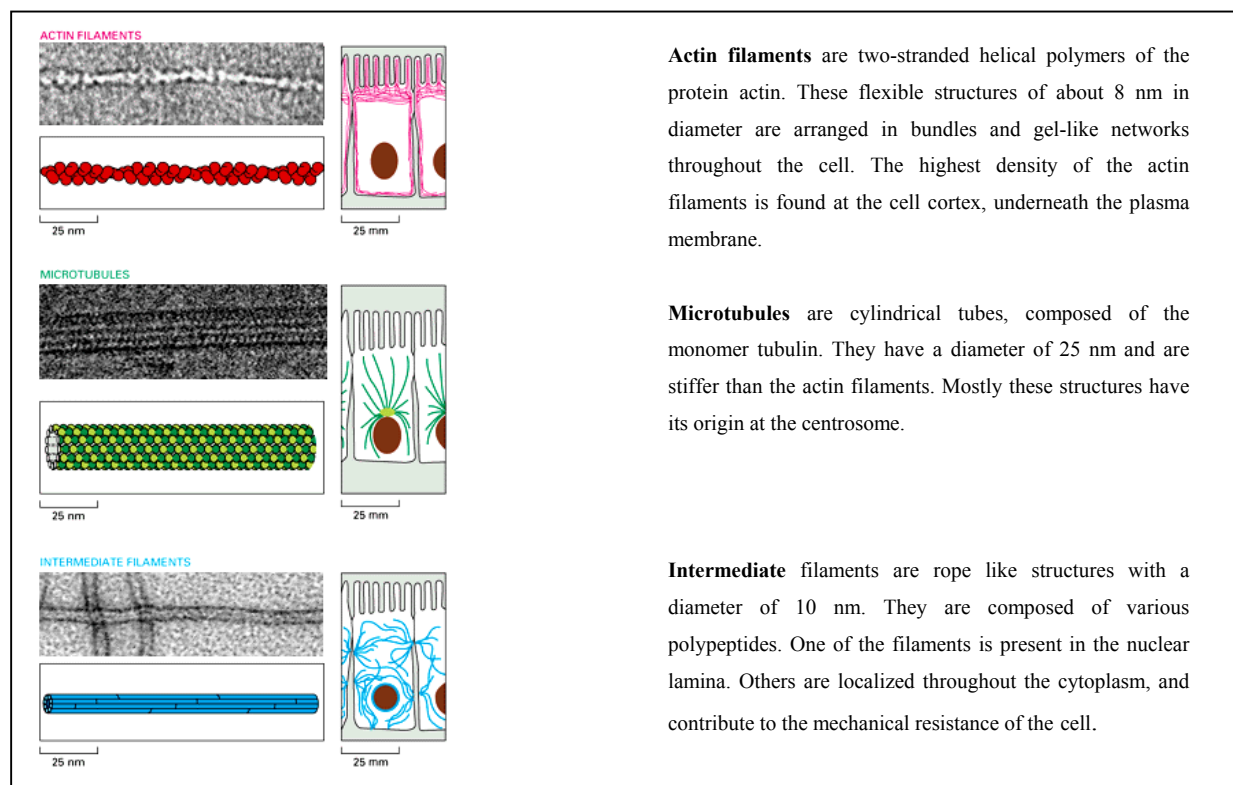


Figure 1.1: The three different filament types of the cytoskeleton, each shown in an electron micrograph, a schematic drawing and the distribution in an epithelial cell. Figure is taken from Alberts *et al.*, 1994.

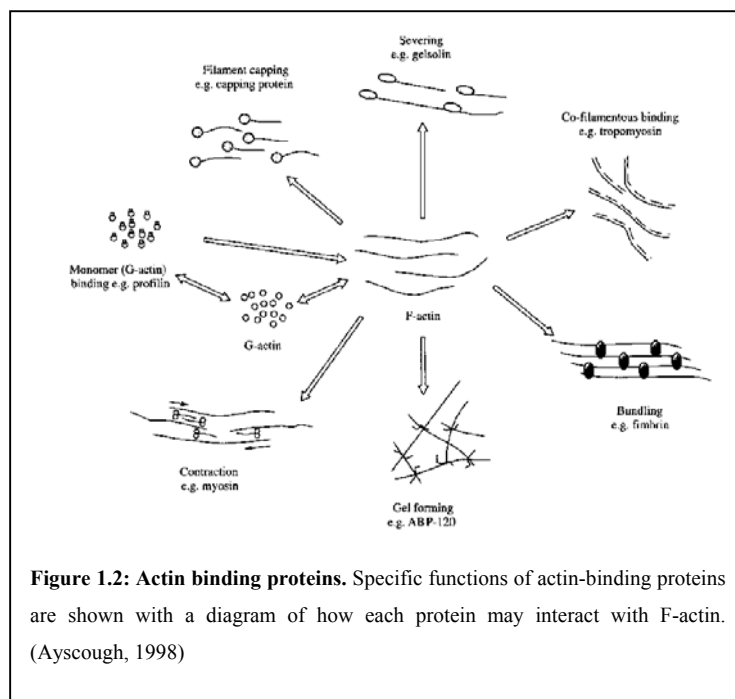
1.2 The Actin Cytoskeleton

The major constituent of the microfilament is actin, and together with several actin-binding and associated proteins, it constitutes the actin cytoskeleton (Stossel, 1993). Some single cell eukaryotes like yeasts have a single gene for actin (Winsor and Schiebel, 1997), whereas many multicellular organisms contain multiple actin genes. Humans for example have six *actin* genes encoding various isoforms of the protein (Kedes *et al.*, 1985), and plants such as *Arabidopsis* has 10 (Meagher *et al.*, 1999). The six known actin isoforms in mammalian cells are two sarcomeric muscle actins (alpha-skeletal and alpha-cardiac), two smooth muscle actins (alpha and gamma), and 2 nonmuscle, cytoskeletal actins (beta and gamma). Actin is highly conserved throughout the evolution and is the most abundant intracellular protein in a eukaryotic cell. The recent discovery of MreB protein as a homologue of actin in bacteria changed the conventional theory that prokaryotes do not have actin (van den Ent *et al.*, 2001). Actin is a protein consisting of 375 amino acids with a molecular mass of about 43 kDa. Actin exists either in a globular monomeric (G-actin) or in a filamentous polymeric form (F-actin). Each actin molecule can bind to ATP, which is hydrolyzed to ADP after incorporation of the actin molecule into the polymer. Polymers assemble spontaneously via noncovalent interactions between the monomeric subunits and are highly dynamic structures with subunit turnover at both ends. Energy is not required but contributes to the polymerization, as shown by the observation that ATP-bound actin polymerizes faster than ADP-bound actin (Engel *et al.*, 1977). The rate-limiting step in actin polymerization is nucleation, the assembly of the first subunits to generate a new filament. Actin filaments are structurally polarized, and the kinetics of polymerization at each end is different. The plus (barbed) end grows more quickly than does the minus (pointed) end. Actin is predominantly present in the cytoplasm and recently confirmed to be present also in the nucleus (Olave *et al.*, 2002).

The actin cytoskeleton is directly involved in cell locomotion (Welch *et al.*, 1997), cytokinesis (Fishkind and Wang, 1995), cell-cell and cell-substratum interactions (Wehrle-Haller and Imhof, 2002; Yamada and Geiger, 1997), vesicular and organelle transport (Kubler and Riezman, 1993; Langford, 1995), establishment and maintenance of cell morphology (Matsudaira, 1994) and the localization of signaling particles and mRNA (Bassell and Singer, 1997). All these functions of actin filaments are modulated and assisted by actin-binding proteins.

1.3 Actin binding proteins

The association of the actin-binding proteins with actin is necessary for modulating the behavior and organization of the actin cytoskeleton. More than 162 distinct and separate actin-binding proteins have been identified excluding the synonyms and isoforms (dos Remedios *et al.*, 2003) and they can be grouped into 48 classes (Kreis and Vale, 1999; Pollard and Cooper, 1986). These include monomer binding proteins [profilin (Ampe *et al.*, 1988), cofilin (Abe *et al.*, 1990)], barbed end capping proteins [capZ (Barron-Casella *et al.*, 1995)], barbed end capping/severing proteins [gelsolin (Kwiatkowski *et al.*, 1986), villin (Pringault *et al.*, 1986)], lateral binding proteins [calponin (Strasser *et al.*, 1993), tropomyosin (Lees-Miller and Helfman, 1991)], Cross linking proteins [α -actinin (Youssoufian *et al.*, 1990), Spectrin (Winkelmann and Forget, 1993), dystrophin (Koenig *et al.*, 1988),] membrane associated actin binding proteins [Synapsins or protein 4.1; (Sudhof, 1990)] and motor proteins such as myosins.



Profilin is a small actin-binding protein (12-19 kDa) originally identified as an actin sequestering protein that can inhibit actin filament growing. Profilins appear to be multifunctional. They regulate actin polymerization, act as adaptor proteins, and possibly link transmembrane signaling to the actin cytoskeleton (Theriot and Mitchison, 1993). Cofilin is a widely distributed intracellular

actin-modulating protein that binds and depolymerises filamentous actin and inhibits the polymerisation of monomeric G-actin in a pH-dependent manner (Kuhn *et al.*, 2000). Capping protein (capZ) is a heterodimeric actin-binding protein found in all eukaryotic cells and it binds to the barbed ends of actin filaments and nucleates polymerisation of actin (Schafer and Cooper, 1995). Gelsolin is best known for its involvement in dynamic changes in the actin cytoskeleton during a variety of forms of cell motility. Gelsolin severs assembled actin filaments in two, and caps the fast-growing plus end of a free or newly severed filament (Kwiatkowski, 1999). Calponin is a 33 kDa protein binding to actin and calmodulin and found

predominantly in smooth muscle and thought to be involved in the regulation or modulation of contraction (Strasser *et al.*, 1993). Tropomyosin, in connection with the troponin complex regulates the interaction of F-actin and myosin (Farah and Reinach, 1995). Synapsin I is a neuronal phosphoprotein associated with the membranes of small synaptic vesicles and thought to regulate synaptogenesis and neurotransmitter release from adult nerve terminals (Ryan *et al.*, 1996).

The organization of the actin cytoskeleton must be tightly regulated both temporally and spatially to perform all its biological functions. Rho-like GTPases are key regulators in signaling pathways that link extracellular growth signals or intracellular stimuli to the assembly and organization of the actin cytoskeleton (Hall, 1994).

1.4 Actin-binding proteins of α -actinin superfamily

At the leading margins of moving or spreading cells, actin filaments are organized into two principal structures, bundles and meshworks. Actin bundles are parallel arrays of closely packed actin filaments that stiffen membrane projections like filopodia, microvilli and stereocilia. An actin meshwork is a criss-crossed array of actin filaments forming the lamellipodia. When laminated to the cytoplasmic face of the plasma membrane, an actin meshwork forms a two-dimensional elastic sheet that stiffens the cell membrane, anchors integral membrane proteins and supports the shape of the cells. Actin cross-linking proteins characterized by a pair of actin-binding sites form actin bundles and meshworks. The α -actinin superfamily is the largest of the F-actin cross-linking protein families. Proteins in this family share an actin-binding domain homologous to the ABD of α -actinin (Matsudaira, 1994). The family includes spectrins, fimbrin/plastins, dystrophins, gelation factor from *Dictyostelium* and filamin subfamilies (Hartwig, 1995). The globular actin-binding domain is contained in the first 250 amino acids at the N-terminus of all the members of the family and may be composed of more than one subdomain (Puius *et al.*, 1998). The actin-binding domain (ABD) found close to the N-terminus in all members of the α -actinin superfamily consists of two calponin-homology domains (Korenbaum and Rivero, 2002). The calponin homology (CH) domain is a protein module of about 100 residues that was first identified at the N-terminus of calponin, an actin-binding protein playing a major regulatory role in muscle contraction (Strasser *et al.*, 1993). Proteins of the α -actinin superfamily utilize a double calponin homology domain to arrange the actin filaments in bundles and meshworks and link them to the plasma membrane (Matsudaira, 1994). Fimbrins are the simplest of the family and are modular proteins consisting of a calmodulin like calcium binding domain at the N-

terminus followed by a pair of α -actinin like actin binding domains (Lin *et al.*, 1994). Filamin or actin-binding protein-280 (ABP-280) is a 280 kDa protein that cross-links actin filaments into orthogonal networks in the cortical cytoplasm and participates in the anchoring of membrane proteins to the actin cytoskeleton (Gorlin *et al.*, 1990). Filamin and its homologues have an ABD at its N-terminus separated from a C-terminal dimerization domain by several immunoglobulin fold containing repetitive elements (Fucini *et al.*, 1999). The third subfamily in the α -actinin superfamily consists of proteins like α -actinin, spectrin and dystrophin. The distinguishing feature of the subfamily is a repeated triple stranded α -helical motif (Yan *et al.*, 1993) called the spectrin repeat. The presence of spectrin repeats in the rod domain classifies these proteins into the spectrin family. The structure of the ABD in dystrophin and utrophin has been solved, revealing a bundle of α -helices arranged in an extended head-to-tail dimer (Keep *et al.*, 1999; Norwood *et al.*, 2000). α -Actinin dimerises to cross-link actin filaments and spectrin forms a tetramer of $(\alpha\beta)_2$ type (Viel, 1999). Even though the ABD of dystrophin also has been proposed to form a dimer by x-ray crystallographic studies (Norwood *et al.*, 2000), the spectrin repeats in dystrophin do not form a dimer at least in-vitro (Chan and Kunkel, 1997).

In myofibrillar cells, α -actinin constitutes a major component of Z-disks in striated muscle and of the functionally analogous dense bodies and dense plaques in smooth muscle. In nonmuscle cells, it is distributed along microfilament bundles and is thought to mediate their attachment to the membrane at adherens-type junctions (Blanchard *et al.*, 1989). Spectrin, first identified as supporting the plasma membrane of erythrocytes, is now found to be in association with other intracellular membranes (De Matteis and Morrow, 2000). Dystrophin and utrophin are identified as proteins involved in Duchenne/Becker muscular dystrophies and associate with the plasma membrane of muscle and neuronal tissues. Dystrophin is a 427 kDa protein which binds to cytoskeletal F-actin and to dystroglycan, a transmembrane protein associated with plasma membrane multimolecular complex. Dystroglycan in turn binds to laminin-2 in the overlaying lamina. Thus dystrophin is a part of a complex that links the cytoskeleton to the extracellular matrix (Sunada and Campbell, 1995). Although utrophin is very similar in sequence to dystrophin and possesses many of the protein-binding properties ascribed to dystrophin, it is confined to the subsynaptic membrane at the neuromuscular junction (Blake *et al.*, 1996).

Another family of large proteins exists with an α -actinin like ABD domain at the N-terminal end and followed by several repeating domains, which are called the plakins. Plakins are cytolinker proteins that associate with cytoskeletal elements and junctional complexes.

The plakin family consists of desmoplakin (Smith and Fuchs, 1998), plectin (Reznicek *et al.*, 1998), bullous pemphigoid antigen 1 [BPAG1 (Leung *et al.*, 1999)], and microtubule–actin crosslinking factor [MACF/ACF7 (Karakesisoglou *et al.*, 2000)]. This family of proteins is defined by the presence of a plakin domain and/or a plakin repeat domain. In addition to these two domains, plakins also harbor other domains that are common in some but not all members: the actin-binding domain (ABD), coiled-coil rod, spectrin-repeat-containing rod and microtubule-binding domain. Many plakins are expressed in tissues that experience mechanical stress, such as epithelia and muscle, where they play a vital role in maintaining tissue integrity by crosslinking cytoskeletal filaments and anchoring them to membrane complexes. The proteins in the spectrin family and plakin family can be classified together as spectraplakin family (Roper *et al.*, 2002) composed of both the spectrin and plakin superfamilies. These superfamilies consist of proteins that contribute to the linkage between the plasma membrane and the cytoskeleton. Spectrin superfamily members bind and cross-link actin filaments and attach them to membrane receptors. Members of the plakin superfamily were first identified as components of desmosomes and hemidesmosomes, connecting the adhesion receptors to intermediate filaments, but they also can cross-link different cytoskeletal elements.

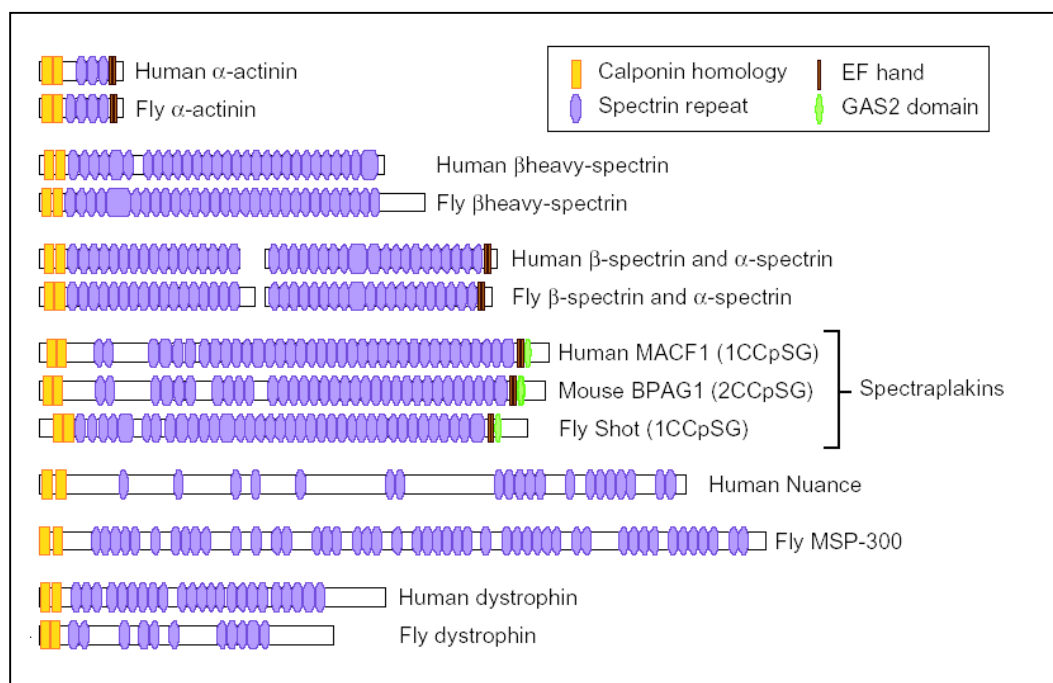


Figure 1.3: The spectrin protein superfamily. The figure depicted is a selection of members of the spectrin family of proteins, comparing human and fly orthologues for each member, and in the case of spectraplakins showing both mammalian genes (*MACF1* and *BPAG1*). Taken from Roper *et al.*, 2002.

1.5 Diseases related to actin-binding proteins

Members of the α -actinin superfamily are also involved in the pathogenesis of diseases. The most famous disease associated with actin-binding proteins may be Duchenne and Becker muscular dystrophy (DMD & BMD). It is a X-linked degenerative disorder of muscle affecting 1 in 3500 live born males (Gospe *et al.*, 1989). Patients with DMD have mutations in the gene encoding dystrophin. Dystrophin is thought to serve as a link from the actin-based cytoskeleton of the muscle cell through the plasma membrane to the extracellular matrix (Sunada and Campbell, 1995). In dystrophic muscle, where this linkage is disrupted, muscle fibers develop normally, but get easily damaged and degenerate (Menke and Jockusch, 1995). Regeneration is insufficient and successive rounds of degeneration lead to a gradual replacement of muscle by connective tissue.

Spectrin, the predominant component of the membrane skeleton of the red blood cell, is essential in determining the properties of the membrane including its shape and deformability. Mutations in the spectrin gene cause elliptocytosis and hereditary pyropoikilocytosis resulting in diminished elasticity or destabilization of the erythrocyte skeleton (Delaunay, 2002; Goodman *et al.*, 1982)

Plectin is a widely expressed high molecular weight protein that is involved in cytoskeleton-membrane attachment in epithelial cells, muscle, and other tissues. Mutations in the gene encoding plectin (PLEC1) have been implicated in the pathogenesis of an autosomal recessive variant of epidermolysis bullosa simplex and is associated with cutaneous blistering starting in the neonatal period and muscular dystrophy in later life (McLean *et al.*, 1996). BPAG1 is a component of the basement membrane of the skin. BPAG1 is the major autoantigenic determinant of autoimmune sera of patients with blistering disease bullous pemphigoid (Stanley *et al.*, 1988). Targeted removal of the BPAG1 gene in mice results in severe dystonia and sensory nerve degeneration (Guo *et al.*, 1995). Dystonin, is a neural isoform of BPGA1 and deletion of dystonin causes a hereditary neurodegenerative disorder called dystonia musculorum (dt) leading to a sensory ataxia in mice (Brown *et al.*, 1995). In the dt mice degenerating sensory neurons show abnormal accumulations of IFs and disorganized MTs in the axons. Animals that survive longer develop less motor neuron degeneration resulting in sensory neuropathy (Dalpe *et al.*, 1998).

1.6 The Nuclear Lamina

The nuclear lamina is a mesh of intermediate filaments that mainly underlies the inner aspect of the inner nuclear membrane and also extends into the nuclear interior (Stuurman *et al.*, 1998). The nuclear lamin filaments are made up of monomeric subunits, which each comprise a central coiled-coil, helical rod domain flanked by globular domains on the C-terminus and N-terminus. They can form parallel dimers and subsequently undergo polymerization to form the filamentous network of the nuclear lamina. In humans, there are three genes encoding the lamins, *LMNA*, *LMNB1* and *LMNB2*. There are two major A-type lamin proteins (lamin A and C) and two major B-type lamins. All vertebrate cells express at least one B-type lamin, whereas the A-type lamins are developmentally regulated and expressed primarily in differentiated cells (Goldman *et al.*, 2002). The locality of the nuclear lamins have implicated them in a wide range of nuclear functions such as nuclear growth, maintenance of nuclear shape, DNA replication, chromatin organisation, RNA splicing, cell differentiation, apoptosis and cell-cycle-dependent control of nuclear architecture (Moir *et al.*, 2000; Zastrow *et al.*, 2004).

1.7 Nuclear envelope

The most prominent feature of the nuclear envelope is a pair of inner and outer nuclear membranes (INM and ONM resp.) with a perinuclear space in between them. These two membranes are periodically interrupted by nuclear pore complexes (NPCs), which are large macromolecular assemblies that form aqueous gated channels across the nuclear envelope and mediate the transport of macromolecules. The ONM is continuous with the peripheral rough endoplasmic reticulum. The INM is enriched with a distinctive set of membrane proteins and

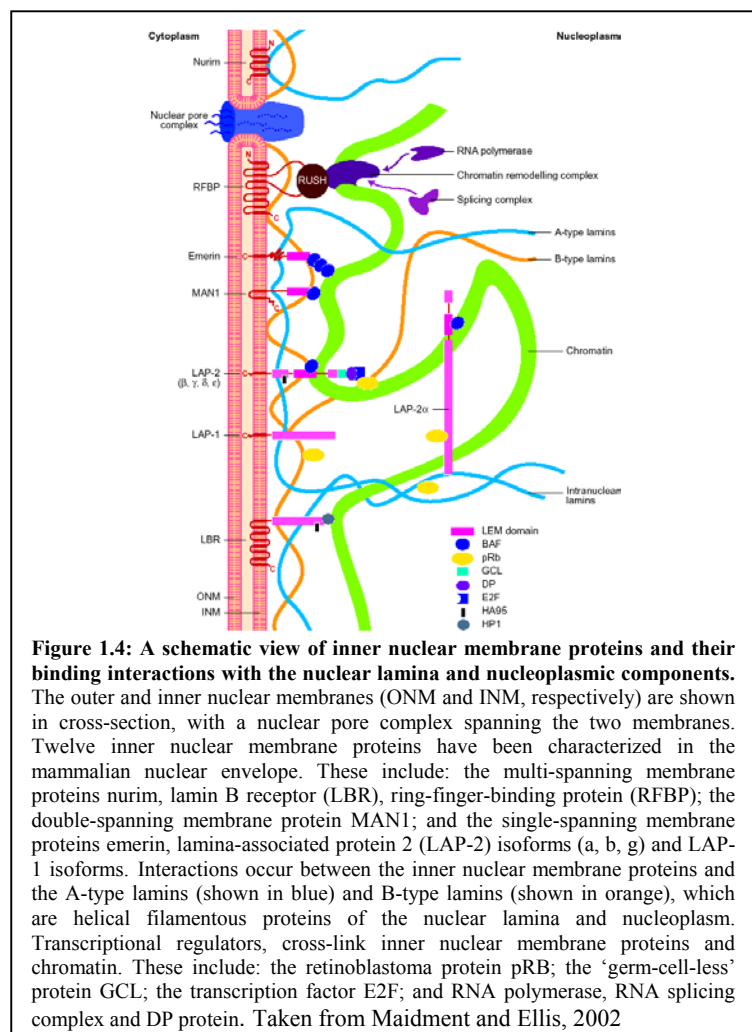


Figure 1.4: A schematic view of inner nuclear membrane proteins and their binding interactions with the nuclear lamina and nucleoplasmic components. The outer and inner nuclear membranes (ONM and INM, respectively) are shown in cross-section, with a nuclear pore complex spanning the two membranes. Twelve inner nuclear membrane proteins have been characterized in the mammalian nuclear envelope. These include: the multi-spanning membrane proteins nurim, lamin B receptor (LBR), ring-finger-binding protein (RFBP); the double-spanning membrane protein MAN1; and the single-spanning membrane proteins emerin, lamina-associated protein 2 (LAP-2) isoforms (a, b, g) and LAP-1 isoforms. Interactions occur between the inner nuclear membrane proteins and the A-type lamins (shown in blue) and B-type lamins (shown in orange), which are helical filamentous proteins of the nuclear lamina and nucleoplasm. Transcriptional regulators, cross-link inner nuclear membrane proteins and chromatin. These include: the retinoblastoma protein pRB; the 'germ-cell-less' protein GCL; the transcription factor E2F; and RNA polymerase, RNA splicing complex and DP protein. Taken from Maidment and Ellis, 2002

maintains close associations with the underlying lamina (Burke and Stewart, 2002). So far at least 20 inner nuclear membrane proteins were described and most of them with the exception of nurim interact with nuclear lamins (Rolls *et al.*, 1999). The inner nuclear membrane proteins include two related families: the LAP-1 family, comprising LAP-1 A, B and C isoforms; and the LAP-2 family, comprising LAP-2 b, g, d and e isoforms (Dechat *et al.*, 2000). LAP-2 has a fifth family member, LAP-2a, which is a soluble nucleoplasmic protein. In addition, there are two related, but distinct, nuclear membrane proteins: emerin (Bione *et al.*, 1994) and MAN1 (Lin *et al.*, 2000). The LAP families and emerin both contain single transmembrane domains at their C-terminus, whereas MAN1 possesses two such domains. These proteins are orientated in the inner nuclear membrane with their N-termini projecting into the nucleoplasm (known as type II orientation). All the LAP-2 isoforms, emerin and MAN1 share a homologous N-terminal domain, referred to as the 'LEM domain' (for LAP–emerin–MAN) (Lin *et al.*, 2000) which confers the ability to bind to 'barrier to auto-integration factor' (BAF), a DNA-bridging protein of unknown function (Haraguchi *et al.*, 2001). Three unrelated multi-membrane-spanning proteins have also been identified: nurim, lamin B receptor (LBR) and a hormonally regulated atypical P-type ATPase termed ring-finger binding protein (RFBP) (Mansharamani *et al.*, 2001; Rolls *et al.*, 1999; Worman *et al.*, 1990).

1.8 The nuclear lamina and inherited disease

The inherited human diseases associated with nuclear lamina components are called laminopathies. Laminopathies are a group of inherited diseases that arise through mutations in genes that code for A type lamins and lamina-associated proteins. The first report of such an association between the NE and disease was Emery–Dreifuss muscular dystrophy (EDMD) which arises with mutations in the X-linked gene STA (Bione *et al.*, 1994). EDMD is the third most common X-linked form of muscular dystrophy (after Duchenne and Becker) and is usually characterized by contractions in the Achilles and elbow tendons, a rigid spine, with muscle weakness during early childhood. Abnormal heart rhythms, heart block and cardiomyopathy leading to cardiac arrest also arise (Emery, 1989). The STA gene encodes the nuclear protein emerin, a 29 kDa type-2 integral membrane protein that traverses the INM through its carboxy-terminal domain.

In the last few years a number of mutations has been identified in the *LMNA* gene, the gene coding for lamin A/C, resulting in several diseases affecting different tissues (reviewed in (Mounkes *et al.*, 2003a). Figure 1.5 shows the identified mutations and the locations in the

lamin A/C gene. Three of these diseases affect striated muscle: autosomal dominant and recessive forms of Emery–Dreifuss muscular dystrophy (AR and AD-EDMD) (Bonne *et al.*, 1999), autosomal dominant limb-girdle muscular dystrophy with a cardiac conduction disturbances (LGMD1B) (Muchir *et al.*, 2000) and an autosomal dominant form of dilated cardiomyopathy with conduction defect (DCM-CD) (Fatkin *et al.*, 1999). The fourth specifically involves the adipose tissue: autosomal dominant familial partial lipodystrophy (FPLD) (Cao and Hegele, 2000). The fifth, an autosomal recessive form of axonal neuropathy (AR-CMT2) (De Sandre-Giovannoli *et al.*, 2002), specifically affects the peripheral nervous tissue. The sixth is an autosomal recessive disorder affecting adipose and bone tissues: mandibuloacral dysplasia (MAD) (Novelli *et al.*, 2002). The autosomal dominant form of Hutchinson–Gilford progeria syndrome (HGPS) is the seventh (De Sandre-Giovannoli *et al.*, 2003). This list is not exhaustive and novel mutations in lamin A/C gene are being identified.

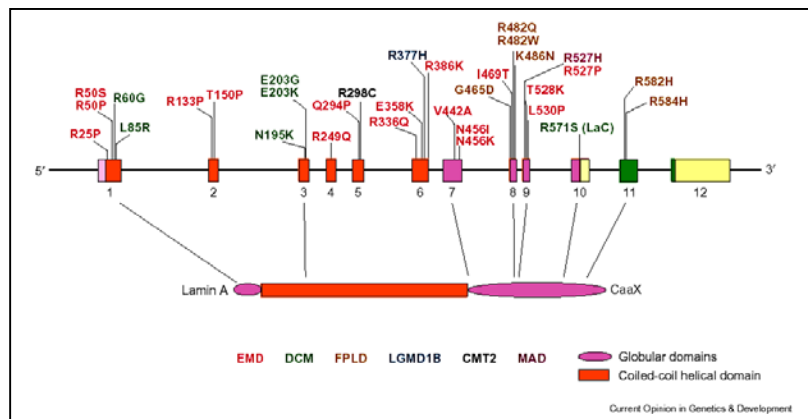


Figure 1.5: Amino acid substitutions in the LMNA gene (top) and the resulting diseases (bottom) are shown, by color code. This is not an exhaustive illustration of all the mutations but illustrates that mutations associated with the skeletal laminopathies are distributed throughout the gene. Those associated with FPLD and MAD tend to be clustered in the carboxyl globular domain. Abbreviations see text.

Taken from (Mounkes *et al.*, 2003a)

Abnormalities in nuclear structure in the cells and tissues of individuals with mutations in lamin A or C have been reported but the pathophysiological mechanism is unclear. Two mouse models are existing for laminopathies, one is a null mice for The *LMNA* gene showing muscular dystrophies similar to EDMD in humans (Sullivan *et al.*, 1999) and another Hutchinson–Gilford progeria syndrome (Mounkes *et al.*, 2003b). Analysis of the two animal models prompted researchers to form two theories about the pathogenesis of these diseases, one is the gene expression theory (Nikolova *et al.*, 2004) and the other is the mechanical stress hypothesis (Lammerding *et al.*, 2004). The “gene expression” hypothesis proposes that the nuclear envelope plays a role in tissue specific gene expression that can be altered by mutations in lamins and is based primarily on observed interactions between the nuclear envelope and chromatin components. The “mechanical stress” hypothesis states that abnormalities in nuclear structure, which result from lamin mutations, lead to increased susceptibility to cellular damage by physical stress. This hypothesis is supported by

observations that fibroblasts from patients with lamin A/C mutations and transfected cells expressing the mutant proteins often have severe abnormalities in nuclear morphology and that fibroblasts from individuals with FPLD are susceptible to damage by heat shock (Ostlund *et al.*, 2001; Raharjo *et al.*, 2001).

1.9 Role of Actin-binding proteins in nuclear positioning

Nuclear migration and positioning are essential for the movement of pronuclei during fertilization, normal mitotic and meiotic cell division and various morphogenetic processes during metazoan development. Disruption of nuclear migration in the cell bodies of the developing cerebral cortex lead to the human neurodevelopmental disease lissencephaly (Lambert de Rouvroit and Goffinet, 2001). Until recently nuclear positioning and migration were thought to be controlled and maintained only by microtubules and microtubule motors alone (Reinsch and Gonczy, 1998). The recent discovery of *D. discoideum* interaptin provided the first example of an actin-binding protein as a potential linker that could directly tether the nucleus to the actin cytoskeleton (Rivero *et al.*, 1998). In *Caenorhabditis elegans*, the novel actin binding protein ANC-1 together with Unc-84 has been shown to be important in the nuclear anchorage in syncytial cells. Mutations in ANC-1 or Unc-84 lead to a nuclear anchorage defective phenotype where the nuclei float freely within the cytoplasm (Starr and Han, 2002). The mammalian protein NUANCE (Zhen *et al.*, 2002) is a giant actin binding protein with an N-terminal ABD and a C-terminal klarsicht like transmembrane domain shown to be localized to the nuclear envelope. NUANCE, syne-1 (a C-terminal homologue of NUANCE, Apel *et al.*, 2000) and *Drosophila* MSP-300 are orthologues of ANC-1 which all together form a group of actin-binding proteins speculated to have a role in nuclear positioning. All these proteins have similar domain architecture with an N-terminal ABD followed by several spectrin like repeats and a C-terminal transmembrane domain. The ABD domain can bind to the actin filaments and C-terminal transmembrane domain can tether the protein to the nuclear envelope, thus forming a bridge connecting the nucleus to the actin cytoskeleton (Starr and Han, 2003). It has been shown that protein 4.1 is essential for proper assembly of functional nuclei *in vitro* in *Xenopus* egg extracts and identified the spectrin-actin binding domain (SABD) as one of the 4.1 domains critical for this process (Krauss *et al.*, 2002). Protein 4.1, a multifunctional structural protein, acts as an adaptor in mature red cell membrane skeletons linking spectrin-actin complexes to plasma membrane-associated proteins.

1.10 Aim of the study

NUANCE (Nucleus and ActiN Connecting Element) is a recently identified giant human protein that shows a similar domain architecture as ANC-1 and MSP-300 (Rosenberg-Hasson *et al.*, 1996). The functional actin-binding domain (ABD) found at the N-terminus of NUANCE directly links the cytoplasmic actin cytoskeleton to the outer nuclear membrane (Zhen *et al.*, 2002). A number of proteins have been identified and partially characterized in higher eukaryotes known as syne-1, myne-1 and nesprins-1 (Apel *et al.*, 2000; Mislow *et al.*, 2002b; Zhang *et al.*, 2001) which share strong homology against the C-terminal transmembrane domain of NUANCE. We have identified previously a 165 kDa protein called Enaptin-165 that displays strong homology to the N-terminal ABD of NUANCE (Braune, 2001). Enaptin-165 and syne-1 were present in the same human chromosome at a distance of about 500 kb. Our first aim was to examine whether Enaptin-165 and syne-1 are part of a larger protein of the size of NUANCE. Our studies included RT-PCR, characterization of the genomic locus, which codes for Enaptin-165 and syne-1 in order to recover and assemble the full-length Enaptin cDNA. To characterize the cell biology of Enaptin protein further we generated antibodies against the C- and N-terminus of Enaptin. Those tools would enable us to characterize the subcellular localization and the tissue distribution of Enaptin. Our studies included experiments to dissect and define functional domains of the C-terminal half of Enaptin. Syne-1 has been shown previously to interact with lamin A/C and emerin (Mislow *et al.*, 2002a), which are the proteins of nuclear lamina known to be involved in various laminopathies. We wanted therefore to find out whether the localization of Enaptin depends on lamin A/C and emerin and whether the localization of Enaptin is also affected in various laminopathies. To investigate the potential link of Enaptin to muscular dystrophies and to get further insight in to the function of this protein, a knockout strategy was initiated.

Materials
and Methods

2 Materials and methods

2.1 Materials

15 ml tubes, type 2095	Falcon
50 ml tubes, type 2070	Falcon
Corex tube, 15 ml, 50 ml	Corex
Coverslips (glass), Ø12 mm, Ø18 mm, Ø55 mm	Assistant
Cryotubes, 1 ml	Nunc
Electroporation cuvette, 2 mm electrode gap	Bio-Rad
Eppendorf tubes, 1.5 ml and 2 ml	Sarstedt
Hybridization tubes	Hybaid
3MM filters	Whatmann
Micropipette tips	Greiner
Micropipette, 1-20 µl, 10-200 µl, 100-1,000 µl	Gilson
Multi-channel pipette	Finnigan
Needles (sterile), 18G, 27G	Terumo, Microlance
Nitrocellulose, type BA85	Schleicher and Schüll
Nylon membrane, Biodyne	PALL
Filter, sterile 0.45 µm and 0.2 µm	Gelman Science
Parafilm	American Nat Can
Pasteur pipette, 145 mm, 230 mm	Volac
Petri dish (35 mm, 60 mm, 100 mm)	Falcon
Petri dish (90 mm)	Greiner
Plastic cuvettes	Greiner
Plastic pipettes (sterile), 1 ml, 2 ml, 5 ml, 10 ml, 25 ml	Greiner
PVDF membrane	Millipore
Quartz cuvettes Infrasil	Hellma
Saran wrap	Dow
Superdex75 PC3.2/30	Pharmacia Biotech
Tissue culture dishes, 6 wells, 24 wells, 96 wells	Nunc
Tissue culture flasks, 25 cm ² , 75 cm ² , 175 cm ²	Nunc
Whatman 3MM filter paper	Whatman
X-ray film X-omat AR-5	Kodak

2.2 Instruments

Blotting chamber Trans-Blot SD	Bio-Rad
Biotech fresco	Heraeus Instruments
Centrifuges (microcentrifuges):	
Centrifuge 5417 C	Eppendorf
Centrifuge	Sigma B Braun
Cold centrifuge Biofuge fresco	Heraeus Instruments
Centrifuges (table-top, cooling, low speed):	
Centrifuge CS-6R	Beckman
Centrifuge RT7	Sorvall
Centrifuge Allegra 21R	Beckman
Centrifuges (cooling, high speed):	
Beckman Avanti J25	Beckman
Sorvall RC 5C plus	Sorvall
Centrifuge-rotors:	
JA-10	Beckman
JA-25.50	Beckman
SLA-1500	Sorvall
SLA-3000	Sorvall
SS-34	Sorvall
Crosslinker UVC 500	Hofer
Freezer (-80 °C)	Nunc
Freezer (-20 °C)	Siemens, Liebherr
Electrophoresis power supply, Power-pac-200, -300	Bio-Rad
Electroporation unit Gene-Pulser	Bio-Rad
Gel-documentation unit	MWG-Biotech
Heating blocks: type DIGI-Block JR	neoLab
Hybridisation oven	Hybaid
Incubator Lab-Therm	Kühner
Ice machine	Ziegra
Incubators:	
CO ₂ -incubator, BBD 6220, BB 6220	Heraeus
CO ₂ -incubator	WTC Binder Biotran
Incubator, microbiological	Heraeus

Incubator with shaker Lab-Therm	Kuehner
Lab-shaker	Kühner
Laminar flow, Hera Safe (HS 12)	Heraeus
Magnetic stirrer, MR 3001 K	Heidolph
Microscopes:	
Light microscope, DMIL	Leica
Fluorescence microscope, DMR	Leica
Fluorescence microscope, 1X70	Olympus
Confocal laser scanning microscope, DM/IRBE	Leica
Stereomicroscope, SZ4045TR	Olympus
Oven, conventional	Heraeus
PCR-thermocycler	MWG-Biotech
pH-meter 766	Knick
Pump system Biologic Workstation	Bio-Rad
Refrigerator	Liebherr
Semi-dry blot apparatus, Trans-Blot SD	Bio-Rad
Shaker 3015	GFL
Spectral photometer type Ultraspec 2000	Pharmacia Biotech
Speed-vac concentrator, DNA 110	Savant
Type thermomixer	Eppendorf
Ultracentrifuge Optima TLX	Beckmann
UV-Monitor TFS-35 M	Faust
UV-transilluminator	MWG-Biotech
Vortex REAX top	Heidolph
Water bath	GFL

2.3 Enzymes, inhibitors and antibodies

2.3.1 Enzymes for molecular biology

Calf Intestinal Alkaline Phosphatase (CIAP)	Roche
DNase I (Desoxyribonuclease)	Sigma
Lysozyme	Sigma
M-MLV reverse transcriptase	Promega
RevertAid™ First Strand cDNA Synthesis Kit	Fermentas
Restriction endonucleases	Life Technologies,

Ribonuclease A	New England Biolabs,
T4-DNA-ligase	Amersham Biosciences
Taq-DNA-polymerase	Sigma
Advantage Taq polymerase	Life Technologies
Pfu polymerase	Roche
SP6 and T3 RNA polymerase	Clontech
	Invitrogen
	Roche
2.3.2 Antibodies	
primary antibodies:	
mouse-anti-skeletal (Fast) myosin	Sigma
mouse-anti-lamin A/C	CHEMICON
mouse-anti-emerin	NOVO Castra
mouse-anti- β -tubulin (WA3)	Gift of U.Euteneuer (München)
mouse-monoclonal anti-NUANCE K49-260-1	Unpublished
mouse-monoclonal anti-NUANCE K20-478-4	(Zhen <i>et al.</i> , 2002)
guinea pig anti-nesprin antibody	Gift of H. Herrmann (Heidelberg)
<i>secondary antibodies:</i>	
goat-anti-mouse-IgG, peroxidase-conjugated	Sigma
goat-anti-rabbit-IgG, peroxidase-conjugated	Sigma
goat-anti-mouse-IgG, Cy3-conjugated	Sigma
goat-anti-mouse-IgG, Cy5-conjugated	Sigma
goat-anti-mouse-IgG, alkaline phosphatase conjugated	Sigma
goat-anti-mouse-IgG, Alexa 488 conjugated	Molecular Probes
goat-anti-rabbit-IgG, Alexa 568 conjugated	Molecular Probes
goat-anti-rabbit-IgG, FITC conjugated	Sigma
goat-anti-guinea pig-IgG, FITC conjugated	Sigma
biotinylated anti-rabbit IgG	Vector Laboratories
TRITC- Phalloidin	Sigma
2.3.3 Inhibitors	
Benzamidine	Sigma
DEPC (Diethylpyrocarbonate)	Sigma
PMSF (Phenylmethylsulfonylfluoride)	Sigma

Ribonuclease-inhibitor (RNAsin)

Promega

Complete Inhibitor-Cocktail

Roche

2.3.4 Antibiotics

Ampicillin

Grünenthal

Geneticin (G418)

Life Technologies

Kanamycin

Biochrom

Penicillin/streptomycin

Biochrom

2.4 Reagents

Acrylamide

National Diagnostics

Agarose (electrophoresis grade)

Life Technologies

Acetone

Riedel-de-Haen

Bacto-Agar, Bacto-Peptone, Bacto-Tryptone

Difco

BSA (bovine serum albumin)

Roth

Chloroform

Riedel-de-Haen

Calcium chloride

Sigma

CNBr-activated sepharose 4B

Amersham Bioscience

Coomassie-brilliant-blue R 250

Serva

p-cumaric acid

Fluka

DAPI

Sigma

DMEM (Dulbecco's Modified Eagle's Medium)

Sigma

Ham's F10 nutrient medium

Biochrom

DMF (dimethylformamide)

Riedel-de Haen

DMSO (dimethyl sulfoxide)

Merck

DTT (1,4-dithiothreitol)

Gerbu

EDTA ([ethylenedinitrilo]tetraacetic acid)

Merck

EGTA (ethylene-bis(oxyethylenenitrilo)tetraacetic acid)

Sigma

Ethanol

Riedel-de-Haen

Ethidium bromide

Sigma

FCS (fetal calf serum)

Biochrom,

Fish gelatine

Sigma

Formamide

Merck

Formaldehyde

Sigma

GST beads

Amersham Bioscience

Glycine

Degussa

IPTG (isopropyl β -D-thiogalactopyranoside)	Sigma
Isopropanol	Merck
β -mercaptoethanol	Sigma
Methanol	Riedel-de-Haen
Methylbenzoate	Fluka
Mineral oil	Pharmacia
Minimum Essential Medium	Gibco
MOPS ([morpholino]propanesulfonic acid)	Gerbu
Ni-NTA-agarose	Qiagen
Paraformaldehyde	Sigma
RNase A	Sigma
SDS (sodium dodecylsulfate)	Serva
Sodium azide	Merck
TEMED (tetramethylethylenediamine)	Merck
Tris (hydroxymethyl)aminomethane	Sigma
Triton X-100 (t-octylphenoxypolyethoxyethanol)	Merck
X-Gal(5-bromo-4-chloro-3-indolyl- β -D-galactopyranoside)	Roth
Xylol	Fluka

Radionucleotides

α - ³² P-deoxyadenosine-5'-triphosphate (10 mCi/ml)	Amersham
α - ³² P-deoxycytosine-5'-triphosphate (10 mCi/ml)	Amersham
α - ³² P Uridine 5'Triphosphate (10 mCi/ml)	Amersham

Reagents not listed above were purchased from Clontech, Fluka, Merck, Roth, Serva, Sigma, Promega and Riedel-de-Haen.

2.5 Kits

Nucleobond PC 500	Macherey-Nagel
NucleoSpin Extract 2 in 1	Macherey-Nagel
NucleoSpin Plus	Macherey-Nagel
RNeasy midi kit	Qiagen
pGEM-T Easy Cloning Kit	Promega
Zero Blunt TOPO PCR Cloning Kit	Invitrogen
EndoFree Plasmid Maxi kit	Qiagen
Stratagene Prime-It II random primer labeling kit	Stratagene

Multiple Tissue Expression Array	Clontech
Human Brain, cerebellum Poly A+ RNA	Clontech
RevertAid First Strand cDNA Synthesis Kit	MBI Fermentas
TRIzol reagent	Invitrogen
TOPO TA cloning kit	Invitrogen
Zero Blunt TOPO PCR cloning kit	Invitrogen
VECTOR M.O.M. immunodetection kit	Vectror Laboratoties

2.6 Bacterial host strains

E. coli DH5 α

E. coli XL1Blue

2.6.1 Media for *E. coli* culture

LB medium, pH 7.4 (Sambrook and Russell, 2001)

10 g bacto-tryptone

5 g yeast extract

10 g NaCl

adjust to pH 7.4 with 1 N NaOH

add H₂O to make 1 liter

For LB agar plates, 0.9% (w/v) agar was added to the LB medium and the medium was then autoclaved. For antibiotic selection of *E. coli* transformants, 50 mg/l ampicillin, kanamycin or chloramphenicol was added to the autoclaved medium after cooling it to approximately 50°C. For blue/white selection of *E. coli* transformants, 10 μ l 0.1 M IPTG and 30 μ l X-gal solution (2% in dimethylformamide) was spread per 90 mm plate and the plate was incubated at 37°C for at least 30 min before using.

SOC medium, pH 7.0 (Sambrook and Russell, 2001)

20 g bacto-tryptone, 5 g yeast extract, 10 mM NaCl, 2.5 mM KCl. Dissolve in 900 ml deionised H₂O, adjust to pH 7.0 with 1 N NaOH. The medium was autoclaved, cooled to approx. 50°C and then the following solutions, which were separately sterilized by filtration (glucose) or autoclaving, were added: 10 mM MgCl₂.6 H₂O, 10 mM MgSO₄.7 H₂O.

20 mM glucose, add H₂O to make 1 liter.

2.7 Eukaryotic cells

C3H/10T1/2 mouse fibroblasts

N2A mouse neuroblastoma cell line

COS-7 monkey SV40 transformed kidney cell line

C2F3 mouse myoblasts

MB50 human myoblast primary cell line

Skin fibroblast cells of patients suffering from Emery-Dreifuss muscular dystrophy (a gift from Prof. Dr. Manfred Wehnert, Ernst-Moritz-Arndt Universität Greifswald)

Lamin A/C ^{-/-} mouse fibroblasts and wild type fibroblasts (Brian Burke, Department of Anatomy and Cell Biology, University of Florida ,Sullivan et al., 1999).

2.7.1 Media for cell culture

COS7 (monkey kidney fibroblasts)- DMEM high glucose-500 ml, 10% FBS, 2 mM glutamine, penicillin/streptomycine

MB50 (human myoblasts)- DMEM low glucose-250 ml, Nutrient F10 medium –250 ml, 20% FBS, 2 mM glutamine, penicillin/streptomycine, basic fibroblast growth factor (bFGF).

Differentiation medium for MB50

DMEM low glucose-250 ml, Nutrient F10 medium -250 ml, 2% horse serum, 2 mM glutamine, penicillin/streptomycine

Human primary fibroblasts

Minimum Essential Medium (Gibco) 500ml, 10%FBS, penicillin/streptomycine, nonessential amino acids (6 ml), Bicarbonate (Gibco)(7.5%), glutamine.

Neuroblastoma cells (N2A)

DMEM low glucose 500ml, 10% FBS, nonessential amino acids, 2 mM glutamine, penicillin/streptomycine.

10T1/2 mouse fibroblasts

DMEM low glucose-500 ml, 10% FBS, 2 mM glutamine, penicillin/streptomycine

2.8 Vectors

pGEM-T Easy	Promega
pCR-Blunt II-TOPO	Invitrogen
pCR-2.1 TOPO	Invitrogen
pEGFP-C2	Clontech
pBluescript	Stratagene
pGEX4T1	Amersham

2.9 Oligonucleotides

Oligonucleotides for PCR (polymerase chain reaction) were purchased from Sigma, MWG-Biotech AG (Ebersberg), Roth GmbH (Karlsruhe, Germany and Metabion (Martinsried).

2.9.1 Oligonucleotides used for amplifying the full length cDNA of Enaptin

All primers are given in the 5' to 3' direction.

PCR321/94a

AW297921 fw2	CGTTCGCTCGCTTCGCCTTGCT
AK051543 rv	CTGCACTCTTGTGGACAGCCCAGGTPCR 321/94/b

AW297921 fw2	CGTTCGCTCGCTTCGCCTTGCT
AK051543 rv	CTGCACTCTTGTGGACAGCCCAGGT

PCR 363

AW297921 fw2	CGTTCGCTCGCTTCGCCTTGCT
AK051543 rv	CTGCACTCTTGTGGACAGCCCAGGT

PCR 360

AI713682 fw	GCCTTGGAAGTTCGTCATCT
AI473752 rv	CCAGGCTCTCCAAGTCAAGCTG

PCR391

BI33827 fw2	GAGAATTCATGAAAATGGAGTTTCTCGAACTGAAG
AK056122 rv2	CATGTGAATCGCATCCGTCATCCAG

PCR250

AK056122 fw	CAGCAATCGCCTCTATGATCTGCCAGC
KIAA1262 rv	GCTTCCAGGTGGACAGCTGTACTCTCTGC

PCR 404

Syne1B fw1	CAGATGACTTGACCCAGTTGAGCCTGCTG
Trans rv	GTGTATCTGAGCATGGGGTGGGAATGAC

2.9.2 Knockout target vector primers

5probe fw	CCACCAAAGTACAAATTAAGGTGAC
5probe rv	CAGCCAACATGTAACCAAATTCATC
3armprobe fw	CTCACTGCACACTCCTACACTC
3armprobe rv	GAGTCCCCTTGGTCTTAGCAATC
5arm-SalI fw	CGGGTCGACCTTCTCTGAGTGACCTTGAC
5arm-EcoRV rv	CCCGATATCGAAGGTACGTTTCTGTACAATCTC
3arm-NotI fw	CATCGGCCGGACTCCCTAATGTGAACCTAAC
3arm-SacII rv	GTCCAGTAACGTATCTCTGTTCGTGGCGCCTAC

2.9.3 Primers for making GFP-dominant negative constructs for Enaptin

GFPDN Construct

GFPDN fw	GTGAATTCCAGTTTAATTCTGACCTCAAC
GFPDN rv	GTGTCGACTTCAGAGTGGAGGAGGACCG

GFP-Trans

GFPDNfw2	CGAATTCAAGGATCTTGAGAAGTTAC
GFPDN rv	GTGTCGACTTCAGAGTGGAGGAGGACCG

2.9.4 Primers for GST-specII fusion protein

Spec fw BamHI	CAGGATCCGTGGCAGCAGTTTAACTCAG
Spec rv EcoRI	GTGAATTCCTTGATATGACGACTGACCTC

2.9.5 Primers of probes used for northern blotting

ABD probe

ABD-EcoRI fw	GGGGAATTCCAGAAACGTACCTTCAC
ABD-Sall rv	CAGTGTGACAAACTGGGCCACGTAAG

2.9.6 Primers for C-terminal syne-1 probe for multiple tissue expression array

Syne 1Bfw	CAGATGACTTGACCCAGTTGAGCCTGCTG
Syne 1Brv	GGAGATGCTGCCACCGGTCGTTGAC

2.10 Construction of vectors

2.10.1 Cloning of cDNA fragments

In order to amplify the cDNA fragments, RT-PCR reactions were done on human cerebellum poly A⁺ RNA (Clontech, Germany) using degenerate primers. Enaptin cDNA fragments were amplified using the first strand cDNA produced by the RT reactions as template using an Advantage cDNA polymerase mix (Clontech) according to the manufacturers instructions. The primers used for the amplification were given above. The amplified fragments such as PCR321/94a, PCR321/94b, PCR363, PCR360, PCR391, PCR250 and PCR404 were cloned in the plasmid vector pGEM-T Easy (Promega) and sequenced first with vector primers and then with specific primers corresponding to the sequence obtained.

2.10.2 Generation of C-terminal Enaptin-GFP fusions

GFP-DN Enaptin

The required Enaptin DNA fragment corresponding to aa 8396-8749 of human Enaptin was amplified with GFPDN fw and GFPDN rv primers from an image clone, containing the mouse Enaptin C-terminus (BC054456). The PCR fragment was cloned into

the plasmid vector TOPO TA (Invitrogen) and sequenced. The DNA fragment was retrieved from the TOPO vector using EcoRI and Sall and ligated into pEGFPC2 vector (Clontech). The GFPDN construct was sequenced to confirm the cloning direction.

GFP-Trans Enaptin

The Enaptin DNA fragment corresponding to aa 8611-8749 of human Enaptin was amplified by PCR with the GFPDNfw2 (EcoRI)/ GFPDN rv (Sall) set of primers using the BC054456 image clone and cloned into pGEM-T Easy. The construct was digested with EcoRI and Sall and the Enaptin-Trans fragment was ligated into pEGFPC2 vector.

2.10.3 Cloning of GST-SpecII

To construct GST-SpecII, the cDNA fragment of Enaptin corresponding to the last two spectrin repeats corresponding to aa 8394-8608 of human Enaptin was amplified from the PCR404 plasmid using primers SpecfwBamHI and SpecrvEcoRI and cloned into TOPO2.1-TA vector (Invitrogen). The SpecII fragment was retrieved from TOPO2.1-TA using EcoRI and ligated into pGFPC2. BamHI site could not be used due to a frame shift mutation. The cloning direction and sequence were confirmed by sequencing.

2.10.4 Probes for northern blot analysis

CPG2 Probe

Enaptin-165 was cloned into pGEM-T Easy with the 3' side located towards the SP6 promotor. This construct was digested with HindIII at position 3646 in the cDNA of Enaptin-165 (Padmakumar, 2004) for generating a digestion site with a 5'overhang. The in-vitro transcription was done using SP6 RNA polymerase (Roche) according to the manufacturer's instructions. The transcription will produce antisense RNA fragment of 650 bases corresponding to nucleotides 3646-4296 in the Enaptin-165 cDNA. The base numbers are counted from the starting codon.

ABD probe

The ABD probe corresponds to nucleotides 517 to 1287 of the Enaptin-165 cDNA and was amplified using primers ABD-EcoRI fw and ABD Sall rv. This PCR fragment was purified and digested with EcoRI and Sall and ligated into EcoRI/Sall digested pGEM.T easy vector. The in-vitro transcription was done using SP6 RNA polymerase (Roche).

Probes for multiple tissue expression (MTE) array analysis.

N-terminal ABD probe

A probe corresponding to nucleotides 318–951 of the human Enaptin cDNA for performing an MTE array analysis was generated by EcoRI digestion of human EST clone 1650727 (AI031971).

C-terminal syne-1 probe

A cDNA fragment corresponding to nucleotides 23398– 23832 was amplified using syne-1 fw and syne-1 rv as primers using PCR404 as template. The PCR product was purified from the gel and used to probe the multiple tissue expression arrays.

2.11 Buffers and other solutions

Buffers and solutions not listed below are described in the methods section.

PBS (pH 7.2):	10x NCP-buffer (pH 8.0):
10 mM KCl	100 mM Tris/HCl
10 mM NaCl	1.5 M NaCl
16 mM Na ₂ HPO ₄	5 ml Tween 20
32 mM KH ₂ PO ₄	2.0 g sodium azide
<u>10x MOPS (pH 7.0/ pH 8.0):</u>	<u>PBG (pH 7.4):</u>
20 mM MOPS	0.5% BSA
50 mM sodium acetate	0.045% fish gelatine
1 mM EDTA in 1x PBS	
<u>20x SSC</u>	<u>TE-Puffer (pH 8.0):</u>
3 M NaCl	10 mM Tris/HCl (pH 8.0)
0.3 M sodium citrate	1 mM EDTA (pH 8.0, adjusted with NaOH)
autoclaved	

2.12 Computer programs

GCG software package (Wisconsin package) and the BLAST (NCBI) program were used for the alignment analysis of cDNA sequences. Protein sequences were aligned using the programs ClustalW, BioEdit and TreeView (available from EMBL, www.ebi.ac.uk). For prediction of motif and pattern searches several tools available in the ExPaSY server (www.expasy.ch) were used. Annealing temperatures of primers were calculated with the program “Primer Calculator” available in the Internet (www.gensetoligos.com).

2.13 Molecular biological methods

2.13.1 Plasmid-DNA isolation from *E. coli* by alkaline lysis miniprep

With this DNA isolation method, plasmid DNA was prepared from small amounts of bacterial cultures. Bacteria were lysed by treatment with a solution containing sodium dodecylsulfate (1% SDS) and 0.5 M NaOH (SDS denatures bacterial proteins and NaOH

denatures chromosomal and plasmid DNA). The mixture was neutralized with 3M potassium acetate, causing the plasmid DNA to re-anneal rapidly. Most of the chromosomal DNA and bacterial proteins precipitate, as does SDS forming a complex with the potassium, and are removed by centrifugation. The re-annealed plasmid DNA from the supernatant was concentrated by ethanol precipitation.

2.13.2 Plasmid-DNA isolation with a kit from Macherey-Nagel

The NucleoSpin kit is designed for the rapid, small-scale preparation of highly pure plasmid DNA (minipreps) and allows a purification of up to 40 µg per preparation of plasmid DNA. The principle of this plasmid-DNA purification kit is based on the alkaline lysis miniprep. Plasmid DNA was eluted under low ionic strength conditions with a slightly alkali buffer. For higher amounts of plasmid DNA, the Nucleobond AX kit from Macherey-Nagel was used. The plasmid DNA was used for sequencing and transfection of eukaryotic cells. The protocols were followed as described in the manufacturer's manual.

2.13.3 DNA agarose gel electrophoresis

10x DNA-loading buffer:	50x Tris acetate buffer (1000 ml) (pH 8.5)
40% sucrose, 0.5% SDS	242.2 g Tris 0.25% bromophenol blue, in TE (pH 8.0)
	57.5 ml acetic acid
	100 ml of 0.5 M EDTA (pH 8.0, adjusted with NaOH)

Agarose gel electrophoresis was performed to analyze the length of DNA fragments after restriction enzyme digests and polymerase chain reactions (PCR), as well as for the purification of PCR products and DNA fragments. DNA fragments of different molecular weight show different electrophoretic mobility in an agarose gel matrix. Optimal separation results were obtained using 0.5-2% gels in TAE buffer at 10 V/cm. Horizontal gel electrophoresis apparatus of different sizes were used. Before loading the gel, the DNA sample was mixed with 1/10 volume of the 10x DNA-loading buffer. For visualization of the DNA fragments under UV-light, agarose gels were stained with 0.1 µg/ml ethidium bromide. In order to define the size of the DNA fragments, DNA molecular standard markers were also loaded onto the gel.

2.13.4 Isolation of total RNA from mouse tissue with TRIzol reagent

Working with RNA always requires special precautions in order to prevent degradation by ubiquitous RNases, e.g. wearing gloves and using RNase-free water and material. TRIzol reagent is a mono-phasic solution of phenol and guanidine isothiocyanate and is used to isolate RNA by a single-step method (Chomczynski and Sacchi, 1987). The tissue is homogenized in liquid nitrogen and the powder is added to TRIzol reagent (1 g/10 ml).

Incubation is done for 5 minutes at room temperature and 0.2 ml of chloroform/ml of TRIzol is added. The tubes are shaken vigorously by hand for 15 seconds and incubation was at 15 to 30°C for 2 to 3 minutes. The samples are centrifuged at no more than $12,000 \times g$ for 15 minutes at 2 to 8°C. Following centrifugation, the mixture separates into a lower red, phenol-chloroform phase, an interphase, and a colorless upper aqueous phase. The RNA remains exclusively in the aqueous phase. The aqueous phase is transferred to a fresh tube. The RNA is precipitated from the aqueous phase by mixing with isopropyl alcohol (0.5 ml of isopropyl alcohol per 1 ml of TRIzol Reagent). The samples are incubated at 15 to 30°C for 10 minutes and centrifuged at no more than $12,000 \times g$ for 10 minutes at 2 to 8°C. The supernatant was decanted and the RNA pellet washed once with 70% ethanol, dried and re-dissolved in RNase free water.

2.13.5 RNA agarose gel electrophoresis and northern blotting (Lehrach *et al.*, 1977)

10X FA gel buffer (pH 8.0)

200 mM 3-[N-morpholino]

propanesulphonic acid (MOPS)

50 mM sodium acetate

10 mM EDTA

the pH was adjusted with NaOH.

5X RNA loading dye

16 μ l saturated bromophenol blue

80 μ l 500 mM EDTA, pH 8.0

720 μ l 37% formaldehyde

2 ml 100% glycerol

3084 μ l formamide

4 ml 10x FA buffer

The running buffer was identical as above (10x FA gel buffer) but the pH was adjusted to pH 7.0.

The 0.7% agarose gels were made under RNase free conditions (0.7% agarose, 148 ml DEPC water, 20 ml 10X FA buffer, 32 ml 36% formaldehyde). After washing the gels with water, the RNA was transferred onto a zeta probe membrane (BioRad) overnight using the set up similar to the one for Southern blotting, but using 50 mM NaOH to reduce the hydrolysis of RNA. The next day the membrane was washed in 2x SSC, briefly air-dried and the RNA was UV-cross linked to the membrane.

2.13.6 Labeling of DNA probes

DNA probes used for radioactive labelling were obtained either by purification of PCR fragments or digestion from plasmids. Stratagene random labelling kit was used for the labelling reaction according to the manufacturer's protocol. Unincorporated nucleotides were separated by applying the probe to a Sephadex G-50-column. Before using, labelled probes were denatured at 100°C for 5 minutes.

2.13.7 Generation of Riboprobes

1. Isolation of pure plasmids

- a. The plasmid DNA used for making riboprobes should be devoid of any RNase contamination. So the plasmid DNA preparation was treated with Proteinase K (100µg/ml) in 10X proteinase buffer [100mM, TrisHCL(pH 8.0) 50 mM EDTA/ 500 mM NaCl] and 0.1 volume of 5% SDS
- b. The reaction mix is incubated for 1hr and DNA is extracted with phenol:chloroform.
- c. The DNA was resuspended in RNase free TE (pH 7.6).

2. Digestion of plasmids

Around 10 µg of DNA was digested with an enzyme producing a 5' overhang. After the digestion the plasmid is purified using phenol:chloroform extraction and dissolved in RNase free water at a concentration of 0.2 µg/ml.

3. Transcription reaction

For the transcription reaction, 8 µl of plasmid (1.6 µg) is used in a total reaction volume of 20 µl. 10X SP6 polymerase buffer (10 µl), ribonucleotide triphosphates rNTPs except rUTP (2 µl), SP6 RNA polymerase (2 µl), RNasin (RNase inhibitor) 40U, and α -³²P-UTP were added and the reaction mix was incubated for 90 minutes at 37°C. After the transcription reaction, the SP6 polymerase was inactivated at 65 °C by incubating for 10 minutes. 1 µl of DNase was added and incubated for 15 minutes to degrade the DNA template. The labelled RNA probes were separated by gel filtration using a Sephadex-50 column. The RNA probes were used for hybridisation.

2.13.8 Elution of DNA fragments from agarose gels

Elution of DNA fragments from agarose gels was performed using the 'NucleoSpin Extract 2 in 1' kit from Macherey-Nagel. Bands of interest were cut out of the gel and the agarose melted at 50°C in a binding buffer. After several centrifugation steps with wash buffer, the DNA bound selectively to a silica membrane column and was eluted with a low salt solution.

2.13.9 Measurement of DNA and RNA concentrations

Concentrations of DNA and RNA were estimated by determining the absorbance at a wavelength of 260 nm. A ratio of OD₂₆₀/OD₂₈₀ >2 indicate negligible protein contaminations. Protein contaminations were estimated from absorbance at 280 nm.

2.13.10 Restriction digestion of DNA

Digestion of DNA with restriction endonucleases was performed in buffer systems provided by the manufacturers at the recommended temperatures.

2.13.11 Dephosphorylation of 5'-ends of linearized vectors

10x CIAP-Puffer (pH 9.0)

0.5 M Tris/HCl (pH 9.0)

10 mM MgCl₂

1 mM ZnCl₂

10 mM spermidin

In order to prevent linearized vectors from re-ligation, the 5' end phosphate groups were hydrolysed with calf intestinal alkaline phosphatase (CIAP) for 30 minutes at 37°C followed by heat inactivation at 70°C for 10 min.

2.13.12 Creation of blunt ends

Due to the 3' exonuclease activity of klenow enzyme, it is possible to transform overhanging 3' ends of DNA (sticky ends) into blunt ends. After the reaction for 30 minutes at 37°C, heat inactivation for 10 minutes at 70°C was necessary.

2.13.13 Ligation of vector and DNA fragments

T4-DNA-ligase catalyzes the ligation of DNA fragments and vector DNA. 1U T4-ligase was incubated with about 25 ng of DNA fragments overnight at 16°C.

2.13.14 Polymerase chain reaction (PCR)

PCR can be used for *in vitro* amplification of DNA fragments (Saiki *et al.*, 1985). A double stranded DNA (dsDNA) serving as a template, two oligonucleotides (primers) complementary to the template DNA, deoxyribonucleotides and heat resistant *Taq*-DNA-polymerase are required for this reaction. Primers may be designed having non-complementary ends with sites for restriction enzymes. The first step in PCR reactions is the denaturing of dsDNA at 94°C. Second, the reaction mix was incubated at different annealing temperatures, depending on the G/C content of the primers. Different programs provide an accurate calculation of the annealing temperature based on the nearest neighbours method and are freely available in the internet. The third step with a temperature of 72°C allows the elongation of the new strand of DNA by the *Taq*-DNA-polymerase. A PCR machine (thermocycler) can be programmed to regulate these different cycles automatically. A “standard program” is presented below:

I. Initial denaturing: 94°C, 5 min

II. Cycles (25-35):

Denaturing (94°C, 15 sec.)

Annealing (60-68°C, 30 sec)

Elongation (72°C, 1-10min)

III. Final elongation: 72°C, 10 min

IV. Cooling to 4°C

2.13.15 Transformation of *E. coli* cells with plasmid DNA

LB-Medium:

10 g Bacto-Tryptone

5 g yeast extracts

5 g NaCl

SOC-Medium:

20 g Bacto-Tryptone

5 g yeast extract

0.5 g NaCl

20 mM Glucose

For transformation of *E. coli* cells the heat shock method was used. DNA and competent cells were incubated for 15 minutes on ice and then for 45 seconds at 42°C. After cooling on ice for 2 minutes, the bacteria were incubated for 1 hour at 37°C in SOC-medium without any antibiotics. Finally, the bacteria were plated on agar plates containing selective antibiotics, and incubated overnight at 37°C. For further analysis single colonies were picked, inoculated and incubated for 12 hours in LB-medium on a shaker. From clones of interest glycerol stocks were made. For this, samples of *E. coli* cultures were mixed with an equal volume of 50% glycerol and frozen at -80°C.

2.14 Protein methods and immunofluorescence

2.14.1 Extraction of protein homogenate from mouse tissues and cell cultures

For the characterization of the polyclonal antibodies and the detection of the endogenous Enaptin protein, homogenates from mouse tissues and cell cultures were extracted. For this, mice were sacrificed using dry ice. Dissected organs were briefly rinsed in ice-cold PBS buffer and frozen in liquid nitrogen. After homogenisation, the cell lysates were mixed with SDS-loading buffer boiled at 95°C for 5 minutes, the DNA was sheared using 1ml syringe and centrifugation was for 10 minutes at 15,000 rpm. For the COS-7 cells protein homogenates, a confluent 10 cm plate was trypsinised and cells were collected by centrifugation for 5 minutes at 1,000 rpm and resuspended in ice-cold PBS containing protease inhibitors. Afterwards the pellet samples were treated and processed as described above.

2.14.2 SDS-polyacrylamide-gel electrophoresis (SDS-PAGE) (Laemmli, 1970)

5x SDS-loading buffer:	10x SDS-PAGE-running buffer:
2.5 ml 1 M Tris/HCl, pH 6.8	0.25 M Tris
4.0 ml 10% SDS	1.9 M glycine
2.0 ml glycerol	1 % SDS
1.0 ml 14.3 M β -mercaptoethanol	
200 μ l 10 % bromophenol blue	
Molecular weight standard marker	
LMW-Marker (Pharmacia) (kDa):	94; 67; 43; 30; 24; 20.1; 14.4
HMW-Marker (Pharmacia) (kDa):	220; 170; 116; 76; 53
Precision plus protein standards	
Prestained marker (BioRad) (kDa) :	250; 150; 100; 75; 50; 37; 25; 20; 15; 10

SDS-polyacrylamide gel electrophoresis (SDS-PAGE) was performed using the discontinuous buffer system of Laemmli (1970). Discontinuous polyacrylamide gels (10-15% resolving gel, 5% stacking gel) were prepared using glass plates of 10 cm x 7.5 cm dimensions and spacers of 0.5 mm thickness. A 12-well comb was generally used for formation of the wells in the stacking gel. The composition of 12 resolving and 12 stacking gels is given in the table below.

Components	Resolving gel			Stacking gel 5%
	10 %	12 %	15 %	
Acrylamide/Bisacrylamide (30:0.8) [ml]:	19.7	23.6	30	4.08
1.5 M Tris/HCl, pH 8.8 [ml]:	16	16	16	-
0.5 M Tris/HCl, pH 6.8 [ml]:	-	-	-	2.4
10 % SDS [μ l]:	590	590	590	240
TEMED [μ l]:	23	23	23	20
10 % APS [μ l]:	240	240	240	360
Deionised H ₂ O [ml]:	23.5	19.6	13.2	17.16

Samples were mixed with suitable volumes of SDS sample buffer, denatured by heating at 95°C for 5 min and loaded into the wells of the stacking gel. A molecular weight marker, which was run simultaneously on the same gel in an adjacent well, was used as a standard to establish the apparent molecular weights of proteins resolved on SDS-polyacrylamide gels. The molecular weight markers were prepared according to the manufacturer's specifications.

After loading the samples onto the gel, electrophoresis was performed in 1x gel-running buffer at a constant voltage of 100-150 V until the bromophenol blue dye front had reached the bottom edge of the gel or had just run out of the gel. After the electrophoresis, the resolved proteins in the gel were either observed by coomassie blue staining or transferred to a nitrocellulose membrane.

2.14.3 Gradient gel electrophoresis

Gradient gels were used for visualising both high molecular weight proteins and low molecular weight proteins. Gradient gels were made with a gradient mixer and typically a gel with a gradient of 3%-15% acrylamide was made. The top of the gel had 3% of acrylamide whereas the bottom part 15% of acrylamide. The middle part of the gel had a gradient from 3% till 15%. The gradient mixer was connected to a peristaltic pump, which delivered the solution into the gel-casting tray. 15% acrylamide was being added into the near well of the outlet from the mixer.

Stock solutions for preparing Gradient gels

100 ml stock solution	3%	6%	10%	12%	15%	4% Stacking Gel
1.5M Tris/HCl, pH 8.8	25 ml	25 ml	25 ml	25 ml	25 ml	-
0.5% tris/HCl, pH 6.8	-	-	-	-	-	20 ml
PAA (30%)	10 ml	20 ml	33.3 ml	40 ml	50 ml	13.3 ml
SDS (10%)	1 ml	1 ml	1 ml	1 ml	1 ml	1 ml
H ₂ O	64 ml	54 ml	40.6 ml	34 ml	24 ml	65.6 ml

Solutions required for individual gradient gels

	Gradient gel solution per mixing well		1 gel	Stacking gel
Stock solution /Gel	4.5 ml	4.5 ml	9.0 ml	3.0 ml
APS 10%	15 µl	15 µl	22 µl	30 µl
TEMED	8 µl	8 µl	10 µl	16 µl

2.14.4 Western blotting (Kyhse-Andersen, 1984)

2.14.4.1 Protein transfer-semidry blotting method

Buffer:

Anode buffer (AP1): 300 mM Tris (pH 10.4)

Anode buffer (AP2): 25 mM Tris (pH 10.4)

Cathode buffer (KP): 40 mM ϵ -aminocapron acid
25 mM Tris/HCl (pH 9.4); all three buffers contain 10% methanol and 0.05% SDS

Western blotting allows the transfer of proteins from a polyacrylamide gel onto a nitrocellulose membrane. In this work the semi-dry blotting method was used: One layer of Whatmann paper, soaked in AP1, was placed in the blotting chamber. Then two layers of Whatmann paper, nitrocellulose membrane and the gel, all soaked in AP2 were overlaid. Finally three layers of Whatmann paper soaked in KP-buffer were placed on top. The transfer was performed at 12 V for 30 minutes with a BioRad semidry blotting machine. Blotting efficiency was controlled with Ponceau S staining.

2.14.4.2 Protein transfer wet-blot method (tank transfer)

Wet blotting of proteins was performed using a hydrophobic PVDF (polyvinylidene fluoride) membrane (Millipore). The membrane is activated using methanol and the polyacrylamide gel is pre equilibrated with transfer buffer (72 g glycine and 15 g Tris dissolved in 5 L of water). The gel and the membrane were arranged in a pad of whatmann papers and kept in a tank with transfer buffer. The overnight transfer was done at 20V at 4°C.

2.14.4.3 Coomassie blue staining

Staining solution:

0.1% Coomassie-brilliant-blue R 250
50% ethanol
10% acetic acid

Destaining solution:

10% ethanol
7% acetic acid

Gels were stained for at least 15 minutes. Unbound Coomassie-blue was washed away with destaining solution.

2.14.4.4 Ponceau S staining

Staining solution:

2 gr Ponceau S (Sigma) solubilized in 100 ml 3% Trichloroacetic acid

Nitrocellulose membrane was incubated for 1 minute in Ponceau S and briefly washed with water. Bands of interest were marked and afterwards the membrane was destained in NCP.

2.14.4.5 Immunolabeling and detection of proteins on nitrocellulose membrane

Luminol:

2 ml 1 M Tris/HCl (pH 8.5)
200 μ l (0.25 M in DMSO) 3-aminonaphthylhydrazide
89 μ l (0.1 M in DMSO) p-cumaric acid
18 ml water
6.1 μ l 30% H₂O₂

After protein transfer, the nitrocellulose membranes (blots) were blocked with 5% milk powder in NCP for 1 hour. Blots were then incubated for one hour with primary antibodies. Before incubation (1hr) with the secondary peroxidase-conjugated antibody, the membrane was washed in NCP three times for 5 minutes. Unspecific bound antibodies were washed away with NCP for 20 minutes. Immunolabeling was visualized by adding the substrate (luminol) to the peroxidase-conjugated antibodies. This reaction was detected exposing the blots to an X-ray film for 5 sec to 30 min.

2.14.5 Immunofluorescence

Cells were grown on coverslips kept on six well plates. Nicely spread cells are used for fixing. Two ways of fixing were used. In the first way, the cells are incubated with 3% paraformaldehyde for 10 minutes at room temperature, washed 3 times with PBS and permeabilised with 0.5% Triton X-100 for 5 minutes. In the second method, the cells are fixed and permeabilised by incubating with cold methanol (-20⁰C) for 10 minutes. The fixed cells were then washed with three times with PBS for 5 minutes followed by three times washing with PBG. After washing, the cells were incubated with the primary antibody for one hour. After one hour, the cells were washed 6 times with PBG for 5 minutes. After the washing step the cells were incubated with the secondary antibody, which has a fluorescent tag for one hour. The cells were then washed again with 3 times PBG and 3 times with PBS and embedded in slides using gelvatol. For the control, the first antibody was replaced by incubation with PBG followed by incubation with the secondary antibody.

2.14.6 Small-scale GST fusion protein expression

Small-scale expression of fusion proteins was performed to check and standardize the expression of various recombinant clones before proceeding to the large-scale expression and purification. Single colonies (5-10) of recombinant cells were picked and grown overnight in 10 ml of LB medium containing ampicillin (100 µg/ml) at 37°C and 250 rpm. 5 ml of the overnight grown culture were inoculated into 45 ml of fresh LB medium containing ampicillin (100 µg/ml). The culture was then allowed to grow at 37°C till an OD of 0.5-0.6 measured at 600 nm was obtained. Now the induction of expression was initiated by adding IPTG. In order to standardize the conditions of maximum expression of the fusion protein, induction was performed with varying concentrations of IPTG (0.1 mM, 0.5 mM and 1.0 mM final concentration) at two different temperature conditions (30°C and 37°C). Samples of 1 ml were withdrawn at different hours of induction (0 hr, 1 hr, 2 hr, 3 hr, 4 hr and 5 hr), the cells were pelleted and resuspended in 100 µl of 1x SDS sample buffer. The samples were denatured by heating at 95°C for 5 min and 10 µl of each sample were resolved on a 12%

SDS-polyacrylamide gel.

2.14.7 Purification of GST-fusion proteins

To obtain large quantities of GST-fusion proteins, bacteria were grown in 1 liter cultures. The protein expression was induced with 1mM IPTG for 4 hrs and the bacteria were collected by centrifugation at 5000 x g for 10 minutes. The pellet was resuspended in 20 ml ice cold PBS and sonicated in ice for 30 sec or till the color turns gray. 10% Triton X-100 was added to a final concentration of 1% and the lysed cells were centrifuged at 10,000 rpm for 5 minutes at 4⁰C. The supernatant was mixed with 1 ml of Glutathione Sepharose 4B slurry and incubated gently by shaking (200 rpm on a rotary shaker) at room temperature for 30 minutes. The beads were centrifuged down at 500 x g for 5 minutes and afterwards washed several times with ice cold PBS. The washes were discarded and to the sedimented matrix, 1 ml of elution buffer (10 mM reduced glutathione in 50 mM TrisHCl, pH 8.0) was added. The beads were mixed gently and incubated for 10 min to elute the bound material from the matrix and centrifuged down at 500 x g for 5 minutes at 4⁰C. Elution steps were repeated two times more and the samples were analyzed by SDS-PAGE.

2.14.8 Affinity purification of polyclonal antibodies by blot method

TBS : 8 g NaCl, 0.2 g KCl and 3 g Tris/HCl in 1 liter, pH 7.2

Buffer I : 1% BSA, 0.05% Tween 20 in PBS

Buffer II : 0.1 M glycine, 0.5 M NaCl, 0.5% Tween 20, pH 2.6

The recombinant protein, which was used to produce the polyclonal antibody, was analysed by SDS-PAGE and the gel was afterwards transferred to a PVDF membrane. The membrane was stained with Ponceau S to confirm the transfer efficiency and the blot corresponding to the recombinant protein was cut out. The blot was then destained with TBS. The portion of the blot where the recombinant protein was immobilized, was blocked by incubating the blot for 2 hours in buffer I. 1 volume of serum is diluted with 4 volumes of TBS and incubated with the stripes at 4°C for 2 hours. The unbound antibody is washed with TBS 4x 5 minutes at 4°C. After washing, the antibodies bound to the recombinant protein on the membrane stripes are eluted with buffer II, 1 ml, 2x, 1.5 minutes at 4°C. The eluted antibody is neutralised with 100 µl of 1 M Tris (pH 8.0) immediately after elution. The antibody can be stabilised with 0.5% BSA.

2.14.9 Affinity purification by the CNBr method

The GST fusion protein GST-SpecII was purified as described above. Instead of eluting it from the beads using reduced glutathione, the GST bead pellet was resuspended in 1 ml PBS and 40 U of thrombin were added to 0.5 ml of glutathione bead volume. Thrombin

digestion will cut the GST fusion protein at a site in between the GST protein and the recombinant protein. Since the GST will stay bound to the beads, it can be removed by centrifugation at 500 x g for 5 minutes while the recombinant protein remains in the supernatant. Thrombin digestion was done for 4-16 hrs at 22-25°C. The eluted fraction was dialysed overnight against the coupling solution (0.1M NaHCO₃ buffer at pH 8.3 containing 0.5 M NaCl). 200 mg of cyanogen bromide activated Sepharose 4B (CNBr-activated Sepharose 4B, Amersham Bioscience) is resuspended for 15 min with cold 1 mM HCl to wash away all the additives. The beads were mixed with the coupling solution containing the ligand (SpecII) and incubated overnight at 4°C on a rotator. This incubation step will enable the ligand (recombinant protein SpecII) to bind to the CNBr beads. The excess ligand was washed away with 5 ml coupling buffer. To block any active groups in the beads, they were incubated with 1 M glycine for 1-2 hr. The beads were washed 3 times with buffers having an alternate pH value. The buffers are 0.1 M acetate buffer pH 4.0 with 0.5 M NaCl and 0.1 M TrisHCl, pH 8.0 with 0.5 M NaCl. The beads were then packed into a column and then the anti-sera against Enaptin-specII were passed through it continuously overnight at 4°C using a peristaltic pump. The column was washed with PBS several times and the antibody specific to SpecII was eluted using 0.2M glycine at pH 2.8. The eluted antibody was immediately neutralised with NaHCO₃ and the protein elution was measured with the spectrophotometer at 280nm.

2.14.10 Immunohistochemical staining of formalin-fixed paraffin-embedded sections

Solutions

Xylene

Ethanol

0.01 M Phosphate buffer saline (pH 7.4)

Solution of 1% gelatine in PBS (PBG)

10 mM Citric buffer, pH 6.0

The paraffin in the sections was removed by incubating the sections 3 times in xylene for 5 minutes. The sections were rehydrated in a series of incubations with 96% ethanol (2 times, 5 minutes), 80% ethanol, 70% ethanol, 50% ethanol and 30% ethanol one minute each, and finally rinsed with water. The slides are washed with freshly prepared citrate buffer pH 6.0 and boiled in a microwave at 300 Watts in the same buffer for 15 to 20 minutes. The sections are kept again in room temperature citrate buffer for about 20 minutes, rinsed in distilled water and then with PBS (3 times, 5 minutes). The sections were blocked for one hour using a PBG solution containing 5% horse serum. The sections are incubated with the

primary antibody for 24 hours at 4°C. Slides were washed 3 times for 4 minutes. Afterwards the sections were incubated with a secondary antibody conjugated to a fluorescent tag for one hour at room temperature. The sections are washed again as before and mounted in Gelvatol/DABCO (Sigma).

The staining of sections with the VECTOR MOM kit (VECTOR laboratories) was done according to the manufactures instructions.

2.14.11 Microscopy

Confocal images of immunolabelled specimens were obtained using the confocal laser scanning microscope TCS-SP (Leica) equipped with a 63x PL Fluotar 1.32 oil immersion objective. A 488-nm argon-ion laser for excitation of GFP fluorescence and a 568-nm krypton-ion laser for excitation of Cy3 or TRITC fluorescence were used. For simultaneous acquisition of GFP and Cy3 fluorescence, the green and red contributions to the emission signal were acquired separately using the appropriate wavelength settings for each photomultiplier. The images from green and red channels were independently attributed with colour codes and then superimposed using the accompanying software.

2.15 Disruption of the cytoskeleton using various drugs

Disruption of the actin cytoskeleton was done using Latrunculin B at a final concentration of 2.5 µM. The cells were treated with latrunculin B for different time limits, washed and fixed in 3% PFA.

To disrupt the microtubule cytoskeleton, colchicin was dissolved in methanol and used at a concentration of 12.5 µM. Cells were treated with colchicin for 90 min and coverslips were fixed at different time points using methanol.

2.16 Digitonin experiment

For the permeabilization experiments with digitonin, fixed cells (3% paraformaldehyde) were washed in ice-cold PBS and afterwards treated with 40 µg/ml digitonin (Sigma) in PBS for 5 minutes on ice.

2.17 Gene targeting protocols

2.17.1 Target vector construction

The pBluescript II SK⁺ vector was used as the backbone for the target vector construction. The Neomycin cassette was taken out from the pGK-NEO plasmid using the EcoRV and Sall and subcloned into the pBluescript vector. The 5'arm-Sall fw and 5'arm-

EcorV rv primers were used to amplify the 5'Enaptin arm (2 kb) of the vector from IB-10 ES cell genomic DNA using the Pfu DNA polymerase (Invitrogen). The amplified fragment was first cloned into pCR BluntII TOPO vector (Invitrogen) and removed using EcoRI and Sall and ligated into the pBluescript-Neo plasmid. The 3'arm (5 kb) of the knockout plasmid was amplified with the 3arm-NotI fw and 3arm-SacII rv primers using the Pfu DNA polymerase and the ES cell genomic DNA as a template. The fragment was first ligated into the pCR BluntII TOPO vector. The 3'arm was cut out from pCR BluntII TOPO with NotI and SacII and ligated into the pBluescript-5'arm-Neo construct using the same enzyme sites. All the constructs were sequenced and cloning directions and sequences were verified. The size of the complete target vector was 11.7 kb.

2.17.2 Probe generation

5'probe (1032)

The 305 bp 5' external probe (1032) was generated by PCR. The genomic ES cell DNA was used as template and the 5'probe fw and 5'probe rv primers in combination with the Advantage Taq polymerase (Clontech). The PCR-fragment was cloned into pGEM.T Easy. The 5' probe can be cut out with the EcoRI enzyme.

3'probe (1031)

The 3' external 470 bp probe was amplified from ES cell genomic DNA using the 3armprobe fw and 3armprobe rv set of primers. The PCR fragment was cloned into the pGEM.T Easy. The probe can be cut out from the plasmid using the EcoRI.

2.17.3 Embryonic stem cell culture

Media and materials

MEF media	DMEM (4500 mg/l glucose) (Sigma):	500 ml
	FCS	: 50 ml
	L-glutamine	: 6 ml
	Non-essential amino acids	: 6 ml
	Pen/Strep	: 6 ml
	Pyruvate	: 6 ml
ES cells media	DMEM knockout (GIBCO)	: 500 ml
	Knockout SR (GIBCO)	: 90 ml
	L-glutamine	: 6 ml
	Non-essential amino-acids	: 6 ml
	Pen/Strep	: 10 ml

Pyruvate	:	6 ml
ESGRO (Murine LIF, 10^7 U/ml, Chemicon)	:	50 μ l
β -mercaptoethanol (Sigma)	:	6 μ l

Selection media	:	ES cell media and 400 μ g/ml of G418
Freezing media	:	ES cell media, 30% FCS and 20% DMSO
Gelatin (2%) (Sigma)	:	Final concentration 0.1% (w/v) in sterile PBS
Mitomycin C (Sigma)	:	Mitomycin dissolved in sterile PBS (400 μ g/ml)
10X Trypsin (0.5%)(GIBCO)	:	Used at 2x dilution
Trypsin Inhibitor (Sigma)	:	Dissolved in sterile PBS at a concentration of 5mg/ml and used with 1:10 dilution with 2x trypsin

2.17.4 MEF cell culture and Mitomycin treatment

ES cells were grown on feeder cells called mouse embryonic fibroblasts (MEF), which are inactivated by the treatment with mitomycin C. MEFs are primary cells isolated from transgenic neomycin mouse which are resistant to G418 selection. MEFs were grown in normal cell culture plates for normal proliferation, but grown on 0.1% gelatin treated cell culture plates (NUNC) when we required to plate the ES cells on them. Once the MEFs were confluent, they were inactivated by the addition of 150 μ l of mitomycin C (400 μ g/ml) for 2 hours. Mitomycin will arrest the cell division, so there will not be any further growth of the cells. After 2hrs, cells were washed thoroughly with PBS to get rid of all the mitomycin C, trypsinised and plated into gelatin coated cell culture plates.

2.17.8 ES cell culture

ES cells are cultured normally on mitotically inactive embryonic feeder cells (MEF). MEF cells should be mitomycin C treated and plated on gelatinised plates, one day in advance of any ES cell manipulation. Confluent MEFs should be washed with PBS and supplied with ES cell media at least two hours before the plating of ES cells. Frozen ES cells were thawed quickly by placing a vial in a water bath at 37⁰C and the content of the vial added to 10 ml ES media in a 15 ml falkon tube. The cells were centrifuged down at 500 rpm for 5 min and resuspended in ES cell medium and plated on feeder cells. ES cell medium should be changed every 24 hrs.

2.17.9 ES cell transfection

For the transfection experiment 100 µg of the targeting vector was linearised by digestion with the Sall enzyme. The linearisation of the plasmid was confirmed on an agarose gel. The DNA was then extracted with phenol:chloroform (1:1) and then with chloroform alone. The DNA was precipitated with 96% ethanol, pelleted at 12,000 rpm for 10 min. The pellet was washed with 96% ethanol and with 76% ethanol. The air dried DNA was dissolved in millipore water at a concentration of 1 µg/µl.

ES cells were cultured on a 10 cm plate and on the day of transfection, the ES cell media were changed 2 hr prior to the transfection. After 2 hrs, the cells were washed with PBS and then 0.1% trypsin was added for 4 min till the cells detached from the plate. Cell clumps were disintegrated by slowly pipetting up and down several times and then centrifuged down at 500 x rpm in a Beckman CS 6R centrifuge. The cells were washed with PBS and resuspended in 350 µl of ES cell media and then transferred into a 4 mm transfection cuvette (BioRad). 50 µl of the target vector DNA was added, mixed properly and kept on ice for 10 minutes. The transfection was done at 250V and 500 µF and typically a time constant between 8-12 was obtained. Cells were again kept in ice for 5 min and then plated into 4 mitomycin treated MEF 10 cm plates.

2.17.10 Antibiotic selection and picking of ES cell clones

Selection of ES cells resistant to neomycin was started after 48 hrs of transfection. For IB10 ES cells, 350 µg/ml (total) of G418 was used for selection and for R1 cells we used 400 µg/ml of G418. Usually on the third day the untransfected cells will start to die. The selection is continued for another 7 days when small ES cell colonies will start to appear. When the colonies grew large enough with firm boundaries, the colonies were picked using a 20 µl pipette under a light microscope with a 2.5X objective. On the day of picking, several 24 well plates plated with MEF were kept ready. Individual colonies were picked into a 96 well round bottom plate along with 7 µl medium and 50 µl of 2X trypsin was added and kept for 10 min at 37°C. The trypsin was later neutralised with 20 µl of trypsin inhibitor and mixed with 50 µl of ES cell media. The cells were pipetted up and down several times slowly to break the cell clumps. The individual colonies were then plated on to the 24 well plate kept ready with feeder cells.

2.17.11 Splitting and freezing ES cells

When the cells in the 24 well plates were grown enough, they were trypsinised and resuspended in 500 µl medium. 250 µl of the resuspended cells were plated into another 24 well feeder cell plate for growing the cells further for genomic DNA isolation and 250 µl

were pipetted into a cryotube, and the cells were frozen. 250 μ l of ice-cold 2x ES cell freezing media were added to the cells and they were immediately transferred to the -80°C freezer in a thermocool box. The cells kept for genomic DNA isolation were further grown and harvested when the plates became confluent.

2.17.13 Genomic DNA isolation

TNES 50 mM Tris (pH: 7.4)
 100 mM EDTA (pH: 8.0)
 400 mM NaCl
 0.5% SDS

6 M NaCl

Proteinase K : 20 mg/ml

Trypsinised ES cells were mixed with 500 μ l of TNES buffer and 10 μ l of 20 mg/ml proteinase K solution and incubated at 55°C overnight in a shaking incubator. 150 μ l of a saturated (5 M) NaCl solution was added the next day to salt out the proteins. The sample was centrifuged at high speed for 5 minutes in order to pellet the precipitated proteins. The genomic DNA in the supernatant was precipitated by 96% ethanol and the pellet was washed with 70% ethanol. The pellet was dried and the genomic DNA was resuspended in 50 μ l of 10 mM Tris/HCl, pH 7.4.

2.17.14 Southern blotting (Southern, 1975)

Southern blotting is the transfer of DNA fragments from an electrophoresis gel to a membrane. After immobilization, the DNA was subjected to hybridization analysis to identify the bands containing DNA complementary to the radioactively labeled probe. In this work the alkaline transfer on a nylon membrane (Zeta-probe genomic GT tested membrane from Bio-rad) was performed according to the manufacturer's instructions. Genomic DNA from ES cell clones was digested with EcoRI and resolved in a 0.7% agarose in TAE buffer gel. DNA is depurinated by keeping the gel in 0.25 M HCl for 10 minutes, and then neutralised and denatured in 0.4 M NaOH for 10 minutes. For the transfer of the DNA to the membrane, it was kept on top of two layers of Whatmann 3MM paper, having contact to a reservoir of 0.4 M NaOH, which is used as the transfer buffer. After overlaying the gel with Zeta-probe GT Genomic Tested Blotting membrane that had been wetted with the transfer buffer, three wet Whatmann 3MM paper and a thick stack of paper towels were kept above the membrane without air bubbles. A weight of 200 gm was kept above it and the transfer was continued for about 18 hours. After washing the membrane in 2% SSC, it was air-dried and processed for hybridization.

2.17.15 Labeling of DNA probes and hybridization

Prehybridisation solution : 0.25 M sodium phosphate (pH 7.2) and 7% SDS
and hybridization solution

Wash buffer : 20 mM sodium phosphate (pH7.2) and 5% or 1% SDS
0.5% sodium phosphate,pH 7.2

Stock A : 0.5 M NaH₂PO₄.H₂O

Stock B : 0.5 M Na₂HPO₄.7H₂O

316 ml of Stock A and 684 ml of Stock B are combined to make 0.5% sodium phosphate, pH 7.2

DNA probes used for radioactive labeling were obtained by removing the the 5' probe and 3' probe from the pGEM.T Easy vector with EcoRI. The insert of interest was extracted from the gel. About 25 ng DNA were mixed with 10 µl random hexanucleotide primers and then denatured by heating for 5 minutes at 92°C. To this solution, we added 5 µl α-³²P-dATP (50 µCi) and 2 U Klenow-Enzyme and the reaction was incubated for 30 min at 37°C. Unincorporated nucleotides were separated from the probe by passing through a column packed with Sephadex G-50. Before hybridisation, labeled probes were denatured at 100°C for 5 minutes. The membrane was prehybridised with prehybridisation buffer for 30 minutes at 65°C. The labeled probes were added to the membrane in 10 ml of hybridisation buffer and hybridised overnight at 65°C.

Results

3 Results

3.1 Sequence analysis of Enaptin

3.1.1 cDNA cloning of the longest isoform of Enaptin

Enaptin was first identified as a protein consisting of 1431 amino acids (Enaptin-165, AAN03487) while searching for novel actin-binding proteins with an α -actinin type actin binding domain (Braune, 2001). The actin-binding domain of Enaptin-165 comprises two calponin homology domains at its N-terminal end followed by a coiled coil rod domain similar to the spectrin repeats found in the dystrophin protein. Enaptin-165 has around 30% homology with NUANCE, another novel giant actin binding protein of around 800 kDa, shown to be localising to the nuclear envelope (Zhen *et al.*, 2002). NUANCE is located on the human chromosome 14q23 locus whereas Enaptin is mapped to human chromosome 6q25. In contrast to Enaptin-165, the C-terminal part of NUANCE contains a single transmembrane domain, which is necessary for proper nuclear membrane targeting. A protein called Syne-1 (Apel *et al.*, 2000) was identified downstream of the Enaptin-165 locus on chromosome 6, which displays strong sequence homology to the C-terminus of NUANCE. Considering that NUANCE is a giant 800 kDa protein and the fact that its N- and C-termini are homologous to the Enaptin and syne-1 proteins respectively, we speculated that the Enaptin-165 and Syne-1 proteins may be shorter isoforms of a giant NUANCE-like protein, containing both an ABD and a transmembrane domain in a single protein. With this hypothesis in mind, we started to amplify and assemble the full-length Enaptin cDNA.

We searched the EST database of human chromosome 6 and found out several EST clones and some assembled sets of open reading frames in this region. All the EST clones obtained were assembled using the gene assembly programme of the Wisconsin package. There were several large gaps between these assembled fragments. We designed therefore primers such that we could get overlapping fragments of the cDNA of Enaptin. Extensive searches for EST clones were done in the human chromosome region 6q24-25 (between 152990K-152470K region) covering 500 kb. cDNA clones such as AK094094, AL13682, AB033088 (KIAA1262), and AK057959 were obtained from the searches which represent short open reading fragments possibly belonging to the long isoforms of the Enaptin locus. Small EST clones such as AW297921, AB051543, AL713682, BF964526, BI033837, AK056122, BF376488 etc were also obtained in-between these fragments in the specified genomic region. Based on the available EST sequence information, we constructed several primers in order to generate overlapping cDNAs. The successful amplification of such PCR fragments would be an indication for a possible continuous open reading frame.

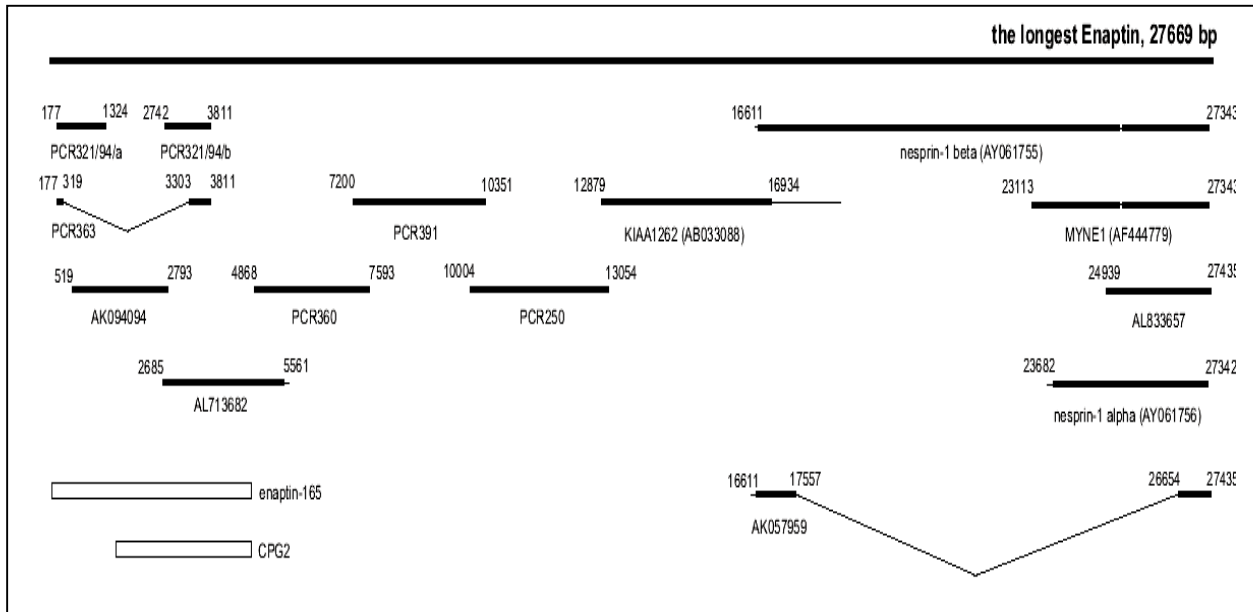


Figure 3.1: cDNA assembly of Enaptin. Schematic representation assembling a 27,669 bp human Enaptin cDNA from overlapping known Enaptin isoforms Nesprin-1a, Nesprin-1b, Myne-1, CPG2 and several other published sequences, RT- and RACE-PCR generated clones using human cerebellum mRNA as template. The location of a small mouse Enaptin N-terminal isoform, previously known as CPG2 and the newly characterised mouse Enaptin-165 is included. Horizontal thick lines represent overlapping PCR-fragments, cDNAs, and published Enaptin isoform sequences. The names and the positions (in nucleotides) along the assembled full length Enaptin cDNA are indicated. Thin horizontal lines indicate parts of clones where the sequence is not identical to the large Enaptin isoform.

We selected human cerebellum mRNA as template for RT-PCR for the cDNA generation because in a multiple tissue expression array used to investigate the mRNA expression pattern of Enaptin, we observed a high expression of Enaptin in cerebellum. We also considered the fact that the short form of Enaptin-165 was amplified from mouse brain cDNA. RT-PCRs were done using degenerate primers and gene specific primers. The quality of the cDNA obtained was verified using the housekeeper G3PDH gene specific primers. We tried to amplify long fragments of about 10 kb size, but were largely unsuccessful. Later, several primers were designed (listed in materials and methods) so that overlapping fragments were produced approximately of the size of 3 kb each, designated in the figure 3.1 as PCR363, PCR360, PCR391, PCR250, PCR321/94a, PCR321/94b. These fragments were assembled using the gene assembly programme of the Wisconsin package. All of these fragments were amplified using the Clontech cDNA amplification kit and cloned into the pGEmteasy vector (Promega) and sequenced first by using vector primers and later using specific primers from the obtained sequence. The full-length cDNA we assembled was 27,669-bp in length (Submitted as AF535142).

3.1.2 Organisation of the *Enaptin* gene

The human *Enaptin* gene is located in the chromosome 6q23.1-q25.3 region, spanning 515 kbs and is encoded by 147 exons. A schematic representation of the intron and exon organisation of *Enaptin* is represented in Figure 3.2.

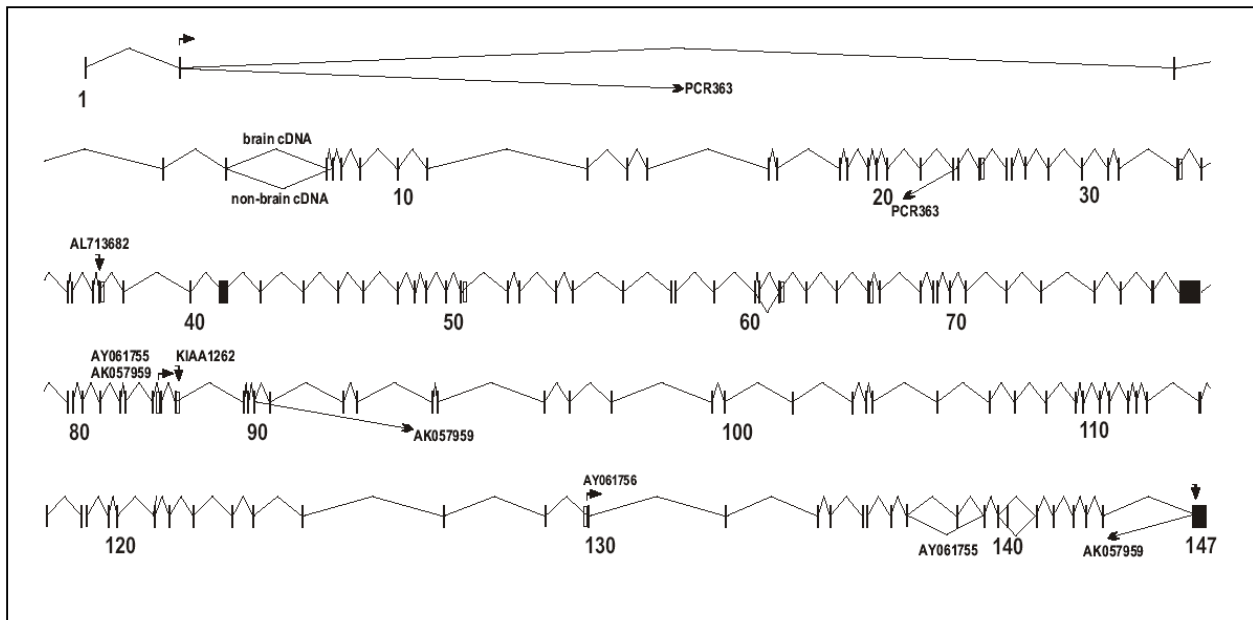


Figure 3.2: Exon-intron organisation of the human *Enaptin* gene. Numbered vertical bars denote exons, lines represent introns. Predicted translational start codons of the various splice variants are denoted by horizontal arrows and labelled with their corresponding accession number. The diagram is drawn to scale.

The intron exon sequence was determined by aligning the obtained cDNA sequence with the genomic sequence. Potential start codons of the various isoforms are shown as horizontal arrows. Vertical arrows represent possible stop codons in the splice variants. Accession numbers of the cDNAs are represented in the figure along with splicing of PCR363.

3.1.3 Domain analysis of *Enaptin*

The deduced amino acid sequence of the longest *Enaptin* cDNA open reading frame consists of 8749 amino acids (Fig. 3.3) with a calculated molecular weight of 1014 kDa and a theoretical pI of 5.37. The SMART programme (www.expasy.ch) analysis predicts 3 major structural domains in the *Enaptin* amino acid sequence, an N-terminal ABD, a C-terminal transmembrane domain and 50 spectrin repeats in the middle of the molecule.

programme. The ABD of Enaptin shares 48% identity to the ABD of NUANCE, 36% with utrophin, 38% with dystrophin, 34% with α -actinin and 38% with β -spectrin. Enaptin and NUANCE have a unique 44 amino acid stretch separating the two calponin homology domains (Figure 3.4) rich in serine residues.

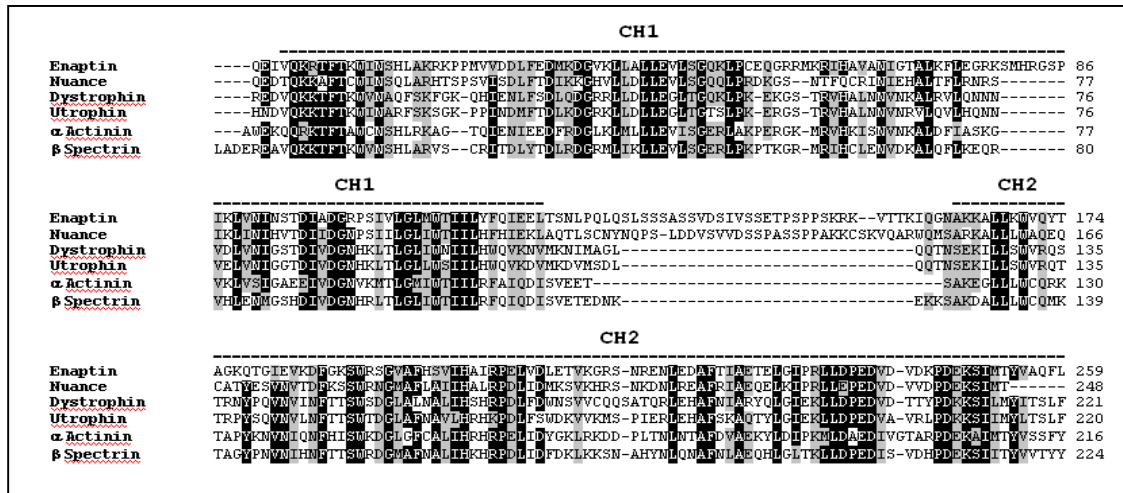


Figure 3.4: Multiple sequence alignment of the actin-binding domains of various members of the α -actinin superfamily. The sequences of Enaptin (accession no. AAN03486, residues 27-292), NUANCE (NP_055995, 32-276), human utrophin (P46939, 32-255), human dystrophin (AAA53189, 16-240), α -actinin-1 (AAH03576, 32-252) and β -spectrin-1 (AAA60580, 55-276) are compared. A stretch of amino acids with several serines separates the CH1 and CH2 in Enaptin and NUANCE in contrast to the conventional type ABDs of utrophin, dystrophin, α -actinin and β -spectrin. The ClustalX programme was used to align the sequences, the alignment was further edited using the Bioedit software. Identical amino acids were shaded black and similar amino acids were shaded gray.

In order to establish the evolutionary relationship between the ABD of Enaptin and the ABDs of other sequence related proteins, a phylogram was generated using the ClustalX alignment programme (Figure 3.5). The analysis included the ABD sequences of *C. elegans* ANC-1, Enaptin, NUANCE, utrophin, dystrophin, ACF-7, α -actinin, β -spectrin, *Drosophila melanogaster* MSP-300 and *Dictyostelium discoideum* interaptin. The phylogenetic analysis showed that Enaptin and NUANCE form a distinct group of proteins and that they are closer to dystrophin and utrophin than other members of the α -actinin superfamily.

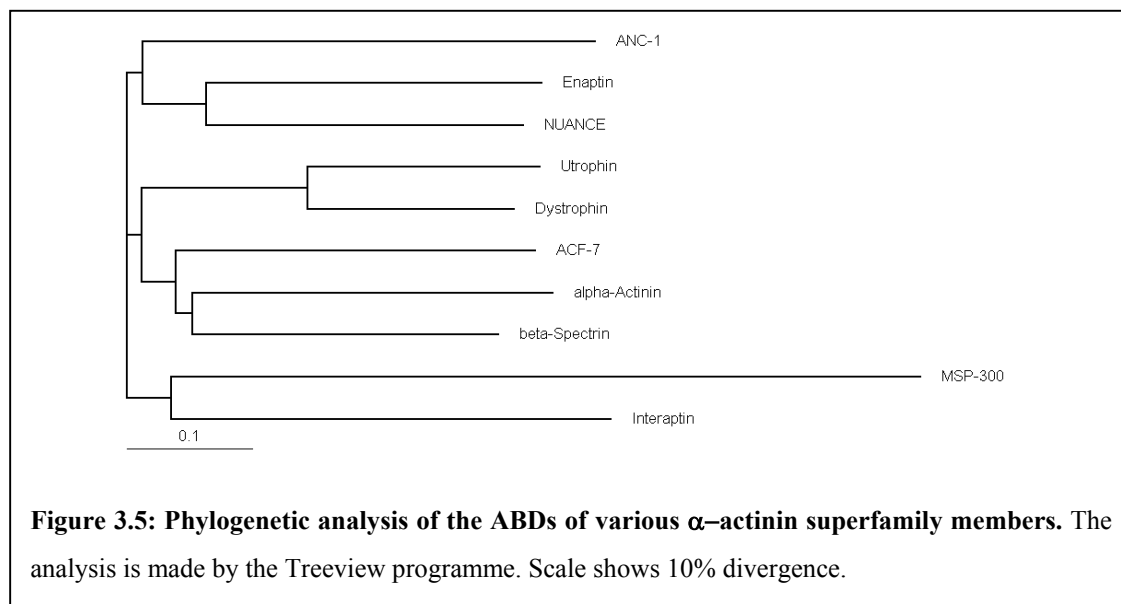


Figure 3.5: Phylogenetic analysis of the ABDs of various α -actinin superfamily members. The analysis is made by the Treeview programme. Scale shows 10% divergence.

Enaptin has a central helical rod domain in which several coiled coils can be predicted using the Multicoil algorithm (Fig. 3.6). The analysis predicts 30 coiled-coils, several coiled-coils have a high probability of forming dimeric and trimeric stranded coiled coils. Around 50 spectrin like repeats were predicted in the rod domain by the SMART programme. In addition to that, seven nuclear localization signals belonging to three different classes were predicted using the PSORT II Prediction programme (<http://psort.nibb.ac.jp/form2.html>). Two NLS predicted were of the pat4 pattern (amino acids 43-49, 4086-4089), another two are of the pat7 (amino acids 171-180, 3214-3218) and three were bipartite nuclear localisation signals (30-49, 7907-7921, 8122-8138). PSORT uses the following two rules to detect it: four residue pattern (called 'pat4') composed of four basic amino acids (K or R), or composed of three basic amino acids (K or R) and either H or P; the other (called 'pat7') is a pattern starting with P and followed within three residues by a basic segment containing three K/R residues out of four (Hicks and Raikhel, 1995). Two segments that are similar to leuzine zipper like repeats (2609-2630, 4754-4775) were also predicted using the 2ZIP programme (web based tool for predicting leuzine zippers). A serine rich region was also detected in between the last spectrin repeat and the transmembrane domains.

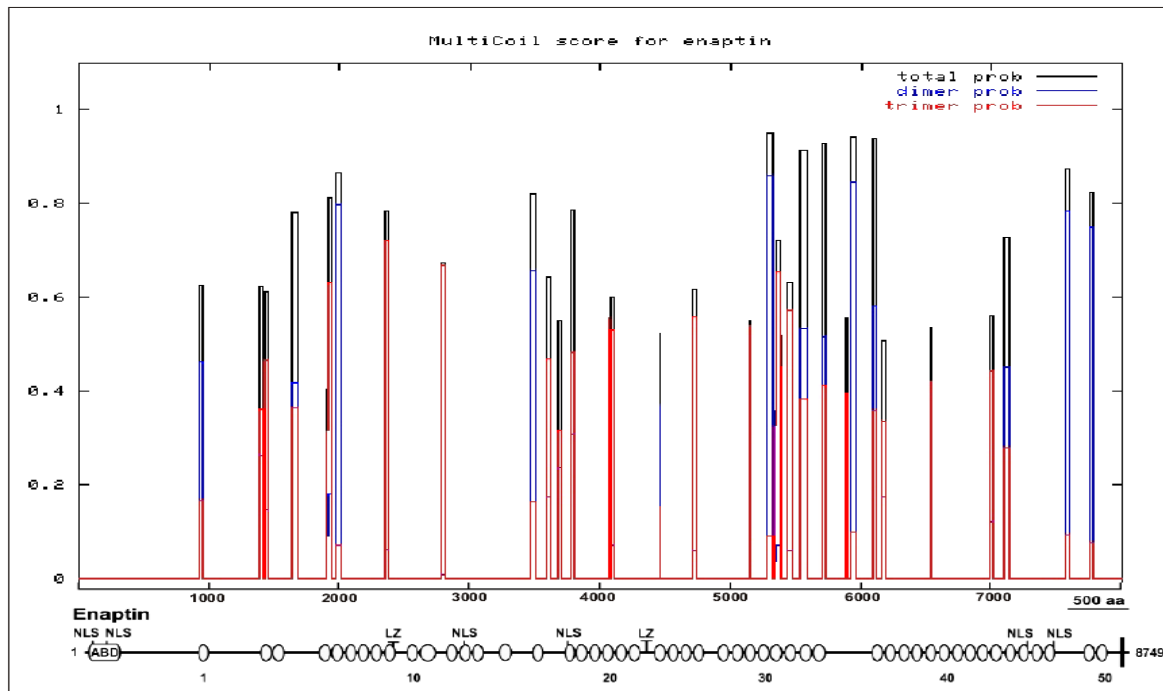


Figure 3.6: Structural features of Enaptin. The ABD is represented by an empty box; 50 spectrin repeats with considerable homology to dystrophin are shown as ovals; and the transmembrane domain is indicated by a black bar. The positions of nuclear localization signals and leucine zippers are indicated. Coiled-coil regions were predicted by the MultiCoil programme (Wolf *et al.*, 1997). Blue and red lines mark the location of predicted dimeric or trimeric coiled-coils, respectively.

The C-terminus of Enaptin displays high homology to NUANCE and to the *Drosophila* klarsicht protein (Mosley-Bishop *et al.*, 1999). All these proteins harbor a stretch of conserved sequences, which include a 23 amino acids long leucine-rich region composed of hydrophobic amino acids (8694-8717). This stretch forms a transmembrane region and a highly conserved C-terminal tail (Figure 3.7). The general structure of the transmembrane domain classifies Enaptin as a type-II integral membrane protein (Kutay *et al.*, 1993), which would contain a long cytoplasmic or nucleoplasmic domain with a C-terminal hydrophobic transmembrane domain (Figure 3.8).

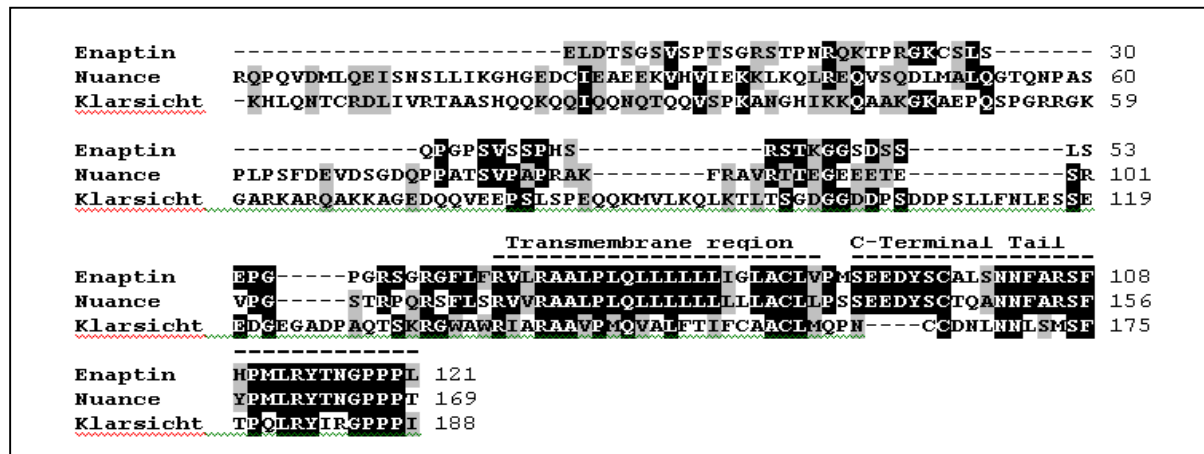


Figure 3.7: Enaptin and NUANCE contain a klarsicht like domain. The C-terminal amino acids of Enaptin (AAN03486), NUANCE (NP_055995), and *D. melanogaster* Klarsicht protein (NM_079149) were aligned using the ClustalX alignment programme. Sequences were edited using the Bioedit software. Identical amino acids are highlighted with black and similar amino acids are shaded gray. Predicted regions in the sequences are shown as transmembrane region and C-terminal tail region.

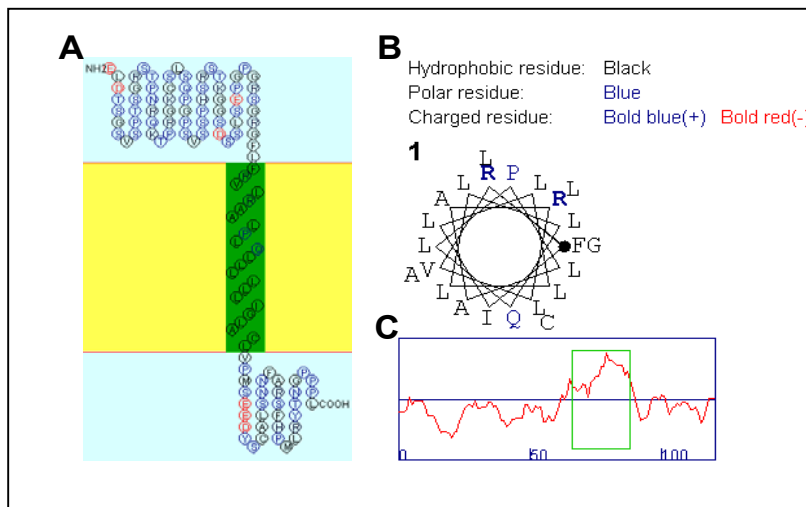
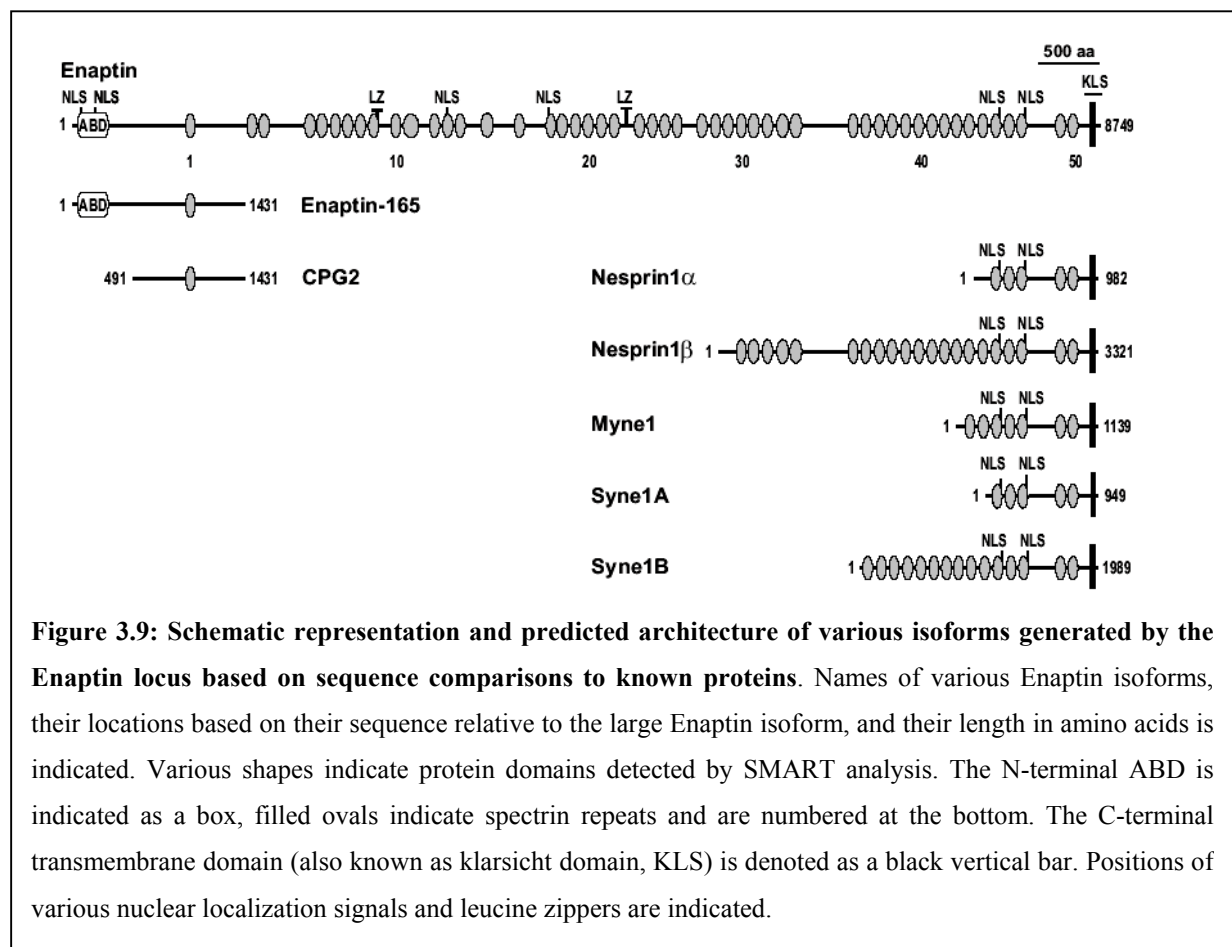


Figure 3.8: Prediction of a transmembrane domain at the C-terminal end of Enaptin. (A) A transmembrane helix is predicted by a web based prediction tool SOSUI, (www.sosui.proteome.bio.tuat.ac.jp). A schematic representation of the putative transmembrane domain is shown. (B) Helical wheel diagram showing the hydrophobic (black) and polar residues (blue) in the transmembrane helix. (C) Hydrophathy plots of the C-terminus of Enaptin showing hydrophobic amino acids, which form the transmembrane helix.

3.1.4 Isoforms of Enaptin

Several isoforms of Enaptin were identified which are produced by alternative splicing of the *Enaptin* gene. These isoforms vary in their expression pattern, domain architecture and sizes. Figure 3.9 is a schematic diagram that summarises various known Enaptin isoforms. The longest isoform is termed Enaptin and is composed of 8749 amino acids harbouring both an N-terminal ABD and a C-terminal transmembrane domain, which are separated by several spectrin-repeats. A shorter isoform labelled as Enaptin-165 with a molecular mass of 165 kDa



contains also an ABD and a single spectrin repeat containing region. Another N-terminal isoform derived from the Enaptin locus is CPG2 (Nedivi *et al.*, 1996), which lacks both an ABD and a transmembrane domain. Several C-terminal splicing forms named as nesprin-1 α , nesprin-1 β , myne-1, syne-1A, syne-1B (Zhang Q *et al.*, 2001, Mislow *et al.*, 2002b., 2002, Apel *et al.*, 2000) contain the C-terminal transmembrane domain with varying numbers of spectrin like repeats and lack completely an ABD.

3.2 Examination of Enaptin's tissue distribution by northern blot analysis

3.2.1 Tissue distribution of Enaptin

To analyse the transcription pattern of human *Enaptin*, a human multiple tissue expression array (MTE, Clontech) was hybridised with probes corresponding to the ABD (bases from 318–951 in AF535142) and to the C-terminus of Enaptin (23398–23832). The MTE array is a positively charged nylon membrane to which poly A⁺ RNAs from different human tissues and cancer cell lines have been immobilised in separate dots, along with several controls. The poly A⁺ RNAs were normalised to the mRNA expression levels of eight different 'house keeping genes'. Table 1 gives the relative expression levels of Enaptin transcripts with both the probes in comparison with NUANCE (Zhen *et al.*, 2002).

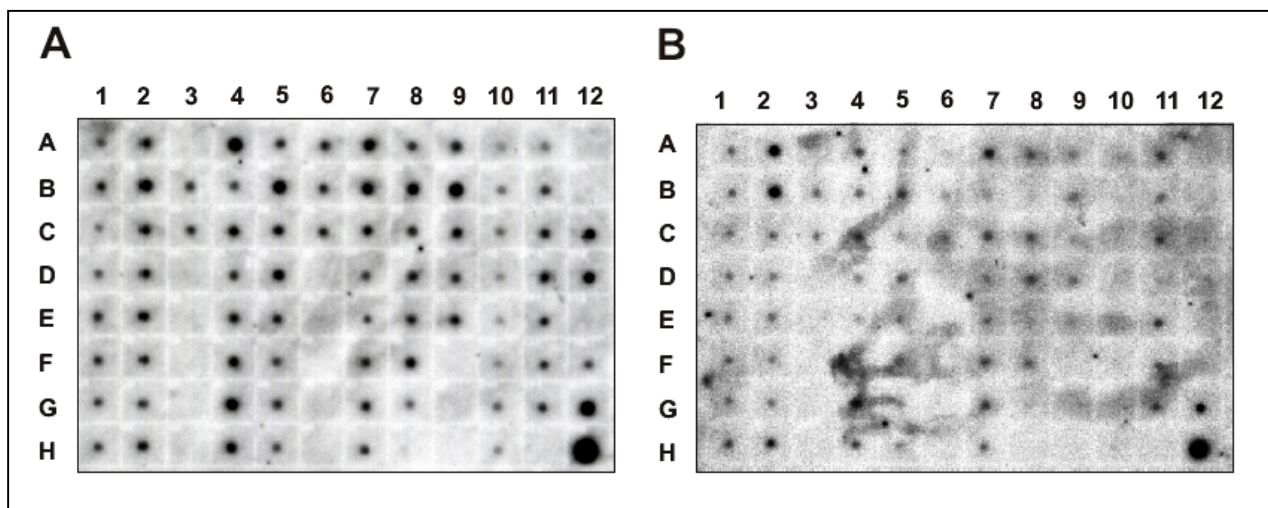


Figure 3.10: Tissue distribution of the Enaptin transcripts using a human multiple tissue and cell line expression array. (A) Northern dot-blot hybridized against Enaptin's ABD (nucleotides 318–951 of human Enaptin cDNA). (B) The same blot was stripped and probed against a C-terminal Enaptin probe (nucleotides 23398–23832). The identification of the positions on the grid is given in Table 1.

The signals obtained with both the C-terminal probe and N-terminal probe showed detectable levels of Enaptin in most of the tissues (Fig. 3.10). Interestingly, different patterns of expression were obtained using both the probes, which underline the existence of alternative splicing forms that display a different level of abundance in various tissues. Comparison of the expression patterns of Enaptin with NUANCE (Zhen *et al.*, 2002) revealed that Enaptin dominates in brain, muscle, heart and pancreas while NUANCE is expressed preferentially in liver, salivary gland, uterus, prostate and lymphatic organs. Enaptin and NUANCE both have a high expression in kidney, stomach and placenta. Cerebellum shows relatively elevated expression in comparison with other parts of the brain.

Table 1. Tissue distribution of the Enaptin transcript using a human multiple tissue expression array.

Tissue type	Expression level			Position on the grid ^a
	Enaptin ABD probe	Enaptin C terminal probe	NUANCE ¹	
Neurological				
whole brain	+	+	tr	1A
cerebral cortex	++	+	tr	1B
frontal lobe	tr	tr	tr	1C
parietal lobe	tr	tr	+	1D
occipital lobe	+	tr	+	1E
temporal lobe	+	tr	+	1F
paracentral gyrus of cerebral cortex	+	tr	tr	1G
pons	+	+	tr	1H
cerebellum, left	++	+++	tr	2A
cerebellum, right	++++	++++	tr	2B
corpus callosum	++	tr	++	2C
amygdala	++	tr	tr	2D
caudate nucleus	++	tr	+	2E
hippocampus	+	tr	+	2F
medulla oblongata	tr	tr	+	2G
putamen	+	++	+	2H
nucleus accumbens	+	tr	tr	3B
thalamus	+	tr	+	3C
Muscle and heart				
aorta	+	+	+	4B
heart	+++++	++	+	4A
atrium, left	+++	+	+	4C
atrium, right	+	tr	+	4D
ventricle, left	++	tr	+	4E
ventricle, right	+++	tr	++	4F
interventricular septum	++++	++	++	4G
apex of the heart	+++	+	++	4H
skeletal muscle	++++	tr	+	7B
Gastro-intestinal				
esophagus	+	tr	tr	5A
stomach	++++	++	++++	5B
duodenum	+++	tr	+++	5C
jejunum	+++	+	++	5D
ileum	+	tr	+	5E
ileocecum	tr	tr	++	5F
appendix	tr	tr	++	5G
colon, ascending	tr	tr	+	5H
colon, transverse	++	tr	+	6A
colon, descending	++	+	+	6B
rectum	+	tr	+	6C
liver	++	tr	++++	9A
pancreas	+++++	+	+	9B
salivary gland	+	tr	+++	9E
Genito-urinary				
kidney	++++	++++	+++++	7A
bladder	+	+	+	8C
uterus	+	+	+	8D
prostate	+	-	++++	8E
testis	++	+	+++	8F
ovary	tr	-	+++	8G
Lymphoid and hematopoietic				
spleen	++	+++	++++	7C
thymus	+	tr	+	7D
lymph node	+	+	+++	7F
bone marrow	+	+	+	7G
peripheral blood leukocyte	tr	tr	++++	7E
Pulmonary				
trachea	+	tr	+++	7H
lung	++	+	++	8A
Other				
adrenal gland	++	tr	++	9C
thyroid gland	++	tr	++++	9D
mammary gland	++	tr	++	9F
Cell lines				
leukemia, HL-60	tr	-	tr	10A
HeLa S3	tr	-	tr	10B

leukemia, K-562	tr	-	tr	10C
leukemia, MOLT-4	tr	-	tr	10D
Burkitt's lymphoma, Raji	tr	-	tr	10E
Burkitt's lymphoma, Daudi	tr	-	++	10F
colorectal adenocarcinoma, SW480	tr	-	+	10G
lung carcinoma, A549	tr	-	tr	10H
Fetal and placenta				
placenta	++++	tr	++++	8B
fetal brain	tr	++	tr	11A
fetal heart	+	tr	+	11B
fetal kidney	+	+	++++	11C
fetal liver	++	-	+	11D
fetal spleen	+	+	+	11E
fetal thymus	+	tr	+	11F
fetal lung	+	tr	+	11G
Control RNA				
yeast total RNA	-	-		12 A
yeast tRNA	-	-		12 B
<i>E. coli</i> rRNA	+	-		12 C
<i>E. coli</i> DNA	+	-		12 D
Poly r(A)	-	-		12 E
human Cot-1 DNA	+	-		12 F
human DNA 100ng	++	+		12 G
human DNA 500ng	+++++	+++++		12 H

^a Grid references to Fig. 3.10

tr – traceable amounts

1 Taken from reference (Zhen *et al.*, 2002)

3.2.2 Northern blot analysis of Enaptin

In order to verify the results obtained from the MTE arrays and find out the various transcripts of Enaptin, northern blot analysis was performed using two different probes, one probe spanning the ABD region equivalent to nucleotides 1878-2557 of human Enaptin cDNA, and another one spanning the CPG2 region (nucleotides 4127-4768). Total RNA from mouse tissues such as brain, heart and skeletal muscle were isolated using the Trizol reagent (Invitrogen) according to the manufacturer's instructions. The RNA was separated in 0.7% formaldehyde agarose gels and blotted onto a zeta-probe membrane (Bio-Rad). For the hybridisation, riboprobes were generated from the corresponding fragments cloned into suitable vectors (see materials and methods). A transcript of >14 kb is observed consistently with both probes in the brain and skeletal muscle samples (Figure 3.11). An additional transcript of 5.5 kb was detected only in brain with the ABD and the CPG2 probe. Smaller transcripts of this size could not be detected in the skeletal and cardiac muscle RNAs using the ABD probe. The CPG2 probe detects in addition to the 14 kb band a 10 kb band in brain, which is visible after prolonged exposure. A 6.5 kb band was consistently observed in both skeletal and cardiac muscle tissues with the CPG2 probe. Such transcripts could not be detected in the muscle tissues using the ABD probe. In our Northern blot analysis however, we were unable to detect the expected 27 kb transcript, which could be corresponding to the longest Enaptin isoform. This may be attributed to the technical difficulties or the absence of the particular transcript in the analysed tissues.

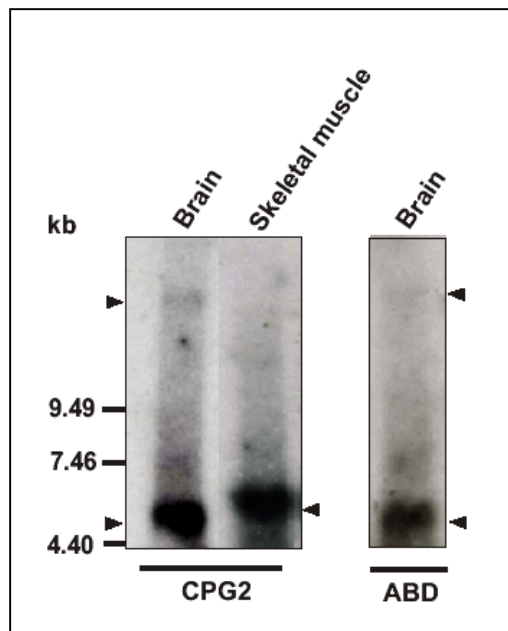


Figure 3.11: Northern blot analysis of RNA from brain, skeletal and cardiac muscle tissues. The blots were hybridised against two specific radiolabelled riboprobes designed against the ABD (equivalent to nucleotides 1878–2557 of human Enaptin cDNA) and CPG2 (equivalent to nucleotides 4127–4768). Arrowheads indicate major transcripts detected.

3.3 Western blot analysis of Enaptin

3.3.1 Western blots with an ABD Enaptin antibody of different tissue lysates

For investigation of Enaptin at the protein level, a polyclonal antibody was raised against the ABD of Enaptin in rabbits. A 6xHIS-ABD-enaptin construct (aa. 2-293) is expressed in PQE30 vector and the protein is purified using a Ni-NTA column. The recombinant protein was used to immunize rabbits and the antiserum was tested for the specificity of the antibody (Braune, 2001; Padmakumar, 2004). The antisera were later purified by affinity chromatography.

The purified ABD Enaptin antibody was used for western blot analysis with various tissue lysates. Mouse tissues were dissected and the protein lysates were prepared as described in Materials and methods. The proteins were resolved in a 5% polyacrylamide gel (Figure 3.12A) or 3%-15% gradient gel (Figure 3.12B) and blotted overnight onto a PVDF membrane (Millipore) by wet blotting. The blots were blocked and incubated with purified Enaptin ABD antibody at the dilution of 1:1000. A secondary anti-rabbit antibody conjugated with peroxidase was used to make a chemiluminescence reaction. In all the tissues tested except kidney, a protein of enormous size of approximately 400 kDa was detected, which may correspond to the 14 kb band transcript that was detected in the northern blot analysis. In brain, heart, kidney, stomach and small intestine a band of 270 kDa was also observed. In addition to that in brain, lung and kidney, a smaller 260 kDa band was detected. Only in the brain sample we could detect a 165 kDa protein (Enaptin-165), which most probably corresponds to the 5.5 kb band detected in the northern blots. The detected proteins in the immunoblot analysis were however significantly lower than the predicted 1000 kDa protein.

Further analysis will be needed to determine the domain organization of the Enaptin isoforms detected in our immunoblot assays.

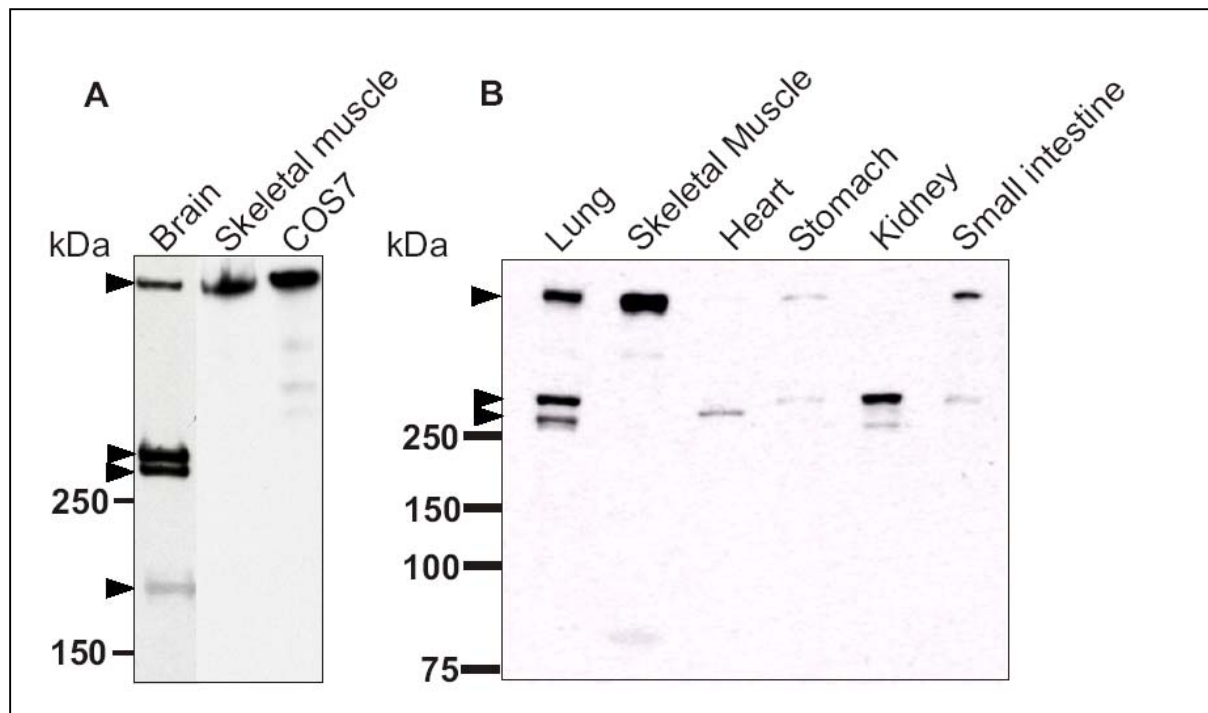
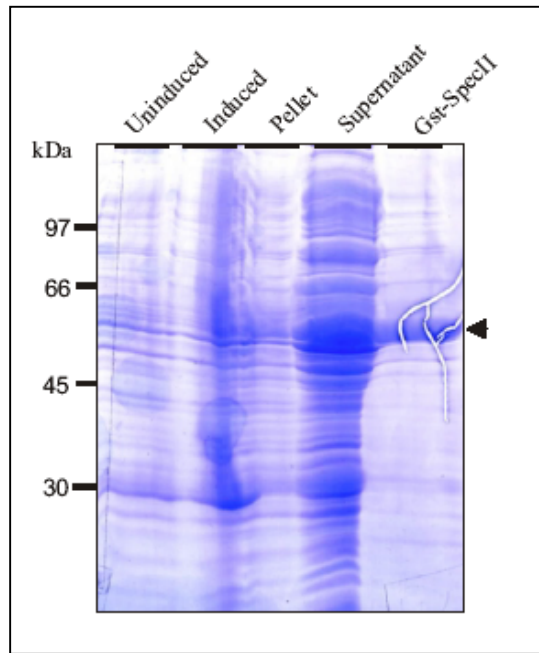


Figure 3.12: Western blot analysis of brain, muscle, lung, heart, stomach, kidney, small intestine and COS7 cell homogenates. The polyclonal Enaptin antibody directed against the ABD recognizes high molecular weight proteins (approximately 400 kDa) in all samples. Additional bands were detected in the brain sample, migrating as 165 and 260 kDa proteins (arrowheads). A, 5% SDS page. B, 3 %-15% gradient gel.

3.3.1 Expression and purification of GST-SpecII

The data presented so far suggest that Enaptin is of enormous complexity and therefore, for a more accurate biochemical and cell biological characterization, additional reagents and tools were required. In order to study the function of the C-terminal isoforms of Enaptin in more detail, an antibody against the C-terminus of human Enaptin was generated. A GST fusion protein (GST-SpecII) was made comprising the last two-spectrin repeats (aa 8394-8608) of human Enaptin using the pGEX4T1 vector (Amersham Bioscience). The Enaptin fragment alone has a theoretical pI of 5.33 and a calculated molecular weight of 25.7 kDa. The molecular weight of the fusion protein was calculated as 51.7 kDa. The GST-SpecII plasmid was transformed into the DH5 α *E. coli* strain and its expression was induced for 4 hrs with 1mM IPTG. The bacteria were collected, lysed and the fusion protein was retrieved from the supernatant using GST beads (Figure 3.13). The recombinant protein migrates on SDS-PAGE with the expected size of 51 kDa. The beads with the GST-SpecII fusion protein were



washed and eluted by reduced glutathione and send for the immunization of rabbit animals (Pineda Antikörper Services).

Figure 3.13: Expression of GST-SpectII protein. The GST-SpectII plasmid was transformed into *E. coli* DH5 α cells. Protein expression was induced by 1 mM IPTG for 4 hrs. Cells were collected, lysed, centrifuged and the supernatant was treated with GST beads for 30 min at room temperature. The beads were collected by centrifugation. An aliquot from uninduced cells, induced cells, pellet, supernatant and GST beads bound to GST-SpectII were resolved on a 12 % SDS polyacrylamide gel and stained with Coomassie blue. Arrowhead indicates the position of the recombinant protein.

3.3.2 Generation and purification of the Enaptin polyclonal antibody

Rabbit serum after 90 days of immunization was tested for the specificity of the antibody produced. For the immunoblot analysis, we used the recombinant GST-SpectII, GST protein as a control, COS7 cell lysate transfected with the GFP-DN construct described in section 3.8, which has the peptide sequence identical to the one used for antibody production, COS7 lysate transfected with GFP alone and nontransfected COS7 cell lysate. The cell lysates and recombinant proteins were resolved on a 12% SDS polyacrylamide gel and blotted onto a nitrocellulose membrane and incubated with the rabbit serum (from the 90th day after immunization) at a 1:1000 dilution (Figure 3.14 A). A secondary anti-rabbit antibody tagged with peroxidase was used and a chemiluminescence reaction was performed for detecting the proteins. The antibody detected the 51 kDa GST-fusion protein along with the GST protein. The bands of lower sizes may be the degradation product of the GST-SpectII fusion protein. The specific detection of the 67 kDa GFP-DN fusion protein in the COS7 lysates confirmed the presence of antibodies specific for the SpecII polypeptide sequence in addition to antibodies that are directed against the GST protein. The antibody did not cross-react with any another protein, which is obvious from the absence of signals in the COS7 lysate and GFP lysate lanes. The presence of the GFP fusion protein is confirmed with a monoclonal antibody for GFP in a similar blot (Figure 3.14 B). Since Enaptin and NUANCE display high homology to each other, we examined the crossreactivity of the serum (Figure 3.14 C) against NUANCE. COS7 cells were transfected with a GFP-NUANCE fusion protein (GFP-

dnNUANCE), which is homologous to the Enaptin region used for generating the antibodies. As shown in Figure 3.14 C, our SpecII antibody detects only the GFP-DN Enaptin fusion and thus proves the specificity of Enaptin-SpecII antibodies towards Enaptin.

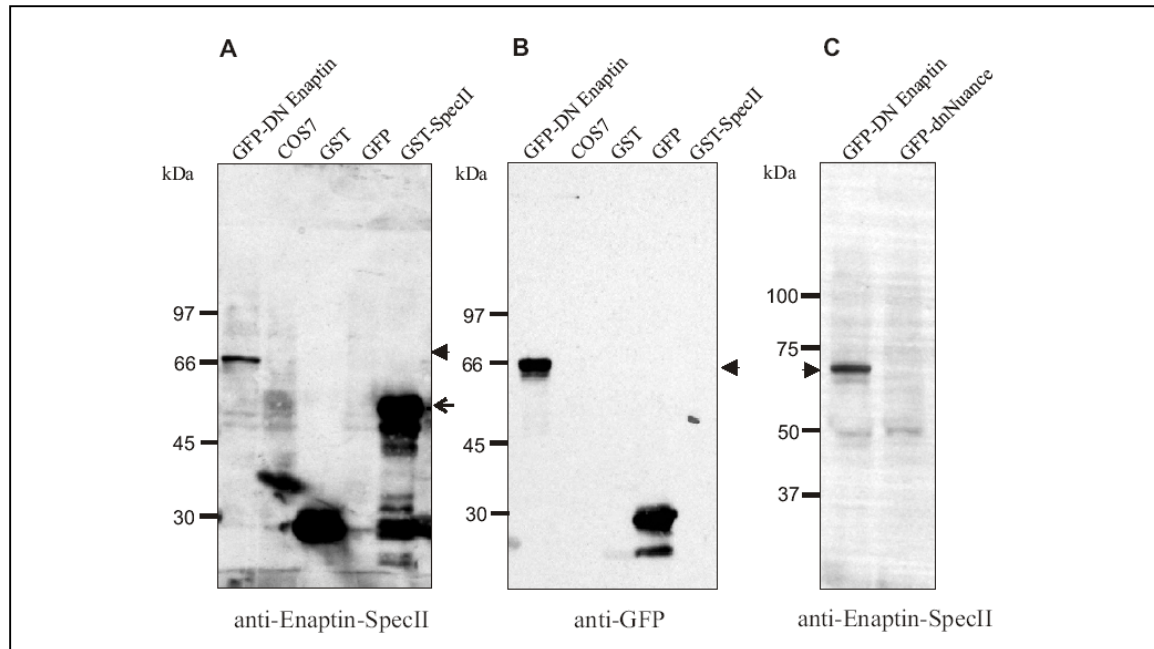


Figure 3.14: Characterization of the C-terminus specific Enaptin antibody (Enaptin SpecII). Cell lysates were prepared from COS7 cells expressing GFP-DN Enaptin, GFP, GFP-dnNUANCE and untransfected COS7 cells. GST and GST-SpecII were purified from *E. coli*. Purified proteins and cell lysates were resolved on a 12% SDS polyacrylamide gel and transferred to a nitrocellulose membrane by semidry blotting. In (A), the blot was incubated with serum from a rabbit after 90 days of immunization with GST-SpecII. A secondary anti rabbit antibody conjugated with peroxidase was used against it and a chemiluminescence reaction was done to detect the proteins. (B) Control blot probed with a GFP specific monoclonal antibody to check the presence of GFP proteins. (C), Specificity test of the Enaptin antibody. Lysates from cells expressing GFP-DN and GFP-dnNUANCE were run on a 12% SDS page gel and immobilized on a membrane by semidry blotting. The blot is probed with the SpecII polyclonal serum and later with an anti-rabbit peroxidase tagged secondary antibody. Signals were developed with a chemiluminescence reaction. Arrowheads indicate the GFP-DN protein and the points to GST-SpecII.

Since the polyclonal antisera detected also GST, we purified the antibody using affinity chromatography. GST-SpecII was digested using thrombin, dialyzed and coupled to CNBr-activated sepharose. Using this Enaptin- SpecII antibody, we could detect a protein of approximately 400 kDa size (data not shown). The purified antibodies were used for immunofluorescence as well as immunohistological studies.

3.4 Subcellular localization of Enaptin using the SpecII antibody

In order to investigate the subcellular localization of Enaptin, various cell lines were fixed in methanol and processed for indirect immunofluorescence. The Enaptin-SpecII antibody was used at a 1:50 dilution along with antibodies recognizing nuclear lamina proteins like laminin and emerin and images were taken using confocal microscopy. In primary human fibroblasts, a prominent Enaptin staining around the nucleus and in the nucleoplasm was observed (Figure 3.15). To examine the nuclear staining of Enaptin in more detail, we co-stained the fibroblasts with laminin A/C (Figure 3.15 G) and emerin (Figure 3.15 C) specific antibodies, which are two inner nuclear membrane proteins. A clear co-localization of these proteins with Enaptin around the nuclear envelope was noticeable (arrow in panel B), suggesting that Enaptin is a component of the nuclear envelope. As mentioned earlier Enaptin is a rather complex gene that codes for various splicing variants. The nucleoplasmic staining (arrow head, panel F) which was visible in our immunofluorescence studies may be therefore attributed to various splicing forms lacking the C-terminal transmembrane domain.

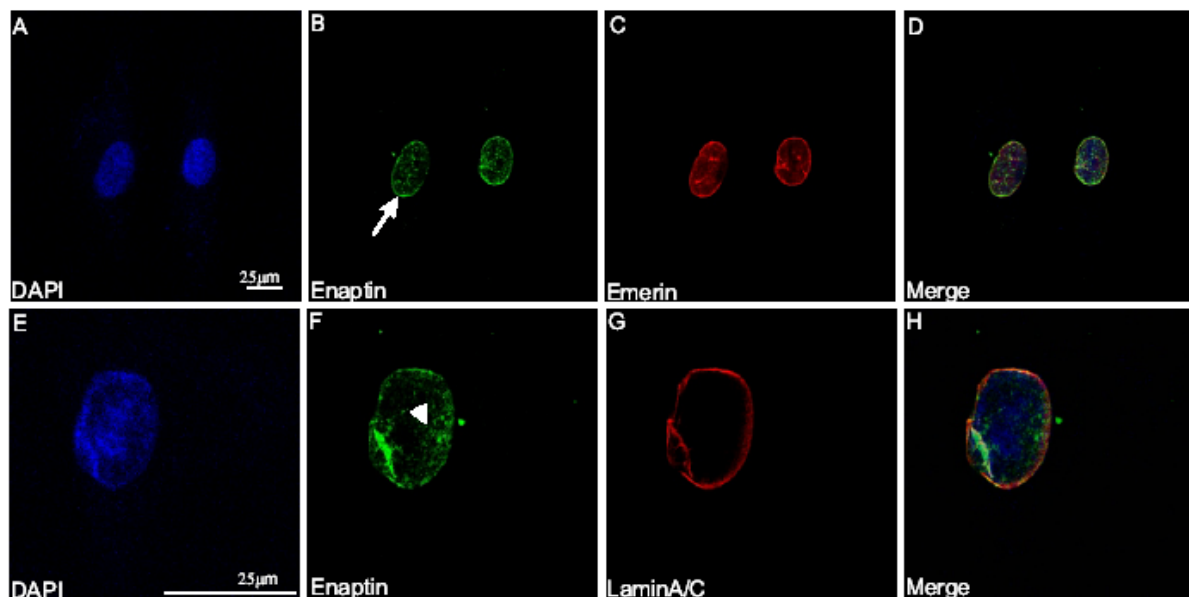


Figure 3.15: Enaptin localizes to the nuclear envelope in human fibroblasts. Human fibroblast cells were fixed with methanol and incubated with monoclonal antibodies for emerin or laminin A/C (Jol2) and the C-terminal Enaptin-SpecII Abs. Secondary antibodies such as anti-mouse Cy3 and anti-rabbit FITC were used. Images were taken using the confocal microscope. The arrow indicates nuclear envelope staining and the arrowhead nucleoplasmic staining.

While Enaptin is present at the nuclear membrane in human fibroblasts, the pattern of its distribution differs in various cell types. In Figure 3.16, Enaptin-SpecII staining of methanol fixed C3H/10T1/2 mouse fibroblasts, MB50 (undifferentiated myoblasts), N2A (undifferentiated neuroblastoma cells) are shown. In mouse fibroblasts, we observed a nuclear membrane staining in addition to a strong cytoplasmic staining. In undifferentiated myoblasts

however, the Enaptin protein is present in the nucleoplasm in addition to localization at the nuclear membrane. Neuroblastoma cells displayed a different staining pattern. We never observed a nuclear membrane staining; instead, a strong nucleoplasmic and cytoplasmic staining was observable. Until now, very little is known about the expression profile of the various Enaptin variants. However one can envision the presence of distinct isoforms in various tissues that differ in their domain architecture in order to accomplish and fulfill the structural and biological needs of each individual tissue.

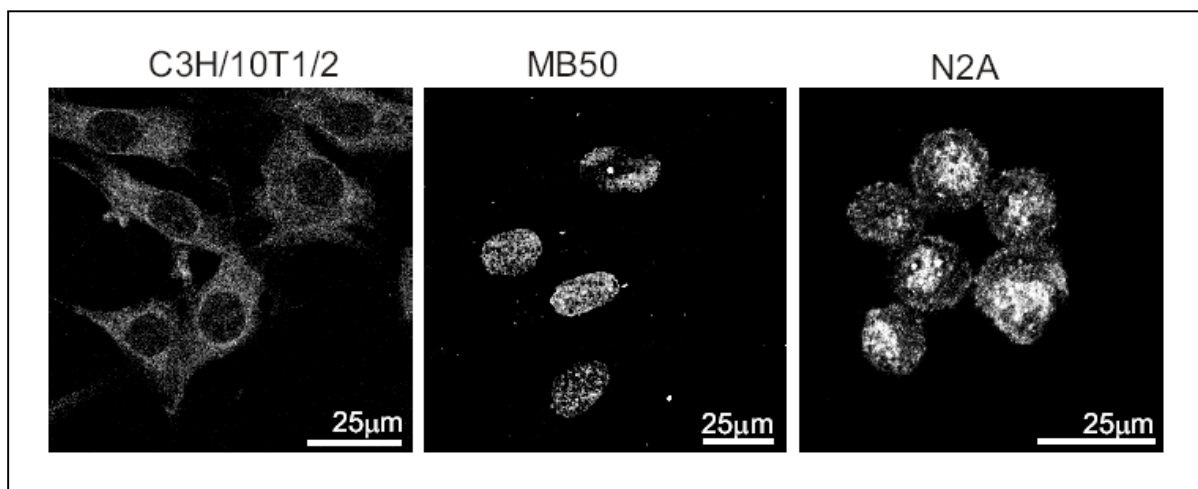


Figure 3.16: Subcellular localization of Enaptin in various cell types. C3H/10T1/2 cells (mouse fibroblasts), MB50 (human primary myoblasts) and N2A (neuroblastoma cell line). Cells were fixed with methanol and stained with rabbit primary Enaptin-SpecII antibody and secondary anti-rabbit-FITC antibody. Images were obtained using the confocal microscope.

3.5 Enaptin is a component of the outer nuclear membrane

The nuclear envelope is composed of two membranes, the outer nuclear membrane, which is continuous with the endoplasmic reticulum, and the inner nuclear membrane. In order to examine the exact topology of Enaptin at the nuclear envelope and to find out whether it is localized in the inner nuclear membrane or outer nuclear membrane, we performed permeabilisation studies. Human fibroblast cells were permeabilized with 40 µg/ml digitonin for 5 minutes or with 0.5% Triton X-100 separately. Triton X-100 permeabilises both the plasma membrane and also the nuclear membrane, while a short incubation with digitonin permeabilises only the plasma membrane and leaves the nuclear membrane intact. Thus the entry of antibodies only to the cytoplasm and not to the nucleoplasm allows the identification of cytoplasmic and outer nuclear membrane components. Human fibroblast cells were fixed with paraformaldehyde and treated with digitonin at different time intervals to optimize the permeabilisation conditions. For controlling the permeabilisation procedure,

we co-immunostained the cells with lamin A/C, which are intermediate filament proteins present close to inner nuclear membrane and also located in the inner aspect of the nucleus. After 5 minutes of digitonin treatment, we could observe strong nuclear envelope staining of the Enaptin antibody but no lamin A/C staining was observed (Figure 3.17 E-H). Triton X-100 permeabilised cells however, displayed strong nuclear membrane staining of both Enaptin and lamin A/C (Figure 3.17 A-D). This experiment demonstrates that Enaptin is a structural component of the outer nuclear membrane. However a presence of Enaptin inside the nucleus cannot be ruled out. Further studies will be necessary including electron microscopy investigations to study the exact location of Enaptin. Interestingly, it has been reported that Nesprin, a C-terminal isoform of Enaptin is present in the inner nuclear membrane (Zhang *et al.*, 2001) using the immunogold-labeling method. Taken together, Enaptin may therefore localize to both inner and outer nuclear membranes.

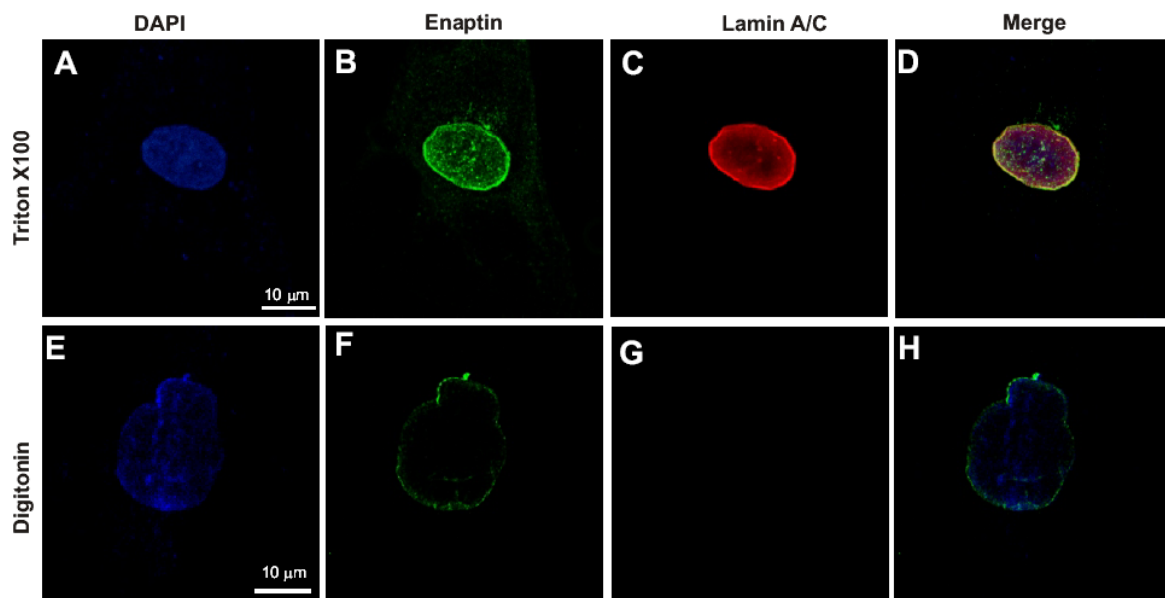


Figure 3.17: Permeabilisation of fibroblast cells with Triton X-100 and digitonin. Human fibroblast cells were fixed with 3% paraformaldehyde and permeabilised with the detergents such as Triton X-100 and digitonin for 5 min. A-D show a Triton X-100 permeabilised cell and panels E-H show a cell after digitonin treatment. Images were taken by confocal microscopy.

3.6 Nuclear membrane localization of Enaptin is not affected by drugs disrupting microfilament and microtubule cytoskeleton

Since Enaptin is an actin binding protein with a functional ABD at its N-terminus (Braune, 2001), we wanted to investigate whether the localization of Enaptin in the nuclear envelope depends upon the actin cytoskeleton. To explore this aspect, we disrupted the actin cytoskeleton using latrunculin B, a microfilament-disrupting drug that binds to G-actin and

prevent its polymerization (Wakatsuki *et al.*, 2001). Human fibroblast cells were treated with the drug at 2.5 μM concentration for 10 min, fixed with 3% PFA and permeabilised with Triton X-100 for 5 min. The polyclonal Enaptin-specII antibody was used for staining Enaptin followed by a FITC conjugated anti-rabbit secondary antibody. Phalloidin was used to visualize the F-actin cytoskeleton and DAPI to stain nuclei. We observed that even after the disruption of the actin cytoskeleton the nuclear envelope staining of Enaptin was retained which suggests that the nuclear envelope staining is not dependent upon an intact actin cytoskeleton (Figure 3.18). The shape of the nucleus is deformed after the treatment of latrunculin B (arrowheads in Figure 3.18 F). The interaction of Enaptin with nuclear lamina proteins and the presence of its C-terminal transmembrane domain may be sufficient for the proper nuclear envelope localization of Enaptin.

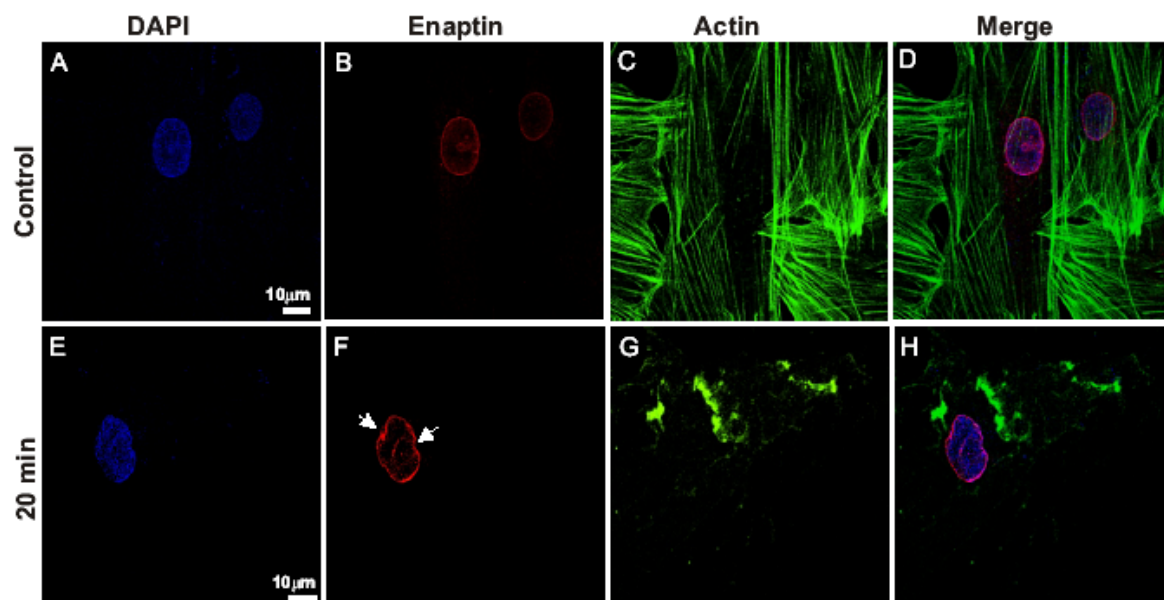


Figure 3.18: Latrunculin treatment of human fibroblast cells. Panels A-D show untreated (control) human fibroblast cells and panels E-H, display cells after a 20 min treatment with latrunculin B (2.5 μM). Cells were fixed in 3% PFA and incubated with the Enaptin-SpecII antibody and anti-rabbit FITC conjugated secondary antibody. F-actin is stained with phalloidin coupled to TRITC. Nuclei are stained with DAPI. Images were prepared with confocal microscope. Arrows indicate the deformation in the shape of the nucleus.

The C-terminus of Enaptin is highly homologous to the *Drosophila melanogaster* klarsicht protein (Figure 3.7). Since klarsicht is required for connecting the MTOC (MicroTubule Organizing Center) to the nucleus (Patterson *et al.*, 2004) and also for vesicle transport along the microtubule network (Jackle and Jahn, 1998), we were interested to examine whether microtubules have a profound role in the localization of Enaptin. In order to address this question we disrupted the microtubule cytoskeleton using colchicin at 12.5 μM concentration. Cells were fixed with methanol after 45 minutes of colchicin treatment,

followed by incubation with Enaptin-SpecII antibodies and anti- β -tubulin specific antibodies. In contrast to untreated cells (Figure 3.18 A-D), which display a nicely organized cytoskeleton (Figure 3.18 C), the colchicin treated cells (Figure 3.18 E-H) contain a disrupted microtubule cytoskeleton (Figure 3.18 G) where very few filaments can be seen in the cytoplasm. The nuclear Enaptin pattern however remained unaffected (Figure 3.18 F, H).

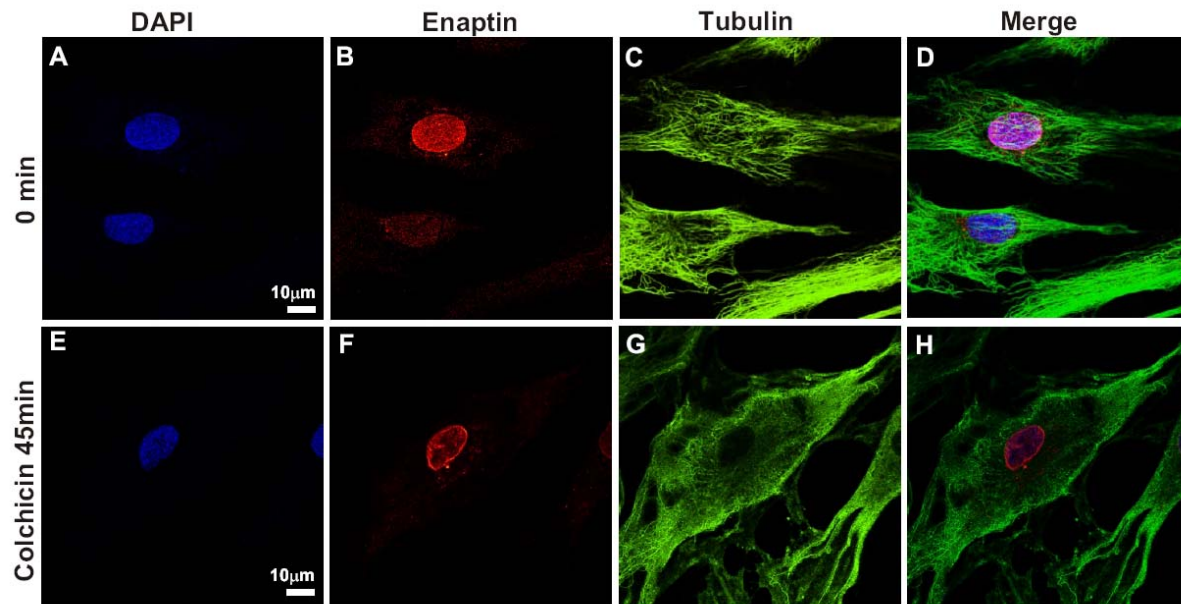


Figure 3.19: Colchicin treatment of human fibroblast cells. Human fibroblast cells were treated with colchicin (12.5 μ M) for 45 min and were fixed afterwards with methanol. The cover slips were incubated with the rabbit polyclonal Enaptin-SpecII antibody and anti- β -tubulin mouse monoclonal antibodies. Anti-rabbit-FITC and anti-mouse-Cy3 were used as secondary antibodies. Images were prepared by confocal microscopy.

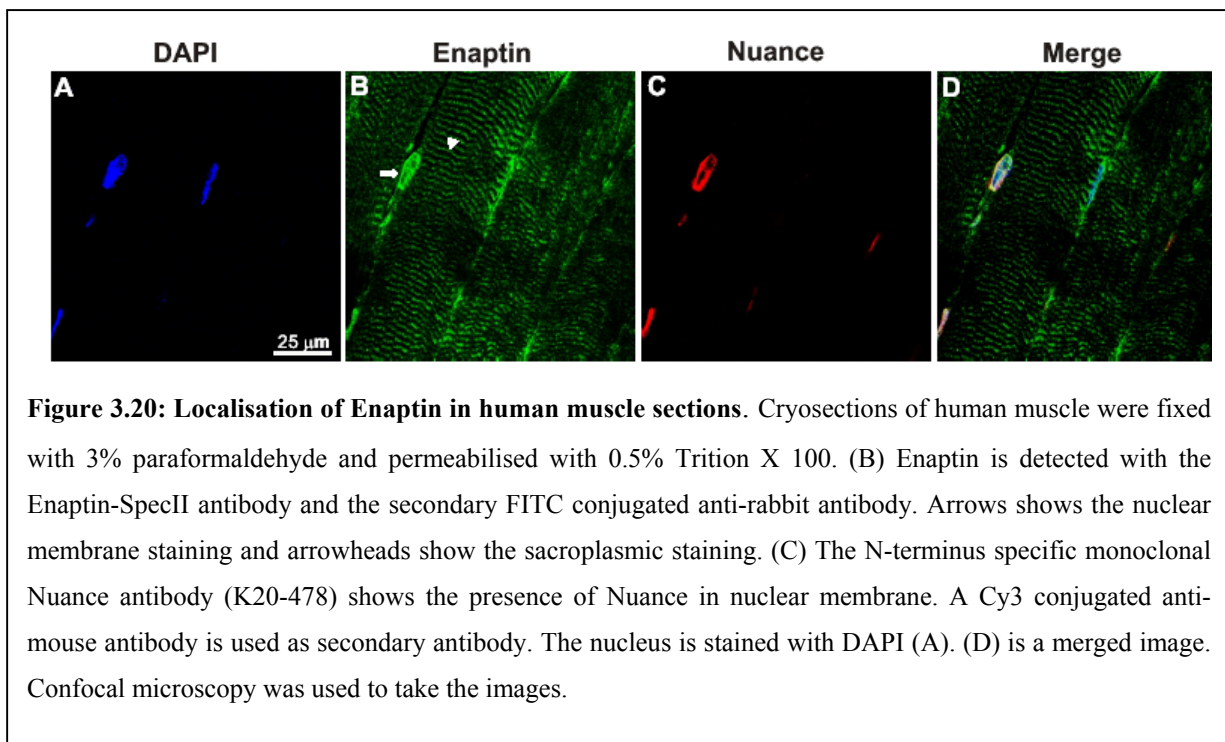
3.7 Tissue expression of Enaptin

From our northern blots, we concluded that Enaptin is present in most of the tissues which were examined however with varying levels of expression. Brain and skeletal muscle were actually two tissues where the highest level of expression for Enaptin were obtained. In order to gain more insight into the expression profile of Enaptin and to verify the data obtained from the northern and dot blot analysis we performed immunohistochemical studies on skeletal muscle and brain tissue sections.

3.7.1 Expression of Enaptin in muscle

From our northern and western blot analysis, we found that Enaptin is strongly expressed in skeletal muscle. So it was interesting to investigate the localization of Enaptin in skeletal muscle. Mutations in nuclear membrane proteins like lamin A/C and emerin were recently postulated to be involved in muscular dystrophies like EDMD (Bonne G *et al.*,

1999). The exact pathological mechanisms of the muscular dystrophic phenotype caused by mutations in these ubiquitously expressed proteins are largely unknown (Hutchison et al., 2001). It has been postulated that lamin A/C or emerin can interact with skeletal muscle specific isoforms of interacting proteins resulting in the skeletal muscle disease phenotypes. The interaction of Enaptin with lamin A/C and emerin and the homology of Enaptin to dystrophin make it thus a potential candidate to carry out such a function. Previously we have used an N-terminal antibody to Enaptin and observed a partial colocalisation of Enaptin with desmin (Padmakumar, 2004). Since Enaptin has many isoforms, their distribution may vary in different tissues and even in the same tissue. Therefore an investigation using the Enaptin-SpecII antibodies, which detect the C-terminal isoforms, was very crucial. Frozen human muscle sections were obtained from the Uniklinik, Bonn, and from the Friedrich-Baur Institute of the LMU, Munich. An investigation regarding the NUANCE expression and distribution in skeletal muscle was also included in our studies. We used the N-terminus specific NUANCE monoclonal antibody (K20-478) for the staining. Microscopical analysis using the confocal microscope demonstrated that both Enaptin and NUANCE stained the nuclear membrane. In the case of Enaptin however, a sarcoplasmic staining was also observed. This sarcoplasmic staining pattern was similar to data we obtained using the N-terminal polyclonal Enaptin antibody. In contrast to Enaptin, NUANCE was found only in nuclei.



3.7.2 Expression of Enaptin in cerebrum, cerebellum and hippocampus

To investigate the localization of Enaptin in different parts of the brain, we used paraffin embedded sagittal sections from 20 days old mice. The sections were deparaffinated with xylol and hydrated with varying percentage of ethanol, boiled in citrate buffer for

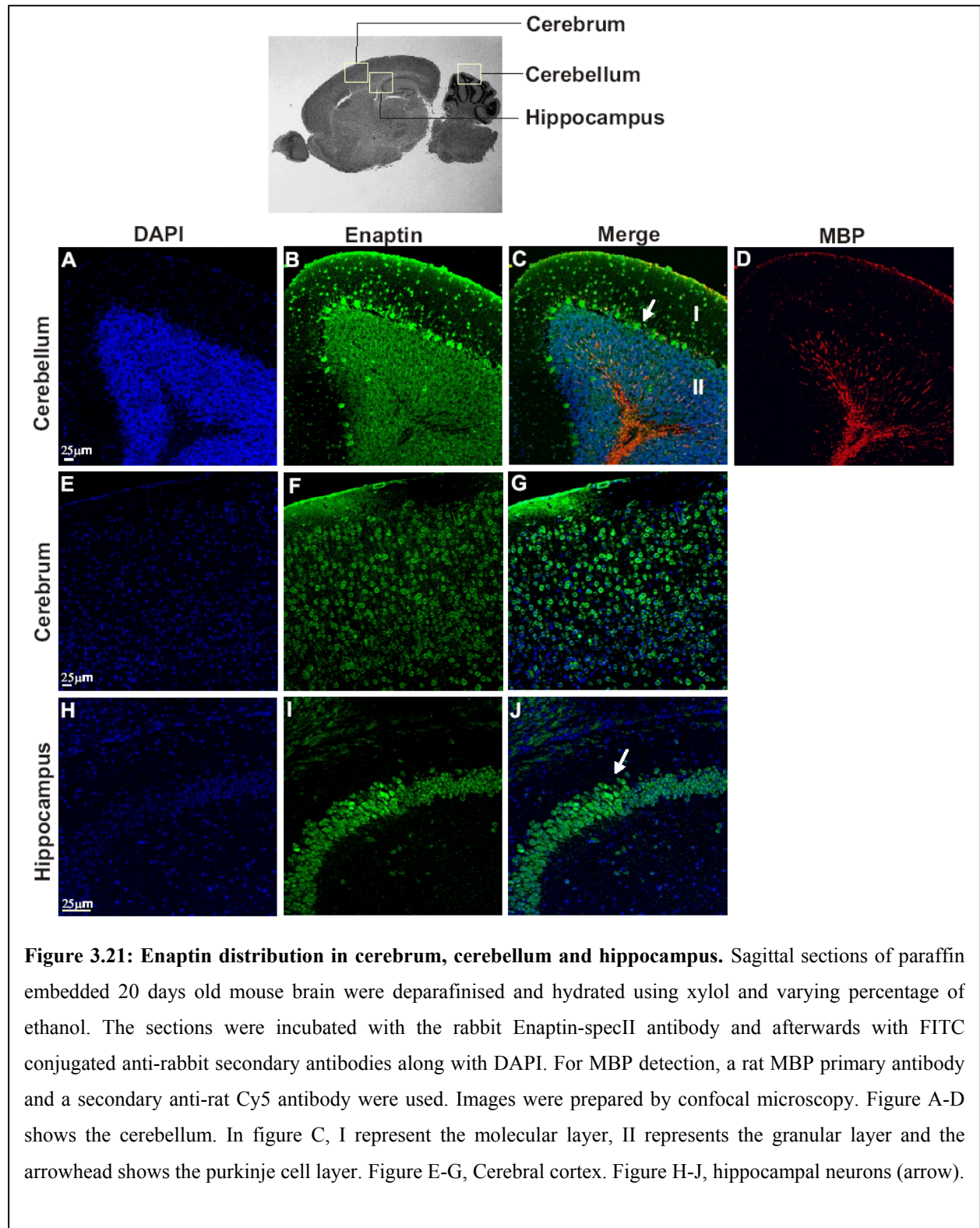


Figure 3.21: Enaptin distribution in cerebrum, cerebellum and hippocampus. Sagittal sections of paraffin embedded 20 days old mouse brain were deparaffinised and hydrated using xylol and varying percentage of ethanol. The sections were incubated with the rabbit Enaptin-specII antibody and afterwards with FITC conjugated anti-rabbit secondary antibodies along with DAPI. For MBP detection, a rat MBP primary antibody and a secondary anti-rat Cy5 antibody were used. Images were prepared by confocal microscopy. Figure A-D shows the cerebellum. In figure C, I represent the molecular layer, II represents the granular layer and the arrowhead shows the purkinje cell layer. Figure E-G, Cerebral cortex. Figure H-J, hippocampal neurons (arrow).

antigen retrieval, blocked and then incubated with the Enaptin-SpecII antibody. FITC labeled anti-rabbit secondary antibody was used along with DAPI. For detection of the myelin basic protein (MBP), which stains the myelinated axons, we used anti-MBP rat antibody and Cy5 conjugated secondary antibody. In the case of cerebellum (A-D), strong staining of Enaptin was observed in the Purkinje cell layer, however a weak staining for Enaptin was also seen in the molecular and granular layers. In the cerebrum (E-G), Enaptin is distributed all over the cortex but seems to be accumulated around the nucleus and also in the cytoplasm. Strong expression for Enaptin could be also detected in the hippocampal neurons (H-J).

3.7.3 Expression of Enaptin in the skin

Skin is a stratified epithelium, where the epithelial cells undergo a dramatic differentiation process that results in a tough, water-impermeable outer covering that is constantly renewed. The epidermis is anchored to a basement membrane. Basal cells are mitotically active, but they lose this potential when they detach from the basement membrane and enter the outward path towards the skin surface. The layer of cells directly contacting the basement membrane, termed the basal layer, contains proliferating cells. During differentiation the epithelial

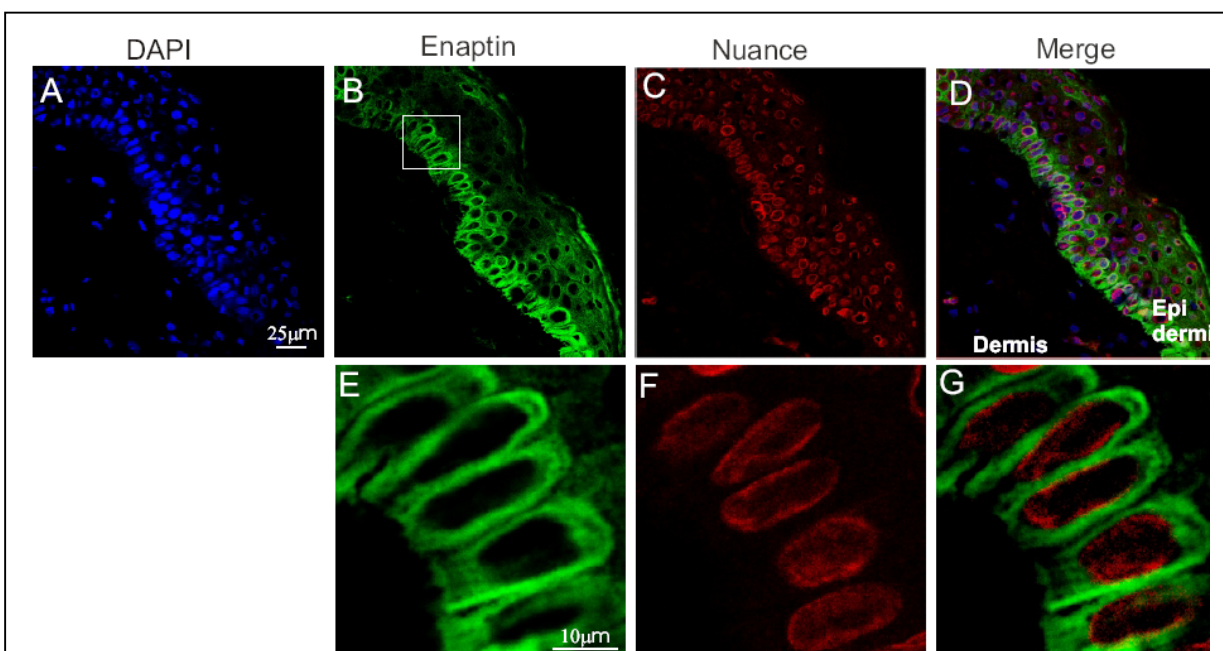
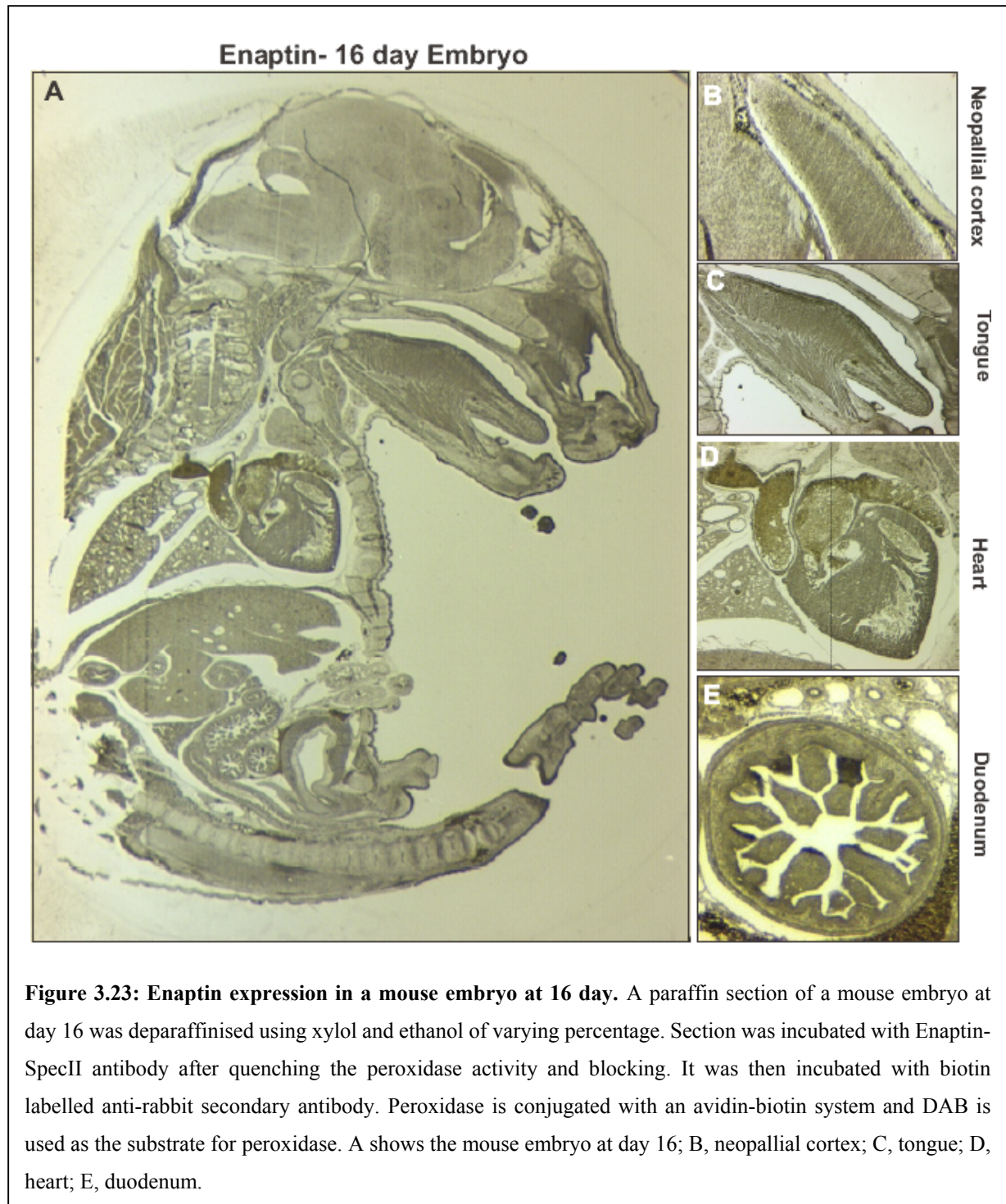


Figure 3.22: Enaptin localization in the skin. Cryosections of human skin fibroblast were fixed in 3% paraformaldehyde and permeabilised with 0.5% Triton X100. (B) Presence of Enaptin in the cytoplasm of epidermal cells. The polyclonal Enaptin-specII is used as primary antibody and an anti-rabbit secondary antibody conjugated with FITC. (C) Nuance distribution in the nuclear envelope as evidenced by staining with mAb K20-478 directed against the Nuance N-terminus and an anti-mouse Cy3 labeled secondary antibody (D) is a merge. The nucleus is stained with DAPI (A). Skin dermis and epidermis are labeled. The images were obtained by confocal microscopy. E-G, a magnified image of the inset in figure B.

cells undergo apoptosis and lose their nuclei and become the dead layer of the epidermis, the stratum corneum (Alonso and Fuchs, 2003). Interestingly, in skin, lamin A/C are differentially expressed. In contrast to lamin C, which is present in all layers of the epidermis including the basal layer, lamin A is found only in suprabasal epithelial cells (Venables *et al.*, 2001). Even though Enaptin is binding to a common region of lamin A and C (Mislow *et al.*, 2002a), we could analyze whether there are any changes in Enaptin distribution if lamin A is absent. Therefore the analysis of the Enaptin pattern in a tissue where gene expression and the nuclei in their morphology undergo dramatic changes was very interesting. The questions were: Is Enaptin expressed in the epidermis? Do the levels of Enaptin change during keratinocyte differentiation? In order to address these questions we stained human skin cryosections (obtained from the Department of Dermatology, Uniklinik, Köln) with the Enaptin-SpecII antibodies (Figure 3.22). For comparing this pattern with NUANCE distribution, mAb K20-478 was used. Our analysis showed that Enaptin was mainly in the cytoplasm and NUANCE was present in the nuclear membrane. This expression pattern is in agreement with the data obtained with the antibody recognizing Enaptin's N-terminus (Padmakumar, 2004). In the epidermis, Enaptin appears to be enriched in the cytoplasm in the basal layer cells in comparison with the other epidermal cell layers.

3.7.4 Expression of Enaptin in a 16-day-old mouse embryo

To investigate the pattern of expression of Enaptin in mouse embryogenesis, we have used a sagittal paraffin section of a 16-day mouse embryo. Images were taken with a stereo microscope. Enaptin is present in several tissues and organs. Organs expressing Enaptin in elevated levels are the neopallial cortex, which is the precursor of cerebrum, the olfactory epithelium, tongue, heart, duodenum, lung and liver.



3.7 Generation of GFP-fusion proteins containing the C-terminus of Enaptin

In the previous immunofluorescence experiments, we demonstrated that Enaptin localizes to the nuclear membrane in various cell lines. The fact that Enaptin has a transmembrane domain at its C-terminus and the findings that the C-terminus of both Enaptin and NUANCE are interacting with nuclear envelope proteins like lamin A/C, emerin, sun1

(Mislow *et al.*, 2002; Libotte, 2004; Padmakumar, 2004), encouraged us to investigate the importance and function of Enaptin's C-terminus for the nuclear membrane localization. Two green fluorescent protein (GFP) fusions of Enaptin, GFP-DN and GFP-Trans were made (Figure 3.24). One harbors the last two spectrin repeats of Enaptin including the tail region and the transmembrane domain (the mouse Enaptin sequence corresponds to amino acids 8396-8749 of human Enaptin) and another one composed of only the tail region and the transmembrane domain. Previous studies with the highly homologous NUANCE protein have shown that such proteins display dominant negative effects, and displace the endogenous NUANCE protein from the nuclear membrane (Zhen *et al.*, 2002). Therefore we wanted to examine the dominant negative effects of similar Enaptin GFP fusions. Since the C-terminal regions of Enaptin and NUANCE are highly similar (Figure 3.7), we postulated that those Enaptin proteins might affect the distribution of the endogenous NUANCE protein as well. The DNA fragments were amplified from a mouse image clone (BC054456) using primers with EcoRI and Sall restriction sites and cloned into the EGFPc2 vector.

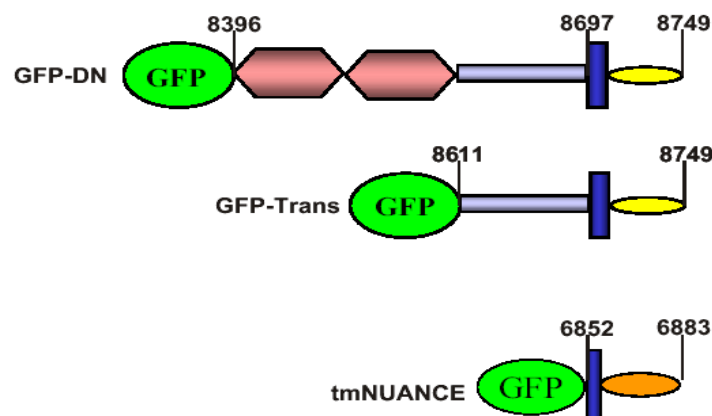
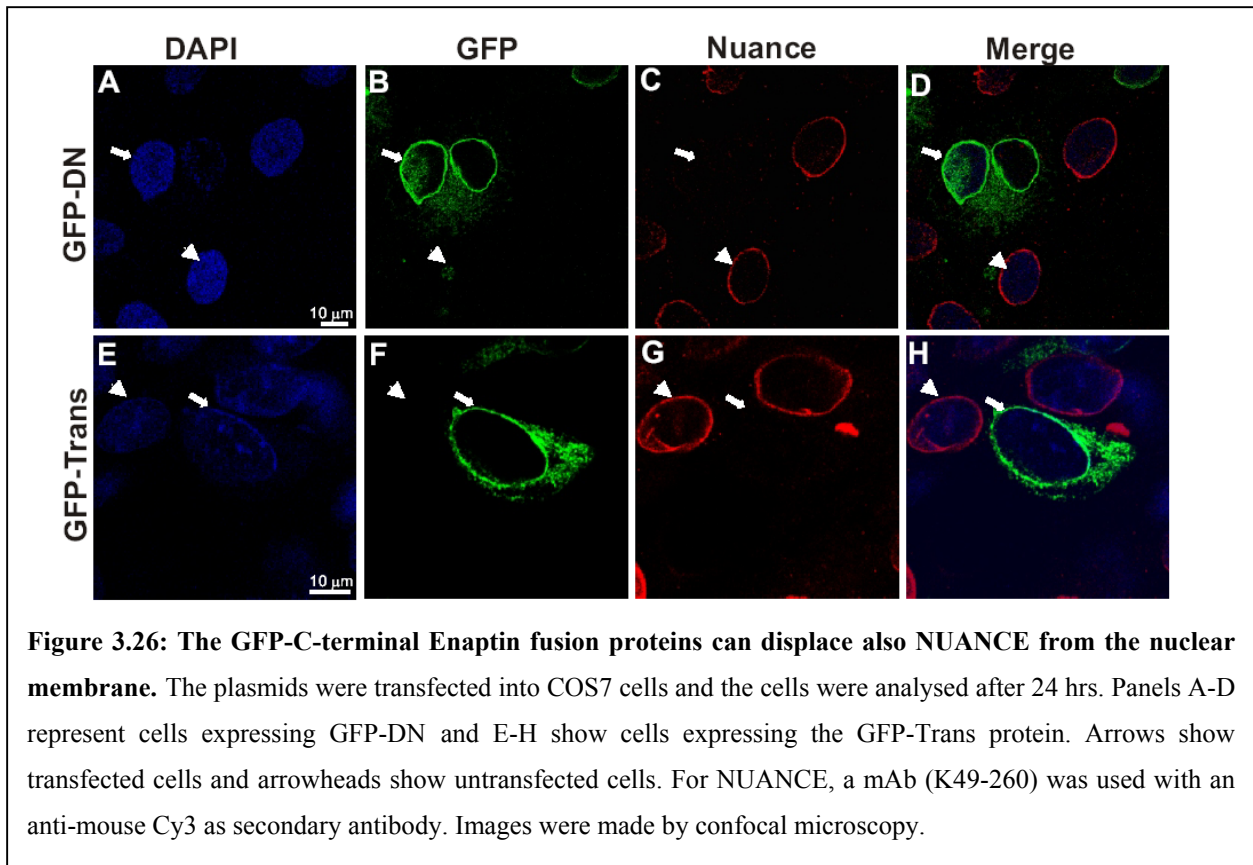


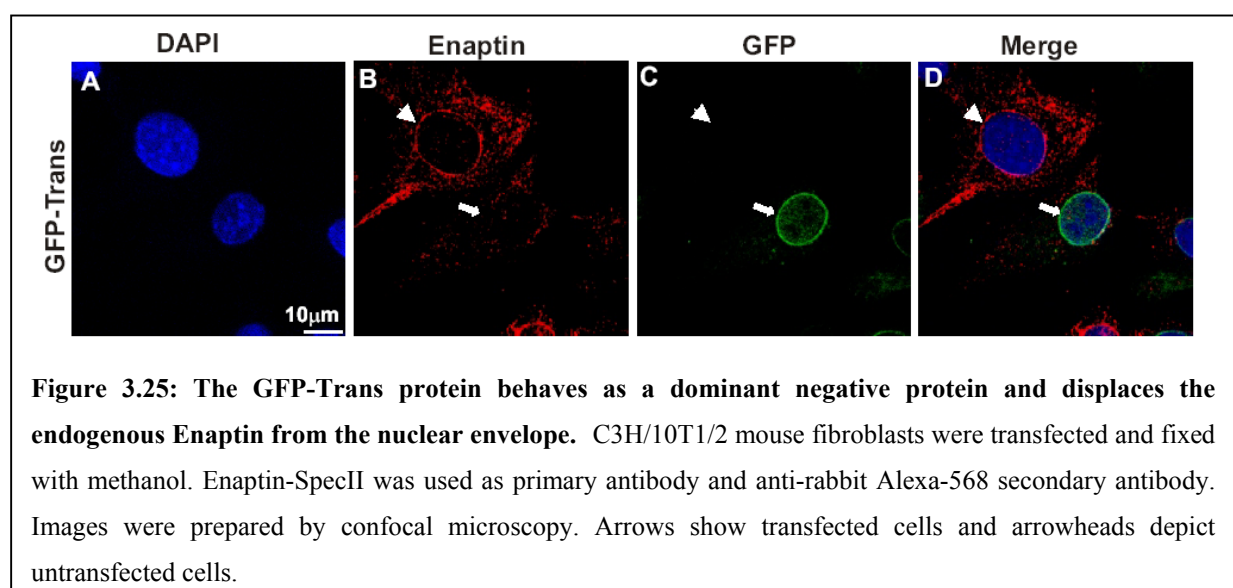
Figure 3.24: Schematic diagram of GFP fusions of Enaptin's C-terminus. C-terminal segments of Enaptin were amplified from an image clone by PCR and cloned into EGFPc2. The oval represents GFP, hexagons represent spectrin repeats and the vertical blue bar stands for the transmembrane domain. The yellow oval depicts the perinuclear segment of Enaptin. The amino acid positions of Enaptin are given with regard to the start methionine in the longest isoform of Enaptin (AAN03486). TmNUANCE is a GFP fusion protein for human NUANCE (Libotte, 2004).

3.8.1 C-terminal Enaptin GFP fusions localize to the nuclear membrane

The plasmids coding for GFP-DN and GFP-Trans of Enaptin were transfected into C3H/10T1/2 cells and COS7 cells by electroporation. Cells were grown for 24 hours after transfection on cover slips and used for immunofluorescence studies using the anti-Enaptin-SpecII antibody and for the detection of NUANCE mAb K49-260 which recognizes the C-terminus.

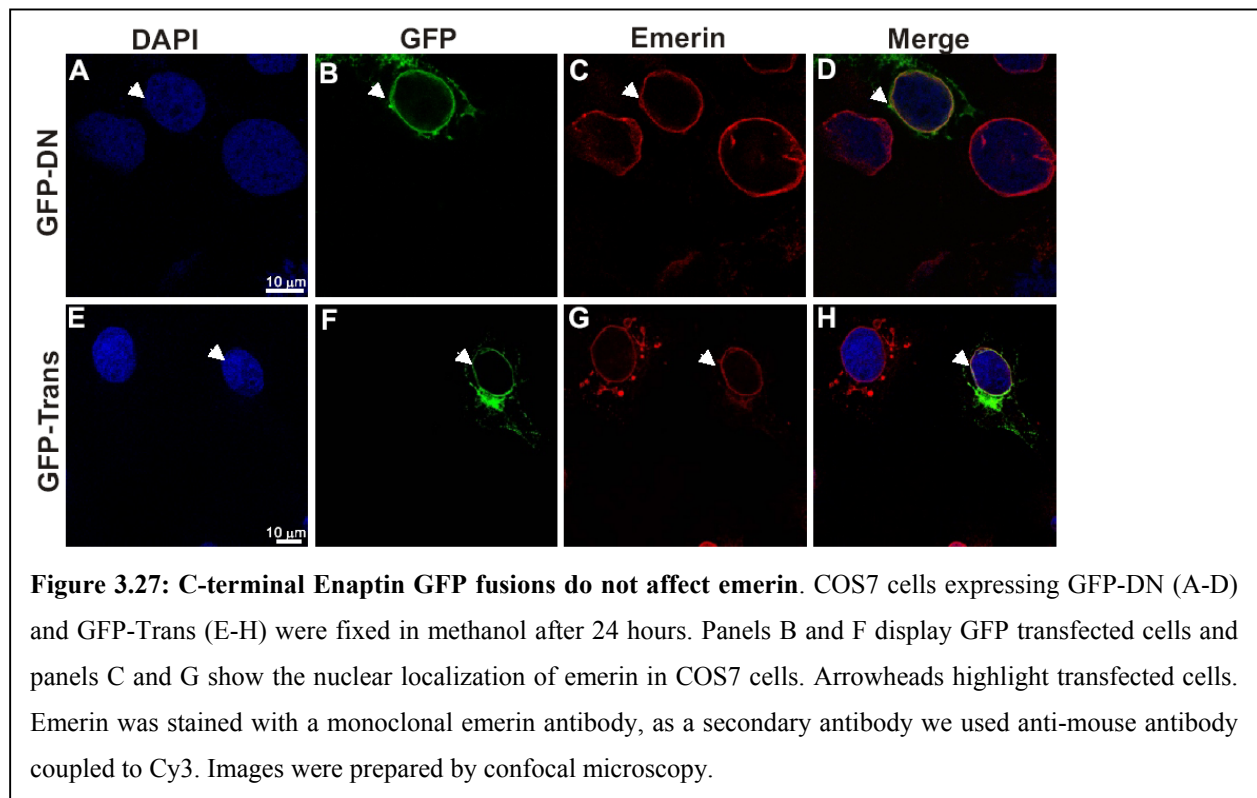


Both Enaptin-GFP fusions were localized to the nuclear envelope (Figures 3.25, 3.26). In C3H/10T1/2, we observed a displacement of endogenous Enaptin from the nuclear envelope using the Enaptin-SpecII antibody, supporting the notion that these proteins can exert a dominant negative effect. Untransfected cells (arrowheads) displayed a nuclear staining of Enaptin. In COS7 cells expressing either GFP-DN or GFP-Trans Enaptin fusion



proteins we could also observe displacement of the endogenous NUANCE protein from the nuclear membrane (Figure 3.26, arrows). We also noted that, in transfected COS7 cells the NUANCE protein appears to be rapidly degraded, which is evident from the lack of staining from the cytoplasm or nucleoplasm. Further studies will be necessary including immunoblot analysis to verify this observation.

The displacement of NUANCE prompted us to look for the localization of emerlin in order to investigate whether the overexpression of the Enaptin GFP fusion proteins constructs has any influence on other inner nuclear membrane proteins. We have already found in our group that a C-terminal NUANCE GFP fusion construct (tmNUANCE Figure 3.24), which consists of only the transmembrane and the tail part, can displace emerlin from the nuclear envelope (Libotte, 2004). In contrast, we could not see any such displacement of emerlin in our GFP fusion constructs of Enaptin transfected cells (Figure 3.27). This may be due to the differences in the lengths of the Enaptin polypeptides used. The GFP-Trans construct of Enaptin has additional 86 amino acids upstream of the transmembrane domain in comparison to the NUANCE polypeptide, which harbors only the transmembrane domain and the C-terminal tail (aa 6,852-6,883 of the human NUANCE). This region is highly conserved in NUANCE, Enaptin and klarsicht protein (Figure 3.7) and may possibly be important for the interaction of emerlin with Enaptin and NUANCE.



3.9 Lamin dependent localization of Enaptin

3.9.1 Localization of Enaptin in Lamin A/C knockout cells

Enaptin and NUANCE were shown to be interacting with lamin A/C and emerin (Mislow, 2002a). Therefore the localization of Enaptin in the nuclear envelope may be dependent on these proteins and correct localization of these proteins may be essential for Enaptin to stay in the membrane. In order to check this possibility, we have analyzed primary mouse fibroblasts derived from lamin A/C knockout mice (Figure 3.28). We detected Enaptin using a Nesprin-1 guinea pig antibody (see Figure 3.1). In wild type cells Enaptin and emerin were localized at the nuclear membrane with Enaptin also present in the cytosol and in the nuclear compartment. But in the lamin A/C^{-/-} cells both the proteins were redistributed from the nuclear envelope. The lack of lamin A/C in the nuclear lamina also affects the shape of the nucleus. Emerin was still present to some extent in the nuclear envelope even though the majority of the protein diffused to the cytoplasm. Enaptin was completely displaced from the nuclear membrane and remained both in the cytoplasmic and nuclear compartment.

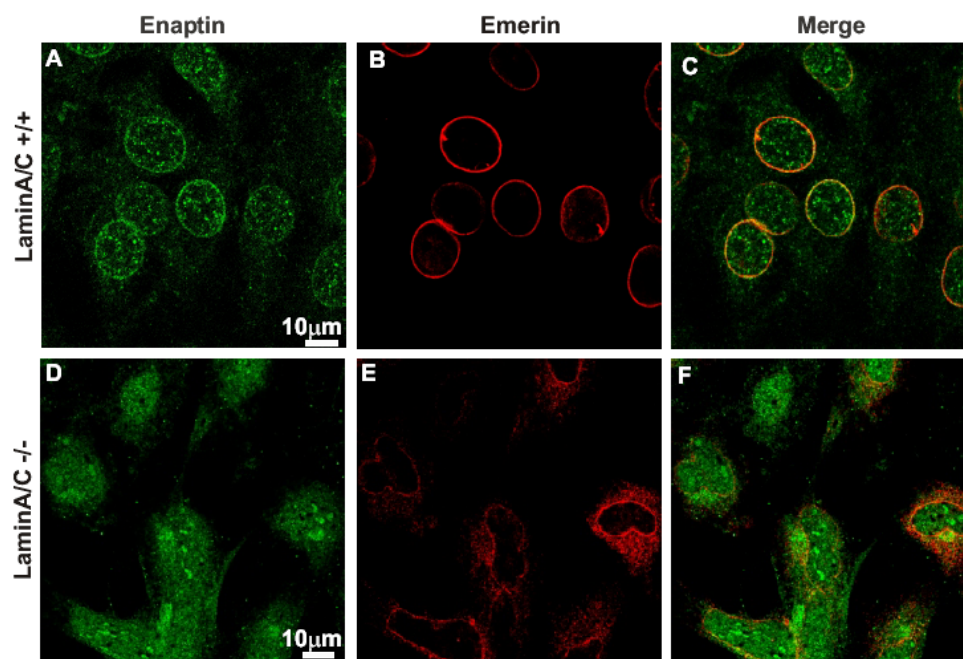


Figure 3.28: Enaptin localization in lamin A/C^{-/-} cells. Mouse primary fibroblast cells were fixed with methanol and incubated with Nesprin-1 guinea pig primary antibody and monoclonal emerin antibody. Anti-guinea pig FITC antibody and Cy3 conjugated anti-mouse antibodies were used as secondary antibodies. Panels A and D show Enaptin and B and D show emerin. C and F are overlays. Images were taken with a laser confocal microscope.

3.9.2 Dominant negative interference of Enaptin using a *Xenopus* lamin B construct

The mislocalization of Enaptin in the lamin A/C^{-/-} cells encouraged us to carry out further investigations concerning the lamin A/C dependent localization of Enaptin. The ability

of a mutated lamin B1 to displace lamin A/C has been demonstrated by Vaughan *et al.* (2001). This construct is a truncated *Xenopus* lamin B1, comprising amino acids 34-420. When transiently transfected, the GFP-lamin B Δ 2+ fusion protein aggregated and was found in nucleoplasmic granules (arrow in panel C, Figure 3.29) and both lamin A and lamin C were reported to be redistributed to these granules (Vaughan *et al.*, 2001), thus inducing a dominant negative effect on lamin A/C. We investigated the distribution of Enaptin in C3H/10T1/2 cells where this particular mutated lamin B is overexpressed. Confocal images obtained showed a redistribution of Enaptin to nuclear granules of GFP-lamin B Δ 2+ (arrow in panel B, Figure 3.29), similar to the reported redistribution of lamin A/C into nucleoplasmic granules.

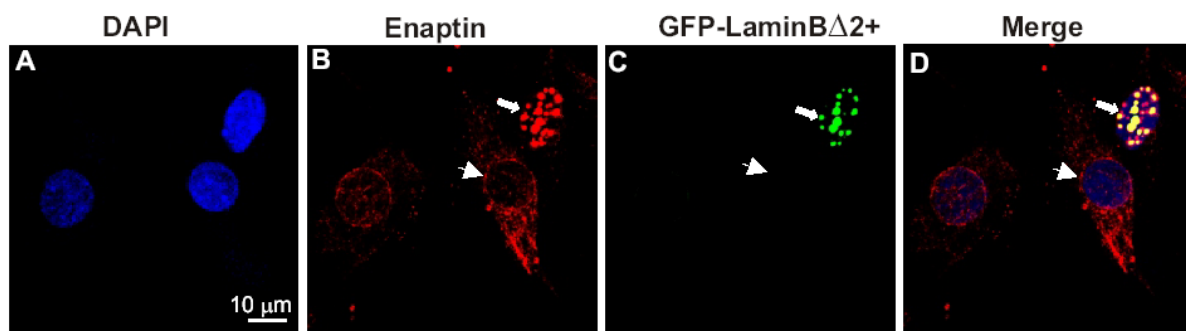


Figure 3.29: Localization of Enaptin in C3H/10T1/2 cells expressing a GFP-tagged lamin B mutant protein. (B) C3H/10T1/2 cells fixed in methanol and labelled with Enaptin-SpecII antibody with an Alexa 568 anti-rabbit secondary antibody. (C) Cell expressing GFP-lamin B Δ 2+. (A) The nucleus is stained with DAPI. Images were obtained by confocal microscopy. Arrows indicate the protein clumps and arrowhead indicates the nuclear envelope localisation of Enaptin.

3.9.3 Nuclear localisation of Enaptin in fibroblasts from laminopathy patients

Redistribution of Enaptin from the nuclear envelope in lamin A/C^{-/-} cells and GFP-lamin B Δ 2+ transfected cells suggested that the localisation of Enaptin in the nuclear envelope might be lamin A/C dependent. Mutations in the *LMNA* gene, which encodes lamin A/C, cause several muscular dystrophies affecting different tissues, which are now classified as laminopathies. Particular mutations in the *LMNA* gene resulting in single amino acid substitutions lead to the autosomal dominant Emery-Dreifuss muscular dystrophy (AD EDMD) and Familial partial lipodystrophy (FLPD). Since the interacting region of lamin A/C with Enaptin was shown to be present in the rod domain of lamin A/C encompassing aminoacids 243-572 (Mislou *et al.*, 2002, Libotte, 2004), it was interesting to investigate the localisation of Enaptin in mutated lamin A/C expressing cells. We obtained skin fibroblasts from patients affected with these diseases and analysed the localisation of Enaptin in comparison with control cells. We analysed cells with 3 mutations in lamin A/C, namely

R453W, R249Q, and R401C, which cause AD EDMD. We observed that Enaptin appears to be redistributed to the cytoplasm in the mutant cells in comparison with control cells, which did not have cytoplasmic staining.

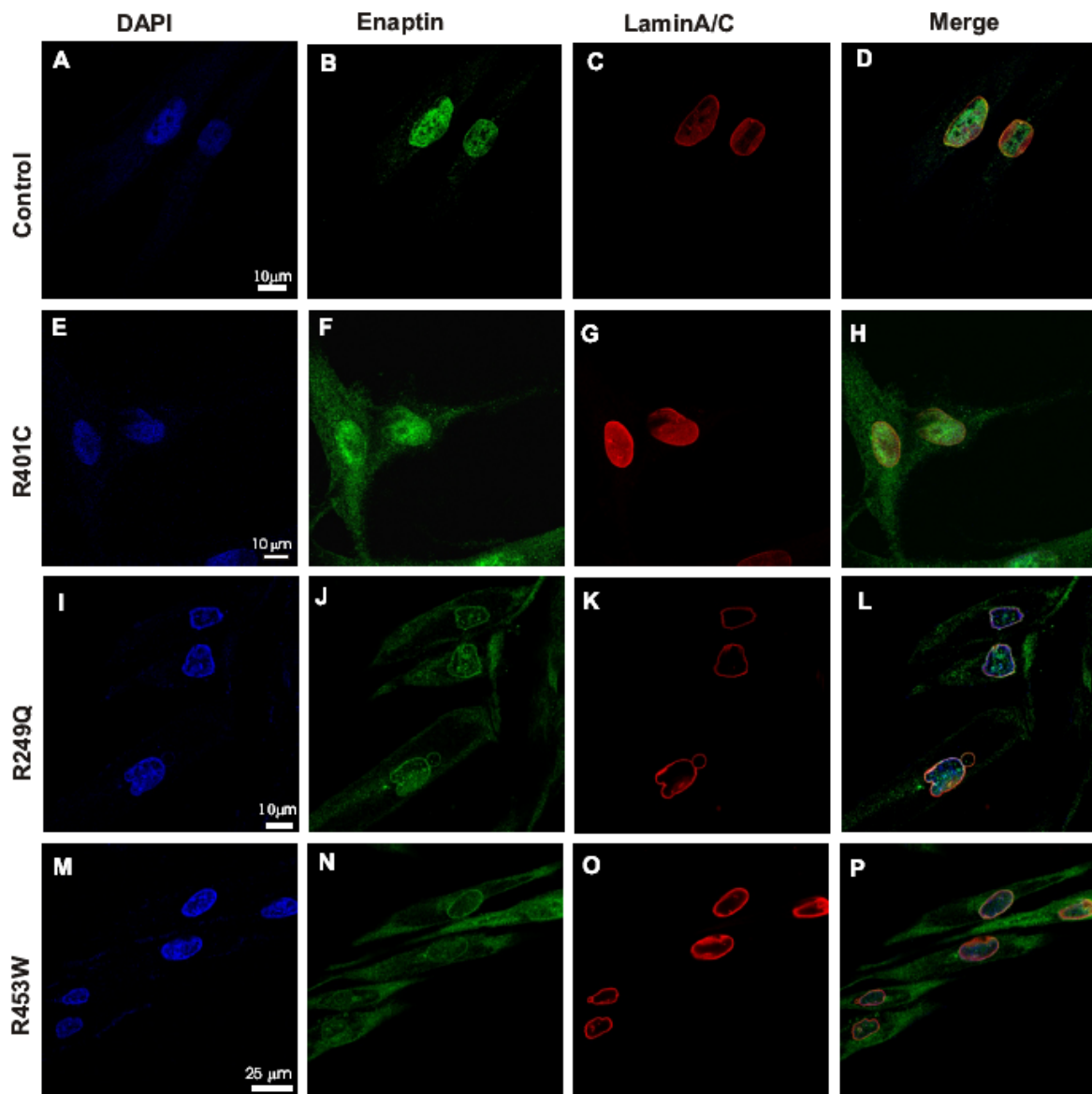


Figure 3.30: Enaptin distribution in fibroblasts obtained from patients with mutations in the lamin A/C gene. Cells were fixed in methanol and stained with Enaptin-SpecII followed by FITC conjugated anti-rabbit secondary antibody. Lamin A/C was detected with Jol2 antibody followed by anti-mouse Cy3 labeled secondary antibody. Nuclei were stained with DAPI and images were taken with a confocal microscope.

3.10 Distribution of Enaptin during myoblast differentiation

Nuclear lamina proteins such as lamin A were demonstrated to be reorganised during muscle differentiation (Muralikrishna et al., 2001). Also Favreau *et al.* (2004) showed that, when a mutant lamin A is expressed in C2C12 myoblast cells, it could inhibit the in-vitro differentiation of myoblasts. Our western blot and immunofluorescence analysis in skeletal

muscle showed that Enaptin was expressed in skeletal muscle and (Zhang et al., 2001) detected a C-terminal isoform of Enaptin (Nesprin-1 α) while searching for vascular smooth muscle differentiation markers. Therefore we were interested to know the expression pattern of Enaptin during muscle differentiation. Primary human myoblasts (MB50) were serum starved for differentiation and fixed with methanol on different days after serum starvation. As a marker for myoblast differentiation, cells were also stained with antibodies against skeletal muscle myosin. Enaptin was detected with the Enaptin-SpecII antibodies in the undifferentiated cells as well as in the differentiated myotubes. During differentiation, myoblast cells fused to form multinucleated myotubes.

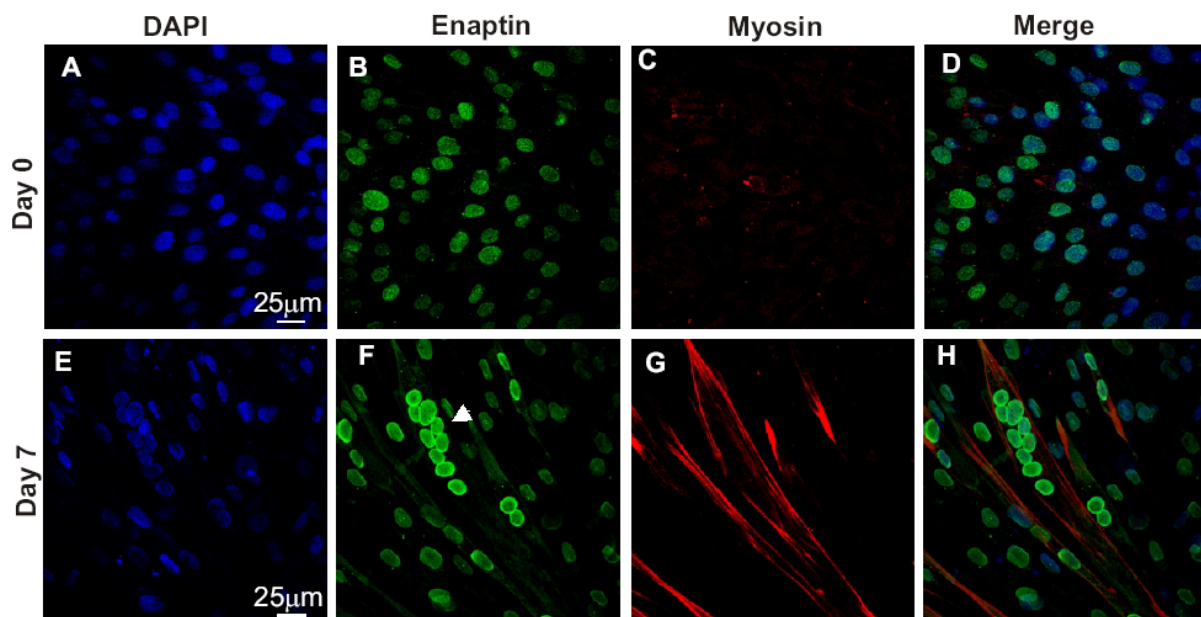


Figure 3.31: Upregulation of Enaptin during myoblast differentiation. MB50 human myoblast cells were changed to a medium with 2% horse serum to induce differentiation. Enaptin was detected using an Enaptin-SpecII antibody and skeletal muscle myosin was detected using monoclonal antibody specific to myosin. Cells were fixed with methanol and images obtained with confocal microscopy. Differentiated cells formed multinucleated myotubes (E-I). Arrowhead points to a group of nuclei in a myotube. Panel I is a phase contrast picture of differentiated myoblasts. A-D, undifferentiated myoblasts.

We observed that the cells, which formed the myotubes by fusing together, had a very intense staining for Enaptin in the nuclear envelope when compared to undifferentiated cells. It appears that during differentiation the expression of Enaptin is upregulated implying a possible role for Enaptin during muscle differentiation.

3.11 Generation of an Enaptin mouse mutant

Gene targeted mice are powerful tool for studying the functional aspects of a protein and its link to human diseases. Enaptin is a novel protein with a proposed function in nuclear positioning as indicated from the data obtained for ANC-1, an orthologue of Enaptin in *C. elegans* (Starr, 2002). Mutations in ANC-1 cause a defect in nuclear positioning and anchorage. From the analysis of a *Drosophila* orthologue of Enaptin, MSP-300 (Rosenberg-Hasson, 1996) it is known that the protein contributes to the integrity of the somatic and visceral muscles during periods of significant morphogenetic changes. A mutant of MSP-300 has a defect in muscle development and is embryonic lethal. Enaptin is shown to interact with lamin A/C and emerin, two inner nuclear membrane proteins forming the nuclear lamina (Mislow *et al*, 2002a). Mutations in lamin A/C and emerin cause a novel group of human disease named as laminopathies (Worman, 2002). As it will be interesting to study whether Enaptin has any role in the pathogenesis of these diseases we decided to generate a mouse model in which the Enaptin gene is ablated.

3.11.1 Analysis of the structure of the mouse Enaptin gene

The *Enaptin* gene is located on mouse chromosome 10. Since Enaptin is a huge gene and has several known isoforms, it was not possible to make a strategy to knockout all the isoforms with a single targeting construct. Enaptin has an actin-binding domain at the N-terminal end and since the actin-binding property of Enaptin may contribute significantly to its functions, we decided to target the isoforms containing the actin-binding domain. We had previously constructed the cDNA of Enaptin-165, a short isoform of Enaptin in mouse which has the ABD domain, we analysed the gene structure of the Enaptin-165 in detail. The analysis with mouse genomic sequence revealed that this Enaptin-165 has 32 exons and the starting codon ATG is located in the second exon. The exons and their intron boundaries are given in Table 3.3. We decided to target the 3rd exon by inserting a neomycin cassette in the middle of exon 3 so that the intron-exon transition is ablated and the transcription will come to an end. Since the first ATG is not ablated, the transcription will start but will come to a stop after the 3rd exon. The possible acceptor from exon 2, in case of a splicing to form an in-frame protein, will be to exon 10. But such a spliced variant of Enaptin will be lacking the two calponin homology domains which may severely affect the functional actin-binding property of the translated protein.

Sequence at <u>intron-exon</u> boundary					Sequence at <u>intron-exon</u> boundary				
<u>Exon</u> <u>No</u>	<u>5'Splice doner</u>	<u>5'splice acceptor</u>	<u>Exon size</u> <u>bp</u>	<u>Intron size</u> <u>bp</u>	<u>Exon</u> <u>No</u>	<u>5'Splice doner</u>	<u>5'splice acceptor</u>	<u>Exon size</u> <u>bp</u>	<u>Intron size</u> <u>bp</u>
1	CAGCCACCAAGCA	ATCAAG/GTAAAT	234	8258	17	ACTCAG/TGGAGG	AAGAAG/GTAAGG	203	1563
2	CTTCAG/GTTCCT	TACAAG/GTGAGC	265	84239	18	GGTTAG/GATTTT	AAGCAA/GTATGT	165	456
3	TTCTAG/ATGAAC	GCCAAG/GTAAACA	63	13790	19	cctcAG/TATGCA	TTGGAG/GTAAGG	153	1524
4	TTGCAG/CGGAAG	AAACTG/GTAAGG	96	6294	20	acgcAG/GATCTG	TCCAAG/GTGGGA	144	2676
5	CCCCAG/CCTTGT	AGGAAG/GTAAGA	84	10454	21	ccaaAG/GTCAAA	CACCAAG/GTAAGA	174	1602
6	TGTCAG/TCGATG	TTCCAAG/GTATTT	21	493	22	TTGTAG/GAACTG	TTCCAAG/GTAAGT	159	1021
7	AAACAG/ATTAAA	TTCCAAG/GTATTT	93	1290	23	ATTAAG/AGCATG	CACACG/GTGAAT	165	1472
8	ACACAG/ATAGAA	AGGCAA/GTAAGT	176	3627	24	TGATAG/GAGTTC	TGGAAAG/GTGAAT	135	167
9	AATAAG/GCAGAT	CCGAAG/GTACGC	97	6894	25	ctacAG/GATCTT	CACAGG/GTATGT	159	177
10	TTACAG/ATGTGG	GATGAT/GTAAGT	110	4197	26	TCttAG/GTttTC	CAGCAG/GTACTG	209	606
11	TTCCAG/AGGGAT	TATCAAG/GTAAGT	108	1439	27	TTTTAG/GTttTC	GTGGAT/GTAAGT	109	836
12	TTTTAG/GCATTT	TCCCAG/GTGAAT	139	1439	28	TTCCAG/GAGATC	TCAGAG/GTATGT	165	1855
13	TTTCAG/CTCTC	CATAAG/GTAAAA	165	22935	29	ATTTAG/GTCAAA	CACCAAG/GTAGAG	168	1269
14	TATTAG/GATCTG	TGGAAG/GTAAGA	113	528	30	TTCCAG/CAAAAG	ATCCAG/GTAGGG	165	1060
15	TCCTAG/GTTCGA	TATATC/GTGAAT	169	5913	31	AATTAG/GTCAGC	ACAAAG/GTACGC	141	2766
16	CTCTAG/TCttTT	GCTCAAG/GTATAG	97	604	32	ccctAG/GAGTTC	AAGAGG/GTttTG	877	

Table 3.3: Intron-exon boundaries and sizes of introns and exons of the mouse *enaptin-165* isoform.

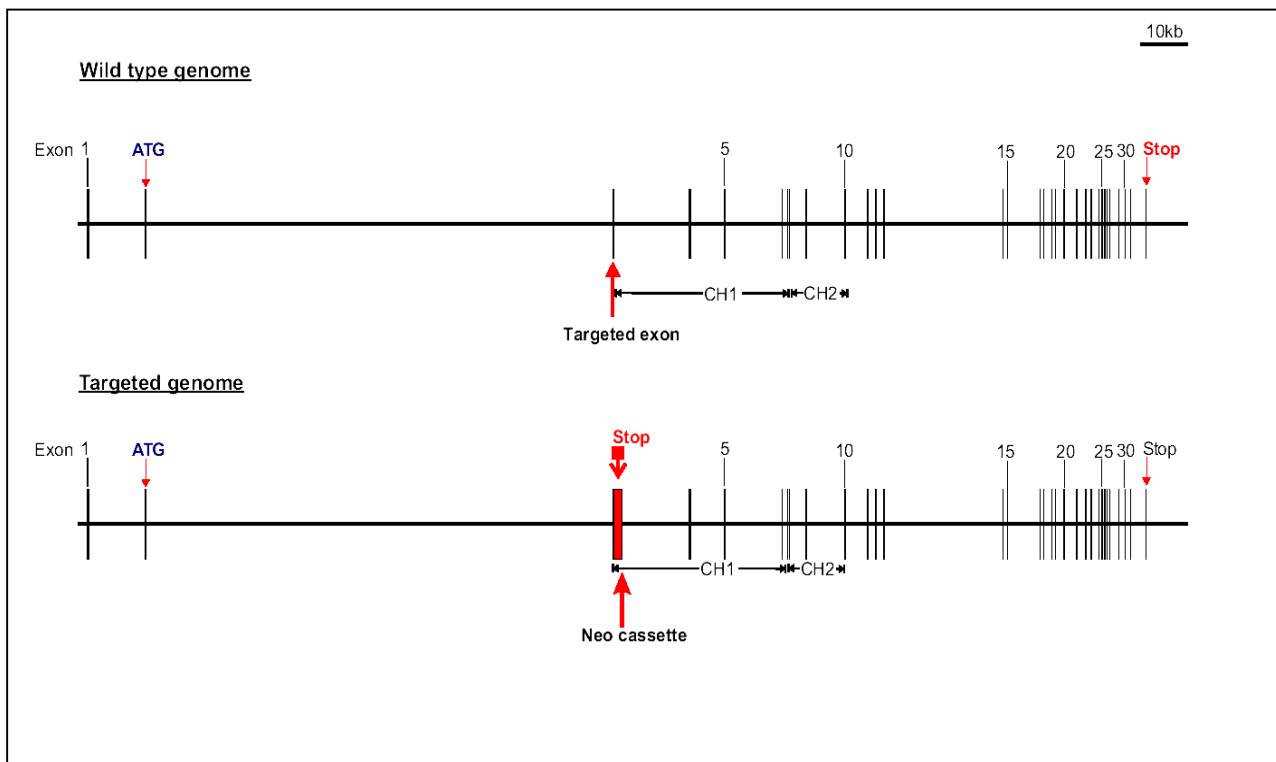


Figure 3.32: Schematic representation of mouse *Enaptin-165*. *Enaptin-165* has 32 exons and introns of varying sizes. The starting codon is located in the 2nd exon and a stop codon in the 32nd exon. The positions of the calponin homology domains (CH1 and CH2) are indicated. When targeted, a neomycin cassette will be inserted in exon 3 disrupting the transcription downstream.

Prior to the generation of a targeting construct, 10 kb intronic sequences upstream and down stream of the exon 3 were tested against mouse genomic database to exclude the presence of any repetitive sequence or duplicated sequence. The analysis found no repetitive sequence in the intended part of vector generation.

3.11.2 Construction of the targeting vector (Enaptin KO)

For the vector construction, genomic DNA was isolated from IB10 mouse embryonic stem cells of the SV126 strain. A schematic diagram of the target vector is given in Figure 3.33. For the 5' arm, a 2 kb genomic fragment at the 5' side of the 3rd exon including a short stretch of bases from the 3rd exon itself was amplified with primers which have restriction sites *Sac*I and *Eco*RV, using a Pfu Turbo DNA polymerase and cloned into a Topo Blunt vector. A 1.8 kb *Eco*RV-*Not*I fragment containing the neomycin resistant cassette was cloned into pBluescript, which was used further as the vector backbone. The 5' arm was cloned into Neo-pBluescript using *Eco*RV and *Sac*I with *Sac*I to the 5' side. The 3' arm was designed avoiding a stretch of unknown sequence of approximately 1 kb (blue block in the figure) downstream of exon 3. The 3' arm was amplified from the ES cell genomic DNA with primers carrying *Sac*II and *Not*I restriction sites with *Sac*II to the 3' side of the 3' arm and cloned first into a TopoBlunt vector. The 3' arm was retrieved from the TopoBlunt using *Not*I and *Sac*II and ligated to the 5' arm-Neo-pBluescript. All the fragments were sequenced and the cloning directions were confirmed.

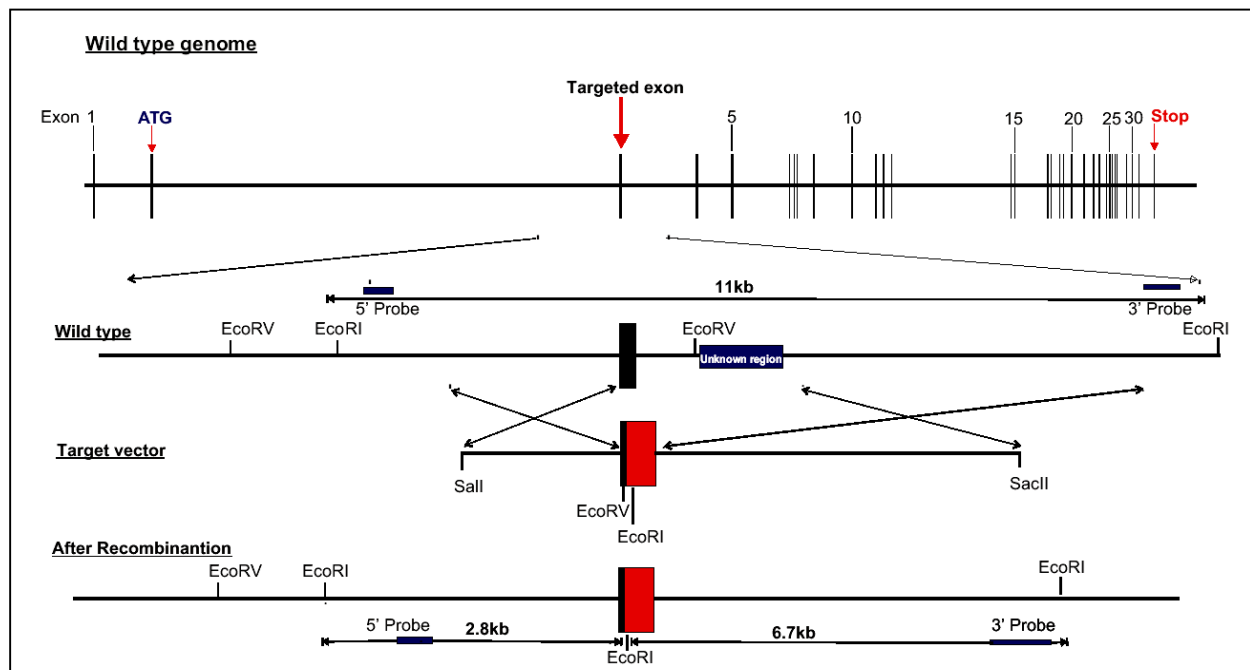


Figure 3.33: Schematic representation of the targeting vector and recombination events.

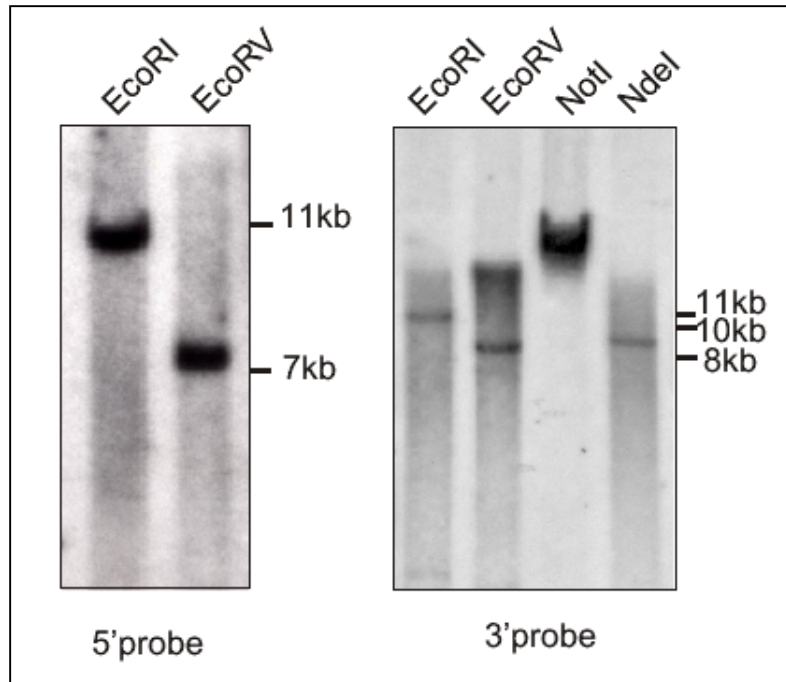


Figure 3.34: Southernblot of mouse genomic DNA for testing the genomic sequence and the probes. The mouse genomic DNA was digested with EcoRI, EcoRV, NotI and NdeI enzymes and resolved on a 0.7% agarose gel and blotted to Zetaprobe membrane. 5'probe and 3'probe labeled with ^{32}P were used for hybridisation.

Two external probes were generated which could be used for the screening of clones and also for checking the recombinant clones. These probes were tested for the genomic sequence digestion pattern and for the specificity of the probes. Southern blotting after digestion of genomic DNA with different enzymes has given the expected pattern of bands. Probes detected specifically single bands at the expected sizes.

3.11.3 ES cell transfection

The target vector was linearised with SalI and 40 μg of purified plasmid DNA were transfected into ES cells from both the IB-10 and R-1 lineage. The clones were selected using G418 for a period of 8 days after transfection. Neomycin resistant clones were picked and grown in 24 well plates. One part of the cells was frozen and another part used for isolating genomic DNA. EcoRI was chosen for digesting the genomic DNA. The expected sizes of the

signals with both wild type and recombinant DNA are given in the Table.

EcoRI Digest		
	5' probe	3'probe
Wild type	11kb	11kb
Recombinant	2.8kb	6.7kb

Table 3.4 Sizes of wild type and knockout bands with 5' and 3'probes when digested with EcoRI

3.11.4 Screening of recombinant clones

We have done three ES cell transfections and more than 500 clones which showed resistance to neomycin were picked and analysed with Southern blotting. Preliminary screening was done with the 5' probe and out of 500 clones, only two clones gave the recombinant band of 2.8 kb in addition to the wild type band of 11 kb.

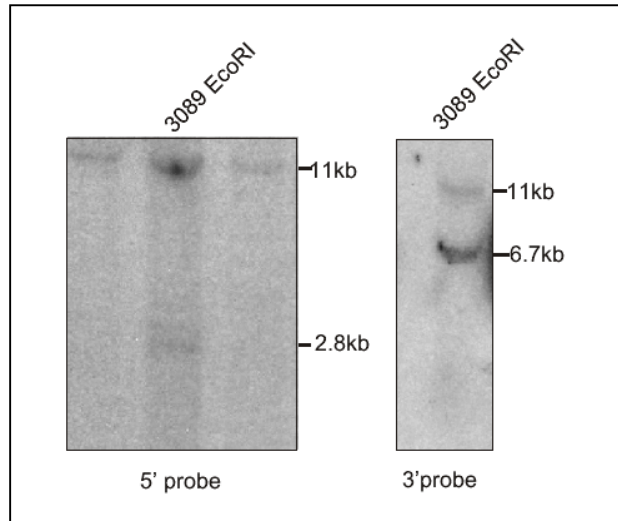


Figure 3.35: Possible recombinant clone 3089.

Genomic DNA was isolated, digested with EcoRI and the fragments resolved in a 0.7% agarose gel. After blotting to Zeta probe membrane, hybridization was done with ^{32}P labeled 3' and 5' probes.

Clones no 3089 and 3196 were selected and probed with the 3' probe. Only clone no 3089 has given an expected recombinant band of the size 6.7 kb with the 3' probe. These clones have to be analyzed further for the recombination events with different enzymes and with the neomycin probe to exclude the random integration into other sites.

Discussion

4 Discussion

4.1 Enaptin is a giant protein of the α -actinin superfamily

Actin is one of the most conserved and ubiquitous proteins in nature. The actin cytoskeleton system is not only abundant but also highly complex and is considered to be very old in the evolutionary sense. Actin and all its associated proteins constitute more than 25% of the total protein in nonmuscle cells and 60% in muscle cells. More than 48 different classes of actin-binding proteins were identified and categorized (Kreis and Vale, 1999). The α -actinin family of F-actin cross-linking proteins includes a range of molecules that share homologous actin-binding domains (Fabbrizio *et al.*, 1993) allowing them to cross-link actin filaments by the formation of dimers or trimers. The family includes spectrins, fimbrins/plastins, dystrophins (Hammonds, 1987), gelation factor/ABP-120 from *Dictyostelium* (Noegel *et al.*, 1989), and members of the filamin subfamily (Hartwig, 1995). The characteristic feature of this family of proteins is an N-terminal actin-binding domain (ABD), which is composed of two calponin homology domains. Calponin homology domains are actin-binding domains of around 100 residues in length, which were first characterised in calponin. Calponin is a protein that plays a major role in smooth muscle contraction (Strasser *et al.*, 1993).

We have identified Enaptin while searching for novel actin-binding proteins of the α -actinin type. Enaptin (greek; enapto: to attach) was initially identified as a 165 kDa protein containing a functional N-terminal ABD and a coiled-coil rod domain (Braune, 2001). Zhen *et al.* (2002) characterised a giant actin-binding protein called NUANCE that connects the nucleus to the actin cytoskeleton. With the cloning of Enaptin, a new member is added into this family of proteins, which may connect the nucleoskeleton and the actin cytoskeleton. The longest open reading frame (ORF) of Enaptin is even bigger than the ORF of NUANCE. Enaptin has 147 exons for its longest isoform whereas NUANCE has 116 identifiable exons. Enaptin has so far eight identified isoforms while five isoforms have been identified for NUANCE, suggesting a complex gene structure for these proteins. Sequence analysis showed that Enaptin has an N-terminal ABD followed by a long coiled-coil domain containing 50 spectrin like repeats and a transmembrane domain at its C-terminus. Both proteins display a similarity to dystrophin (Blake *et al.*, 1996), a large membrane associated protein expressed in muscle and brain and utrophin, which is present at the sarcolemma of skeletal muscle during fetal development. In our ABD domain phylogenetic tree analysis, Enaptin and NUANCE form a distinct sub-family. The ABDs of these two proteins are closer to dystrophin and

utrophin than other members of the α -actinin superfamily. The 44 amino acid long serine rich linker between the CH1 and CH2 domains found in Enaptin may provide more flexibility to the globular ABD domain as suggested for utrophin, where the extended conformation of the ABD gives more flexibility to the molecule (Keep *et al.*, 1999). A recently identified brain protein, calmin (Takaishi *et al.*, 2003), has also a similar stretch of amino acids between the calponin homology domains.

The rod domain of Enaptin contains 50 spectrin like repeats (SR), where the coiled-coils are predicted. Spectrin repeats are typically 100 aa residues in length and in Enaptin, they are arranged as groups with several breaks in between them. These breaks may provide the molecule more flexibility by acting like a hinge (Figure 3.6). The long coiled-coils can form dimers or oligomers as had been demonstrated for spectrin and α -actinin (Chan and Kunkel, 1997; Puius *et al.*, 1998). The dimerisation of two spectrin repeats at the C-terminus of Enaptin has been recently demonstrated (Mislow *et al.*, 2002a). It is probable that out of the 50 spectrin repeat domains, there could be more self-interacting regions in Enaptin, forming dimers or oligomers. Such molecular interactions would provide structure and support for the protein itself. Spectrin repeats have been implicated additionally in cell membrane and organelle membrane interactions. First identified as the supporting infrastructure of the plasma membrane of erythrocytes, spectrin is now recognized as the most central player in a ubiquitous and complex linkage between membranes and the cytosol (De Matteis and Morrow, 2000). Overall, they are considered as scaffolding molecules, which organize and stabilize the cytoskeleton. Whether NUANCE and Enaptin are the nuclear scaffolders of the nuclear membrane needs to be seen.

4.2 Enaptin is a nuclear membrane protein

Our immunofluorescence data from primary fibroblasts using the Enaptin-specII antibodies and our transfection studies with C-terminal Enaptin constructs demonstrated the presence of Enaptin at the nuclear envelope. Thus together with NUANCE, both form a novel group of α -actinin family actin-binding proteins, which localise to the nuclear envelope in higher eukaryotes. Enaptin has seven nuclear localisation signals (NLS) (Figure 3.3) distributed all over the protein, which could mediate the nuclear localisation of the protein. In order to study in more detail and identify the regions implicated, we performed a domain analysis of the highly conserved Enaptin C-terminus using various GFP fusion proteins. Our studies suggest that the C-terminal klarsicht like domain (Figure 3.7) is sufficient for the nuclear membrane localization of Enaptin which is evident from the proper nuclear membrane

localisation of our GFP constructs (Figure 3.21), which interestingly are lacking a nuclear localization signal. It could be possible that the anchoring of the C-terminal GFP constructs to the nuclear envelope is mediated by its interaction to other nuclear membrane proteins. Details of such interactions are emerging from work performed in the *C. elegans* field. UNC-84 is an inner nuclear membrane protein in *C. elegans*, which has an important role in the nuclear migration and nuclear anchorage (Starr and Han, 2002). The presence of UNC-84 is necessary for the proper localization of ANC-1 (the worm orthologue of Enaptin/NUANCE) at the nuclear envelope. While the biochemical details of the ANC-1/UNC-84 interaction were not known, recently in our lab, we have shown that the conserved C-terminal tail domain of Enaptin is interacting directly both in vitro as well as in vivo with SUN-1 (Padmakumar, 2004). SUN-1 is the mammalian homologue of *C. elegans*'s UNC-84. The highly conserved C-terminus of Enaptin displays strong homology to the klarsicht protein. Klarsicht in *Drosophila* (Mosley-Bishop *et al.*, 1999) is required for nuclear migration of differentiating cells in the *Drosophila* eye. Along with klarsicht, Enaptin and NUANCE can be classified as type II integral membrane proteins (Kutay *et al.*, 1993). The discrete NLS throughout the molecule may be necessary for the nuclear localisation of various isoforms lacking the transmembrane domain. In accordance with such a scenario, the Enaptin-165 isoform, which lacks a transmembrane domain is found predominantly in the nucleoplasm in transfection studies carried out in COS7 cells (Padmakumar, 2004).

Interestingly, beside the presence of Enaptin at the nuclear membrane we have observed a nucleoplasmic staining of Enaptin in myoblasts and neuroblastoma cells. Until now however, very little is known about the isoform diversity of Enaptin and it is not clear what domain architecture the various nucleoplasmic, nuclear envelope and cytoplasmic splicing forms has. Interestingly we have also demonstrated a nuclear membrane localisation for Enaptin with polyclonal antibodies designed against Enaptin's ABD (Padmakumar *et al.*, 2004). So it could be inferred that a long isoform may exist with an ABD and transmembrane domain. The nucleoplasmic and cytoplasmic stainings suggest that splicing variants of Enaptin can exist which includes the last two spectrin repeats used for the antibody production, but lacking the transmembrane domain. Even though we could never detect such a splicing form from the sequence analysis, a Golgi localization of Enaptin has been reported with an antibody directed against a spectrin repeat domain in the middle region of Enaptin (Gough *et al.*, 2003). Such an isoform is also postulated for NUANCE (Zhen *et al.*, 2002). Membrane proteins like calmin and lamina-associated polypeptide-2 (LAP2) also have soluble splicing variants (Dechat *et al.*, 2000; Ishisaki *et al.*, 2001) lacking the transmembrane

domain. In the case of the LAP2 family of proteins, four isoforms ($\beta, \gamma, \delta, \epsilon$) exist with the transmembrane domain and LAP2 α and LAP2 ζ are isoforms without a transmembrane domain. LAP2 β is a type II integral protein of the inner nuclear membrane, which binds to lamin B and the chromosomal protein BAF, and may link the nuclear membrane to the underlying lamina and provide docking sites for chromatin. LAP2 α is a nonmembrane protein associated with the nucleoskeleton and may help to organize higher order chromatin structure by interacting with A-lamins and chromosomes.

The localisation of Enaptin in other cellular compartments beside the nuclear membrane suggests that the protein may also have additional roles inside the cell besides its known actin-nuclear membrane tethering function.

The nuclear membrane is composed of two membranes, the outer nuclear membrane, which is continuous with the rough ER, and the inner nuclear membrane. Our observations from the immunofluorescence and transfection studies suggested the presence of Enaptin at the nuclear membrane. However the exact topology of Enaptin at the nuclear membrane still remains uncertain with the absence of immunogold labelling studies. Our digitonin experiments prove the presence of Enaptin at the outer nuclear membrane. NUANCE (Zhen *et al.*, 2002) and Enaptin form a novel class of nuclear envelope proteins localizing to the outer nuclear membrane. Most nuclear membrane proteins characterized so far are positioned in the inner nuclear membrane like emerin (Bione *et al.*, 1994), Man1 (Lin *et al.*, 2000), LAP1 and LAP2 (Foisner and Gerace, 1993) etc. Nesprin 1 α , a splicing variant of Enaptin, has been shown to be associated with the inner nuclear membrane using immunogold labelling (Zhang *et al.*, 2001). Taken together, we presume that Enaptin is present in both inner and outer nuclear membranes. One scenario could be that the long Enaptin isoforms that contain an ABD are located at the outer nuclear membrane whereas the smaller C-terminal isoforms (Nesprin 1 α , β) are located in the inner nuclear membrane. Both Enaptin variants are retained at the membrane due to their transmembrane domains and to the presence of the highly conserved C-terminal tail which locates into the lumen in between the two nuclear membranes, where it can interact with other inner nuclear membrane proteins.

Disruption of the F-actin cytoskeleton using latrunculin-B showed that the nuclear membrane localization of Enaptin remained undisturbed. The existence of Enaptin isoforms without the actin-binding domain and the usage of a C-terminus specific antibody in this experiment make it complicated to explain whether the full length Enaptin isoform still remains in the nuclear envelope. It is possible that the shorter isoforms, which can be detected with the C-terminal Enaptin-SpecII antibody, still remain in the nuclear membrane while the

longest one, which has the actin-binding domain, might have been affected by the depolymerisation of the actin cytoskeleton. However more experiments with cell lines, which express only the full length Enaptin transcript need to be done to address this issue. We have also observed a shrinkage of the nucleus upon latrunculin-B treatment, suggesting a role of the actin cytoskeleton in the maintenance of nuclear integrity which could be mediated through Enaptin and NUANCE.

4.3 Expression and tissue distribution of Enaptin and its isoforms

Enaptin is widely expressed according to our tissue expression array, but the level of expression varies in different tissues. The complementary expression of Enaptin and NUANCE probably hints to the functional importance of these proteins. Dystrophin and utrophin are homologous genes that are expressed apparently in a reciprocal manner and may be co-ordinately regulated (Blake *et al.*, 1996). During embryonic development, utrophin is present in the sarcolemma and dystrophin replaces it in the adult skeletal muscle while utrophin is redistributed to the neuromuscular junction. At present little is known about the expression profile of Enaptin/NUANCE during mouse development. MSP-300, the *Drosophila* orthologue of Enaptin has been reported to be contributing to the integrity of the somatic and visceral muscle during embryonic muscle development (Rosenberg-Hasson *et al.*, 1996). Higher levels of Enaptin in tissues like neopallial cortex, muscles in the tongue and heart are evident in staining of 16-day mouse embryo. More studies have been conducted to find out the role of Enaptin/NUANCE during development.

The Enaptin expression dominates in brain, muscle and heart whereas NUANCE is present there in trace amounts. Stainings of various tissue sections also hint the different subcellular localizations of Enaptin and NUANCE. In skeletal muscle, NUANCE preferentially stains the nuclear envelope while Enaptin stains both the nuclear membrane and the sarcolemma. Our ABD antibody gives only the sarcoplasmic staining, which partially colocalises with desmin (Padmakumar, 2004). Eventhough we have not done co-staining experiments with the Enaptin-specII antibody and with desmin antibodies, it appears that the sarcoplasmic staining may be along the Z discs. For a long time a candidate protein has been speculated, which can connect the nucleoplasm to the sarcolemma for explaining the phenotypes in laminopathies (Nikolova *et al.*, 2004; Zhen *et al.*, 2002). Our stainings may suggest that Enaptin could be an ideal candidate providing such tethering function. The strong signals in cerebellum and cerebrum in the expression array are in well agreement with the immunofluorescence data obtained. However, in both the cases Enaptin appears to be

enriched in the cytoplasmic part of the cell body rather than in the nuclear membrane. Interestingly, we also could not observe a nuclear membrane staining in the N2A neuroblastoma cells. A variety of transcripts of Enaptin were obtained in brain in our western and northern blots analysis. Those data suggest the presence of various Enaptin isoforms in the brain. Interestingly, an N-terminal isoform of Enaptin (CPG2) has been studied in relation to the plasticity in adult cortex and hippocampus (Nedivi *et al.*, 1996). CPG2 has been found to be developmentally regulated in the rat brain and also found to be modulated in a light inducible manner. Taken together, the isoforms of Enaptin may have important functions in brain that could be different from the role the protein has in other tissues. Such a diversity in function is also attributed to dystrophin where the lack of it causes cognitive impairment in DMD brain (Lidov *et al.*, 1990); (Blake and Kroger, 2000). Interestingly, a C-terminal isoform of Enaptin (Syne-1) was reported to be associated with the nucleus in the neuromuscular junctions where it may interact with the muscle specific tyrosine kinase (MuSK) (Apel *et al.*, 2000). MuSK is demonstrated to have role in postsynaptic differentiation (Valenzuela *et al.*, 1995).

Northern blot analysis of brain RNA using probes against the ABD and the CPG2 regions of Enaptin showed three different species, >14, 5.5 and 10 kb, whereas RNA from skeletal muscle gave a band at around 6.5 and >14 kb using the CPG2 probe. The 14-kb band detected in northern blotting could give rise to the 400 kDa protein detected in brain, skeletal muscle, lung, stomach, small intestine and in COS7 cells, the 5.5-kb message to the 165 kDa protein and the 10-kb message to the 270 or 260 kDa protein in brain, heart and kidney homogenates. The detection of Enaptin transcripts in these tissues was consistent with our tissue expression array data. However, we failed to detect the full-length Enaptin of 1014 kDa in northern and western blot analysis probably due to technical limitations attributed to its gigantic size in conjunction with a low abundance. Alternatively, the giant Enaptin transcript may also be developmentally regulated or enriched in cell lines that have not been included in the present study. Spectrin repeats containing molecules are known to mediate membrane cytoskeletal interactions. The increased complexity of the brain as compared to muscle tissues may require various Enaptin isoforms that differ in their domain composition and function.

4.4 Lamin dependent localization of Enaptin

The importance of the lamin A/C network in the proper anchoring of Enaptin to the nuclear membrane is evident from our experiments using lamin A/C^{-/-} cells. Nuclear lamins are type V intermediate filaments and they form a network of filaments underlying the inner

nuclear membrane, providing shape and rigidity to the nucleus forming a molecular interface between the nuclear membrane and the chromatin (Stuurman *et al.*, 1998). Several inner nuclear membrane proteins are thought to be interacting with lamin A/C (Zastrow *et al.*, 2004). The short isoform of Enaptin, nesprin 1- α , and NUANCE were shown to interact directly with lamin A/C in vitro as well in vivo (Mislow *et al.*, 2002a; Libotte, 2004). Our results show that this interaction is essential for the retention of Enaptin in the nuclear membrane. Our transient transfection studies in COS7 cells overexpressing the GFP-Trans fusion protein showed that, the protein can however localise properly to the nuclear membrane, even though it does not contain the demonstrated lamin A/C binding domains of Enaptin. The localisation of the Enaptin GFP-Trans fusion protein could be facilitated by the transmembrane domain and the interaction of the C-terminal tail region to other inner nuclear membrane proteins in the perinuclear space. As evident from Figure 3.23, emerin is also displaced in the lamin A/C^{-/-} cells. It has been shown that UNC-84, a protein in the inner nuclear membrane, also depends upon lamin A/C for its localization (Lee *et al.*, 2002). UNC-84 has been postulated to interact with ANC-1, an orthologue of Enaptin in *C. elegans* (Starr and Han, 2003). The mammalian homologues of UNC-84 are the SUN proteins (Hodzic *et al.*, 2004) and recently they were shown to interact with the tail region of Enaptin in the perinuclear space (Padmakumar, 2004). The mislocalisation of the SUN-1 proteins in the inner nuclear membrane of the lamin A/C^{-/-} cells may eventually lead to the destabilisation and degradation of Enaptin from the nuclear membrane. Interestingly, interaction of Enaptin with lamin A/C was strong enough to redistribute the endogenous Enaptin protein to the mutated lamin-B GFP Δ 2+ nucleoplasmic granules (Figure 3.29) and emerin is retained in the endoplasmic reticulum of cells over-expressing these constructs (Ellis *et al.*, 1997; Vaughan *et al.*, 2001). It appears that many complex protein interactions may exist in the nuclear lamina and the strength of these interactions may vary according to the proteins involved.

The dominant negative effect of Enaptin-GFP fusion protein on endogenous Enaptin and NUANCE suggests that the interaction partners or interaction sites of both these proteins are the same. These interaction sites may be limited in number and the over-expression of the small Enaptin-GFP dominant negative fusion proteins breaks the equilibrium of networking of these proteins by competitive binding to the interacting partners, causing the endogenous Enaptin or NUANCE to displace from the nuclear envelope. We could not observe any mislocalised NUANCE in the cytoplasmic or nuclear compartments and it appears that NUANCE gets degraded fast once it is displaced from the nuclear membrane. In comparison with the tmNUANCE-GFP fusion protein (Libotte, 2004), the Enaptin-GFP-Trans fusion

protein has an additional 86 amino acids (Figure 3.24). Previously we have demonstrated in our group (Libotte, 2004) that tmNUANCE can displace emerin from the nuclear envelope in contrast to the Enaptin-GFP-Trans fusion protein transfected cells, where emerin is properly localized in the nuclear envelope. Our observation with the Enaptin-GFP-Trans fusion protein suggests the importance of the 86 amino acids region between the last spectrin repeat and the transmembrane domain for the retention of emerin in the nuclear envelope. Mislow *et al.* (2002) showed that emerin is interacting with the last seven spectrin repeats before the transmembrane domain of nesprin-1 α (C-terminal isoform of Enaptin). The emerin binding domain was suggested to be present throughout these spectrin repeats with increase in the binding affinity of emerin with increase in the number of spectrin repeats. Eventhough the 86 amino acids region between the last spectrin repeat and transmembrane domain was not included in this study, our results suggest that these short stretch of amino acids could also contribute significantly towards the interaction of emerin to Enaptin.

4.5 Enaptin and Laminopathies

Laminopathies represent a group of human hereditary diseases that arises through mutations in genes encoding nuclear lamina components and lamina associated proteins (Mounkes *et al.*, 2003). At least seven diseases were described that are caused by mutations in the *LMNA* gene (Ostlund and Worman, 2003). Our analysis of the fibroblast cells from patients having mutations in the *LMNA* gene showed a partial mislocalisation of Enaptin into the cytoplasm. All the three mutant cells analysed, having missense mutations in position R401C (Hanisch *et al.*, 2002), R249Q (Ki *et al.*, 2002), and R453W (Holt *et al.*, 2003), were in the rod domain of lamin A/C where the putative nesprin-1 α interaction site was mapped (Mislow *et al.*, 2002a; Zastrow *et al.*, 2004). The mislocalised Enaptin appears to be diffused in the cytoplasm which was never observed in the control cells. A homozygous missense mutation Y259X of *LMNA* causing type 1B limb-girdle muscular dystrophy (LGMD1B) is reported to have mislocalised emerin and nesprin1 α (Muchir *et al.*, 2003) in to the endoplasmic reticulum. The partial cytoplasmic redistribution of Enaptin may be the result of a less stable nuclear lamina formed by mutated lamin A/C proteins.

4.6 Possible functions of Enaptin

The cloning of *D. discoideum* interaptin provided the first example of a potential linker that could directly tether the nucleus to the actin cytoskeleton (Rivero *et al.*, 1998). Until then, most of our knowledge regarding nuclear positioning was focused and based upon

the role of microtubule motors and the microtubules themselves (Reinsch and Gonczy, 1998). The role of the actin cytoskeleton in nuclear migration and positioning was unequivocally demonstrated in genetic studies in *C. elegans*. Mutations in ANC-1 (nuclear anchorage defective) resulted in irregular spacing and clumping of nuclei (Starr and Han, 2002). Similar to interaptin, ANC-1 is composed of an N-terminal actin-binding domain and a C-terminal transmembrane domain, which are separated in contrast to interaptin's coiled-coil rod by spectrin repeats. ANC-1, together with *Drosophila* MSP-300 protein (Rosenberg-Hasson *et al.*, 1996) and the mammalian syne-1, and NUANCE proteins (also known as nesprins) define a novel family of nuclear dystrophins that are related by sequence, domain composition and may be involved in nuclear architecture and organization.

Actin has often been observed in isolated nuclei and for a long time. This has been attributed to the cytoplasmic contamination or to the ability of actin to move freely between cytoplasm and nucleus (Olave *et al.*, 2002). More recently this view has changed and functional roles for nuclear actin are emerging with the finding of actin-related proteins and of actin-associated proteins in the nucleus and of nuclear myosin (Pederson and Aebi, 2002). The identification of further nuclear ABD containing proteins underlines an active role of the actin nucleoskeleton in nuclear physiology.

Our data show a profound enrichment of Enaptin at the nuclear envelope of differentiated myoblasts and may suggest a role for Enaptin in myoblast differentiation. It has been reported recently that a mutant form of lamin A could prevent the in-vitro differentiation of C2C12 myoblasts, underlining the importance of nuclear lamina and associated proteins in muscle differentiation and in pathogenesis of laminopathies (Favreau *et al.*, 2004). We could not observe the intranuclear foci localisation or redistribution of Enaptin into the cytoplasm as has been suggested previously (Mislow *et al.*, 2002b; Zhang *et al.*, 2001). Instead, our observation was closer to the pattern observed for syne-1 at the nuclei in the neuromuscular junction (Apel *et al.*, 2000). We could detect Enaptin at the nuclear envelope and nucleoplasm in the myoblasts and it appears to be enriched at the nuclear membrane during differentiation from myoblasts to myotubes. The nuclear lamina is thought to have regulatory role in gene expression during differentiation of myocytes and more work has to be done to clarify what kind of role Enaptin may have in such a scenario.

Enaptin and NUANCE are not only related by sequence to each other but they also seem to have similar functions. While *C. elegans* and *Drosophila* have a single gene each, ANC-1 and MSP-300 respectively, mammals have two genes Enaptin and NUANCE of similar nature. Why do mammals contain then two similar giant genes? One would assume

that this is a precaution of nature to preserve vital and important genes. It is however interesting to note that this is not a specific feature attributed only to NUANCE and Enaptin genes. The mammalian spectraplakin genes ACF7 and BPAG1 (Fuchs and Karakesisoglou, 2001) or the dystrophin/utrophin genes (Deconinck *et al.*, 1997) are such examples. Preliminary data however suggests that while NUANCE and Enaptin are similar in design, they harbour differences in regard not only to their expression pattern, but also to the isoform diversity and the subcellular distribution of their isoforms.

Our studies using the embryonic stem cell technology could shed some light on the potential involvement of Enaptin in human neuromuscular diseases and also whether Enaptin and NUANCE correspond to the biological Atlas of the cell, holding up and keeping the nucleus (universe) in position. Revealing their function is still a great challenge since they are molecules of complex nature and the largest ones of the α -actinin super family.

Summary

5 Summary

The α -actinin superfamily is the largest of the F-actin cross-linking protein families. Members of this superfamily have an actin-binding domain (ABD) consisting of a pair of calponin homology domains. We have cloned and characterized a novel giant actin-binding protein called Enaptin, which belongs to this family. Together with NUANCE, Enaptin forms a group of giant proteins that associate with the F-actin cytoskeleton as well as the nuclear membrane. Enaptin is composed of an N-terminal α -actinin type ABD, followed by a long coiled-coil rod and a transmembrane domain at the C-terminus. We have cloned and assembled a cDNA for Enaptin and found that the longest open reading frame of Enaptin encompasses 27,669 bp and predicts a 1014 kDa protein. The human *Enaptin* gene located on 6q23.1-25.3 spreads over 515 kb and gives rise to several splicing isoforms (Nesprin-1, Myne-1, Syne-1, CPG2). Northern blot analysis identified a >14 kb transcript and an additional transcript of 5.5 kb in brain. Using a polyclonal antibody against the ABD of Enaptin we detected a protein of approximately 400 kDa in tissues like brain and skeletal muscle. Further analysis showed that Enaptin is expressed in a wide range of tissues.

Polyclonal antibodies generated against the C-terminus of Enaptin detected the protein at the nuclear envelope and in the cytosol of human fibroblasts. We showed that Enaptin is located in the outer nuclear membrane by selective permeabilisation of the plasma membrane with digitonin, furthermore its nuclear envelope localization was not affected by disruption of the actin cytoskeleton. Our studies also indicated that the nuclear envelope localization of Enaptin depended on lamin A/C. This is underlined by our findings in fibroblast cells from patients affected with laminopathies where we observed an altered distribution of Enaptin.

With the N-terminal ABD domain and its C-terminal transmembrane domain, Enaptin has the potential to connect the nucleus to the actin cytoskeleton. Studies on Enaptin orthologues in lower eukaryotes proposed a role for these proteins in nuclear positioning and anchorage and in embryonic muscle development. Our myoblast differentiation studies showed an altered expression of Enaptin during differentiation. In order to reveal the functions of Enaptin and its link to human disease, we initiated a project for targeted disruption of Enaptin in the mouse.

5 Zusammenfassung

Enaptin ist ein neues F-Aktin bindendes Protein, das wir bei einer Suche nach neuartigen Proteinen der α -Aktinin Familie im Genom von Maus und Mensch identifiziert haben. Enaptin besitzt eine α -Aktinin-ähnliche Aktinbindedomäne am Aminoterminal, die von einem langen helikalen Bereich mit mehreren Spektrindomänen gefolgt wird. Am C-Terminus ist eine Transmembrandomäne lokalisiert, mit der Enaptin in der Kernmembran verankert werden kann. Zusammen mit NUANCE, das ebenfalls in unserer Gruppe beschrieben wurde, gehört Enaptin zu einer neuen Klasse von Proteinen, die potentiell das Aktinzytoskelett mit dem Zellkern verbinden.

In dieser Arbeit wurde die cDNA von Enaptin assembliert. Der längste offene Leserahmen kodiert für eine 27.669 b lange mRNA und führt zu einem Protein von 1014 kDa. Das menschliche Enaptin ist auf Chromosom 6 an der Position 6q23.1-25.3 lokalisiert und umfasst 515 kb. Für Enaptin sind die Spleissvarianten Nesprin-1, Myne-1, Syne-1 und CPG2 beschrieben worden. In Northernblots konnten wir in Gehirn Transkripte von mehr als 14 kb und 5.5 kb nachweisen; ein polyklonaler Antikörper, der gegen die Aktinbindedomäne von Enaptin erzeugt wurde, erkennt ein Protein von 400 kDa in Gehirn und Skelettmuskel. Polyklonale Antikörper, die gegen die C-terminale Region von Enaptin gerichtet sind, färben in Immunfluoreszenzanalysen die Kernmembran in humanen Fibroblasten. Für diese Lokalisation ist der C-terminale Bereich verantwortlich. Die Lokalisation an der Kernmembran wird aber auch von LaminA/C beeinflusst, da die Enaptinverteilung in Fibroblasten von Patienten verändert ist, die an Laminopathien leiden.

Basierend auf Befunden, die für Enaptin-ähnliche Proteine in niederen Eukaryonten erzielt wurden, nehmen wir an, dass Enaptin eine Rolle bei der Zellkernverankerung und/oder Zellkernpositionierung besitzt und an Kernwanderungsprozessen in der Entwicklung beteiligt sein kann. Mit Hilfe von Mausmutanten soll diese Frage geklärt werden.

Bibliography

6 Bibliography

- Abe, H., Endo, T., Yamamoto, K. and Obinata, T. (1990) Sequence of cDNAs encoding actin depolymerizing factor and cofilin of embryonic chicken skeletal muscle: two functionally distinct actin-regulatory proteins exhibit high structural homology. *Biochemistry*, **29**, 7420-7425.
- Alberts, B., Bray, D., Lewis, J., Raff, M., Roberts, K. and Watson, J.D. (1994) *Molecular Biology of the Cell*. Garland Publishing, Inc., New York & London.
- Alonso, L. and Fuchs, E. (2003) Stem cells of the skin epithelium. *Proc Natl Acad Sci U S A*, **100 Suppl 1**, 11830-11835.
- Ampe, C., Markey, F., Lindberg, U. and Vandekerckhove, J. (1988) The primary structure of human platelet profilin: reinvestigation of the calf spleen profilin sequence. *FEBS Lett*, **228**, 17-21.
- Apel, E.D., Lewis, R.M., Grady, R.M. and Sanes, J.R. (2000) Syne-1, a dystrophin- and Klarsicht-related protein associated with synaptic nuclei at the neuromuscular junction. *J Biol Chem*, **275**, 31986-31995.
- Ayscough, K.R. (1998) In vivo functions of actin-binding proteins. *Curr Opin Cell Biol*, **10**, 102-111.
- Barron-Casella, E.A., Torres, M.A., Scherer, S.W., Heng, H.H., Tsui, L.C. and Casella, J.F. (1995) Sequence analysis and chromosomal localization of human Cap Z. Conserved residues within the actin-binding domain may link Cap Z to gelsolin/severin and profilin protein families. *J Biol Chem*, **270**, 21472-21479.
- Bassell, G. and Singer, R.H. (1997) mRNA and cytoskeletal filaments. *Curr Opin Cell Biol*, **9**, 109-115.
- Bione, S., Maestrini, E., Rivella, S., Mancini, M., Regis, S., Romeo, G. and Toniolo, D. (1994) Identification of a novel X-linked gene responsible for Emery-Dreifuss muscular dystrophy. *Nat Genet*, **8**, 323-327.
- Blake, D.J. and Kroger, S. (2000) The neurobiology of duchenne muscular dystrophy: learning lessons from muscle? *Trends Neurosci*, **23**, 92-99.
- Blake, D.J., Tinsley, J.M. and Davies, K.E. (1996) Utrophin: a structural and functional comparison to dystrophin. *Brain Pathol*, **6**, 37-47.
- Blanchard, A., Ohanian, V. and Critchley, D. (1989) The structure and function of alpha-actinin. *J Muscle Res Cell Motil*, **10**, 280-289.
- Bonne, G., Di Barletta, M.R., Varnous, S., Becane, H.M., Hammouda, E.H., Merlini, L., Muntoni, F., Greenberg, C.R., Gary, F., Urtizberea, J.A., Duboc, D., Fardeau, M., Toniolo, D. and Schwartz, K. (1999) Mutations in the gene encoding lamin A/C cause autosomal dominant Emery-Dreifuss muscular dystrophy. *Nat Genet*, **21**, 285-288.
- Braune, S. (2001) Identification and characterisation of Enaptin, a novel protein of a-actinin type. *Medical Faculty*. University of Cologne, Cologne.
- Brown, A., Bernier, G., Mathieu, M., Rossant, J. and Kothary, R. (1995) The mouse dystonia musculorum gene is a neural isoform of bullous pemphigoid antigen 1. *Nat Genet*, **10**, 301-306.
- Burke, B., Mounkes, L.C. and Stewart, C.L. (2001) The nuclear envelope in muscular dystrophy and cardiovascular diseases. *Traffic*, **2**, 675-683.
- Burke, B. and Stewart, C.L. (2002) Life at the edge: the nuclear envelope and human disease. *Nat Rev Mol Cell Biol*, **3**, 575-585.
- Cao, H. and Hegele, R.A. (2000) Nuclear lamin A/C R482Q mutation in canadian kindreds with Dunnigan-type familial partial lipodystrophy. *Hum Mol Genet*, **9**, 109-112.
- Chan, Y. and Kunkel, L.M. (1997) In vitro expressed dystrophin fragments do not associate with each other. *FEBS Lett*, **410**, 153-159.
- Chomeczynski, P. and Sacchi, N. (1987) Single-step method of RNA isolation by acid

- guanidinium thiocyanate-phenol-chloroform extraction. *Anal Biochem*, **162**, 156-159.
- Cutler, D.A., Sullivan, T., Marcus-Samuels, B., Stewart, C.L. and Reitman, M.L. (2002) Characterization of adiposity and metabolism in Lmna-deficient mice. *Biochem Biophys Res Commun*, **291**, 522-527.
- Dalpe, G., Leclerc, N., Vallee, A., Messer, A., Mathieu, M., De Repentigny, Y. and Kothary, R. (1998) Dystonin is essential for maintaining neuronal cytoskeleton organization. *Mol Cell Neurosci*, **10**, 243-257.
- De Matteis, M.A. and Morrow, J.S. (2000) Spectrin tethers and mesh in the biosynthetic pathway. *J Cell Sci*, **113 (Pt 13)**, 2331-2343.
- De Sandre-Giovannoli, A., Bernard, R., Cau, P., Navarro, C., Amiel, J., Boccaccio, I., Lyonnet, S., Stewart, C.L., Munnich, A., Le Merrer, M. and Levy, N. (2003) Lamin A truncation in Hutchinson-Gilford progeria. *Science*, **300**, 2055.
- De Sandre-Giovannoli, A., Chaouch, M., Kozlov, S., Vallat, J.M., Tazir, M., Kassouri, N., Szepietowski, P., Hammadouche, T., Vandenberghe, A., Stewart, C.L., Grid, D. and Levy, N. (2002) Homozygous defects in LMNA, encoding lamin A/C nuclear-envelope proteins, cause autosomal recessive axonal neuropathy in human (Charcot-Marie-Tooth disorder type 2) and mouse. *Am J Hum Genet*, **70**, 726-736.
- Dechat, T., Vlcek, S. and Foisner, R. (2000) Review: lamina-associated polypeptide 2 isoforms and related proteins in cell cycle-dependent nuclear structure dynamics. *J Struct Biol*, **129**, 335-345.
- Deconinck, A.E., Rafael, J.A., Skinner, J.A., Brown, S.C., Potter, A.C., Metzinger, L., Watt, D.J., Dickson, J.G., Tinsley, J.M. and Davies, K.E. (1997) Utrophin-dystrophin-deficient mice as a model for Duchenne muscular dystrophy. *Cell*, **90**, 717-727.
- Delaunay, J. (2002) Molecular basis of red cell membrane disorders. *Acta Haematol*, **108**, 210-218.
- dos Remedios, C.G., Chhabra, D., Kekic, M., Dedova, I.V., Tsubakihara, M., Berry, D.A. and Nosworthy, N.J. (2003) Actin binding proteins: regulation of cytoskeletal microfilaments. *Physiol Rev*, **83**, 433-473.
- Ellis, D.J., Jenkins, H., Whitfield, W.G. and Hutchison, C.J. (1997) GST-lamin fusion proteins act as dominant negative mutants in *Xenopus* egg extract and reveal the function of the lamina in DNA replication. *J Cell Sci*, **110 (Pt 20)**, 2507-2518.
- Emery, A.E. (1989) Emery-Dreifuss muscular dystrophy and other related disorders. *Br Med Bull*, **45**, 772-787.
- Engel, J., Fasold, H., Hulla, F.W., Waechter, F. and Wegner, A. (1977) The polymerization reaction of muscle actin. *Mol Cell Biochem*, **18**, 3-13.
- Fabbrizio, E., Bonet-Kerrache, A., Leger, J.J. and Mornet, D. (1993) Actin-dystrophin interface. *Biochemistry*, **32**, 10457-10463.
- Farah, C.S. and Reinach, F.C. (1995) The troponin complex and regulation of muscle contraction. *Faseb J*, **9**, 755-767.
- Fatkin, D., MacRae, C., Sasaki, T., Wolff, M.R., Porcu, M., Frenneaux, M., Atherton, J., Vidaillet, H.J., Jr., Spudich, S., De Girolami, U., Seidman, J.G., Seidman, C., Muntoni, F., Muehle, G., Johnson, W. and McDonough, B. (1999) Missense mutations in the rod domain of the lamin A/C gene as causes of dilated cardiomyopathy and conduction-system disease. *N Engl J Med*, **341**, 1715-1724.
- Favreau, C., Dubosclard, E., Ostlund, C., Vigouroux, C., Capeau, J., Wehnert, M., Higuete, D., Worman, H.J., Courvalin, J.C. and Buendia, B. (2003) Expression of lamin A mutated in the carboxyl-terminal tail generates an aberrant nuclear phenotype similar to that observed in cells from patients with Dunnigan-type partial lipodystrophy and Emery-Dreifuss muscular dystrophy. *Exp Cell Res*, **282**, 14-23.
- Favreau, C., Higuete, D., Courvalin, J.C. and Buendia, B. (2004) Expression of a mutant lamin A that causes Emery-Dreifuss muscular dystrophy inhibits in vitro differentiation of

- C2C12 myoblasts. *Mol Cell Biol*, **24**, 1481-1492.
- Fishkind, D.J. and Wang, Y.L. (1995) New horizons for cytokinesis. *Curr Opin Cell Biol*, **7**, 23-31.
- Foisner, R. and Gerace, L. (1993) Integral membrane proteins of the nuclear envelope interact with lamins and chromosomes, and binding is modulated by mitotic phosphorylation. *Cell*, **73**, 1267-1279.
- Fuchs, E. and Cleveland, D.W. (1998) A structural scaffolding of intermediate filaments in health and disease. *Science*, **279**, 514-519.
- Fuchs, E. and Karakesisoglou, I. (2001) Bridging cytoskeletal intersections. *Genes Dev*, **15**, 1-14.
- Fucini, P., Koppel, B., Schleicher, M., Lustig, A., Holak, T.A., Muller, R., Stewart, M. and Noegel, A.A. (1999) Molecular architecture of the rod domain of the Dictyostelium gelation factor (ABP120). *J Mol Biol*, **291**, 1017-1023.
- Goldman, R.D., Gruenbaum, Y., Moir, R.D., Shumaker, D.K. and Spann, T.P. (2002) Nuclear lamins: building blocks of nuclear architecture. *Genes Dev*, **16**, 533-547.
- Goodman, S.R., Shiffer, K.A., Casoria, L.A. and Eyster, M.E. (1982) Identification of the molecular defect in the erythrocyte membrane skeleton of some kindreds with hereditary spherocytosis. *Blood*, **60**, 772-784.
- Gorlin, J.B., Yamin, R., Egan, S., Stewart, M., Stossel, T.P., Kwiatkowski, D.J. and Hartwig, J.H. (1990) Human endothelial actin-binding protein (ABP-280, nonmuscle filamin): a molecular leaf spring. *J Cell Biol*, **111**, 1089-1105.
- Gospe, S.M., Jr., Lazaro, R.P., Lava, N.S., Grootsholten, P.M., Scott, M.O. and Fischbeck, K.H. (1989) Familial X-linked myalgia and cramps: a nonprogressive myopathy associated with a deletion in the dystrophin gene. *Neurology*, **39**, 1277-1280.
- Gough, L.L., Fan, J., Chu, S., Winnick, S. and Beck, K.A. (2003) Golgi localization of Syne-1. *Mol Biol Cell*, **14**, 2410-2424.
- Gregory, S.L. and Brown, N.H. (1998) kakapo, a gene required for adhesion between and within cell layers in Drosophila, encodes a large cytoskeletal linker protein related to plectin and dystrophin. *J Cell Biol*, **143**, 1271-1282.
- Guo, L., Degenstein, L., Dowling, J., Yu, Q.C., Wollmann, R., Perman, B. and Fuchs, E. (1995) Gene targeting of BPAG1: abnormalities in mechanical strength and cell migration in stratified epithelia and neurologic degeneration. *Cell*, **81**, 233-243.
- Hall, A. (1994) Small GTP-binding proteins and the regulation of the actin cytoskeleton. *Annu Rev Cell Biol*, **10**, 31-54.
- Hammonds, R.G., Jr. (1987) Protein sequence of DMD gene is related to actin-binding domain of alpha-actinin. *Cell*, **51**, 1.
- Hanisch, F., Neudecker, S., Wehnert, M. and Zierz, S. (2002) [Hauptmann-Thannhauser muscular dystrophy and differential diagnosis of myopathies associated with contractures]. *Nervenarzt*, **73**, 1004-1011.
- Haraguchi, T., Koujin, T., Segura-Totten, M., Lee, K.K., Matsuoka, Y., Yoneda, Y., Wilson, K.L. and Hiraoka, Y. (2001) BAF is required for emerin assembly into the reforming nuclear envelope. *J Cell Sci*, **114**, 4575-4585.
- Hartwig, J.H. (1995) Actin-binding proteins. 1: Spectrin super family. *Protein Profile*, **2**, 703-800.
- Hicks, G.R. and Raikhel, N.V. (1995) Protein import into the nucleus: an integrated view. *Annu Rev Cell Dev Biol*, **11**, 155-188.
- Hodzic, D.M., Yeater, D.B., Bengtsson, L., Otto, H. and Stahl, P.D. (2004) Sun2 is a novel mammalian inner nuclear membrane protein. *J Biol Chem*.
- Holt, I., Ostlund, C., Stewart, C.L., Man, N., Worman, H.J. and Morris, G.E. (2003) Effect of pathogenic mis-sense mutations in lamin A on its interaction with emerin in vivo. *J Cell Sci*, **116**, 3027-3035.

- Hutchison, C.J., Alvarez-Reyes, M. and Vaughan, O.A. (2001) Lamins in disease: why do ubiquitously expressed nuclear envelope proteins give rise to tissue-specific disease phenotypes? *J Cell Sci*, **114**, 9-19.
- Hutchison, C.J., Bridger, J.M., Cox, L.S. and Kill, I.R. (1994) Weaving a pattern from disparate threads: lamin function in nuclear assembly and DNA replication. *J Cell Sci*, **107 (Pt 12)**, 3259-3269.
- Ishisaki, Z., Takaishi, M., Furuta, I. and Huh, N. (2001) Calmin, a protein with calponin homology and transmembrane domains expressed in maturing spermatogenic cells. *Genomics*, **74**, 172-179.
- Jackle, H. and Jahn, R. (1998) Vesicle transport: klarsicht clears up the matter. *Curr Biol*, **8**, R542-544.
- Karakesisoglou, I., Yang, Y. and Fuchs, E. (2000) An epidermal plakin that integrates actin and microtubule networks at cellular junctions. *J Cell Biol*, **149**, 195-208.
- Kedes, L., Ng, S.Y., Lin, C.S., Gunning, P., Eddy, R., Shows, T. and Leavitt, J. (1985) The human beta-actin multigene family. *Trans Assoc Am Physicians*, **98**, 42-46.
- Keep, N.H., Winder, S.J., Moores, C.A., Walke, S., Norwood, F.L. and Kendrick-Jones, J. (1999) Crystal structure of the actin-binding region of utrophin reveals a head-to-tail dimer. *Structure Fold Des*, **7**, 1539-1546.
- Ki, C.S., Hong, J.S., Jeong, G.Y., Ahn, K.J., Choi, K.M., Kim, D.K. and Kim, J.W. (2002) Identification of lamin A/C (LMNA) gene mutations in Korean patients with autosomal dominant Emery-Dreifuss muscular dystrophy and limb-girdle muscular dystrophy 1B. *J Hum Genet*, **47**, 225-228.
- Koenig, M., Monaco, A.P. and Kunkel, L.M. (1988) The complete sequence of dystrophin predicts a rod-shaped cytoskeletal protein. *Cell*, **53**, 219-226.
- Korenbaum, E. and Rivero, F. (2002) Calponin homology domains at a glance. *J Cell Sci*, **115**, 3543-3545.
- Krauss, S.W., Heald, R., Lee, G., Nunomura, W., Gimm, J.A., Mohandas, N. and Chasis, J.A. (2002) Two distinct domains of protein 4.1 critical for assembly of functional nuclei in vitro. *J Biol Chem*, **277**, 44339-44346.
- Kreis, T. and Vale, R. (1999) *Guidebook to the cytoskeletal and motor proteins*. Oxford University Press Inc., New York.
- Kubler, E. and Riezman, H. (1993) Actin and fimbrin are required for the internalization step of endocytosis in yeast. *Embo J*, **12**, 2855-2862.
- Kuhn, T.B., Meberg, P.J., Brown, M.D., Bernstein, B.W., Minamide, L.S., Jensen, J.R., Okada, K., Soda, E.A. and Bamberg, J.R. (2000) Regulating actin dynamics in neuronal growth cones by ADF/cofilin and rho family GTPases. *J Neurobiol*, **44**, 126-144.
- Kutay, U., Hartmann, E. and Rapoport, T.A. (1993) A class of membrane proteins with a C-terminal anchor. *Trends Cell Biol*, **3**, 72-75.
- Kwiatkowski, D.J. (1999) Functions of gelsolin: motility, signaling, apoptosis, cancer. *Curr Opin Cell Biol*, **11**, 103-108.
- Kwiatkowski, D.J., Stossel, T.P., Orkin, S.H., Mole, J.E., Colten, H.R. and Yin, H.L. (1986) Plasma and cytoplasmic gelsolins are encoded by a single gene and contain a duplicated actin-binding domain. *Nature*, **323**, 455-458.
- Kyhse-Andersen, J. (1984) Electrophoretic transfer of multiple gels: a simple apparatus without buffer tank for rapid transfer of proteins from polyacrylamide to nitrocellulose. *J Biochem Biophys Methods*, **10**, 203-209.
- Laemmli, U.K. (1970) Cleavage of structural proteins during the assembly of the head of bacteriophage T4. *Nature*, **227**, 680-685.
- Lambert de Rouvroit, C. and Goffinet, A.M. (2001) Neuronal migration. *Mech Dev*, **105**, 47-56.

- Lammerding, J., Schulze, P.C., Takahashi, T., Kozlov, S., Sullivan, T., Kamm, R.D., Stewart, C.L. and Lee, R.T. (2004) Lamin A/C deficiency causes defective nuclear mechanics and mechanotransduction. *J Clin Invest*, **113**, 370-378.
- Langford, G.M. (1995) Actin- and microtubule-dependent organelle motors: interrelationships between the two motility systems. *Curr Opin Cell Biol*, **7**, 82-88.
- Law, R., Harper, S., Speicher, D.W. and Discher, D.E. (2004) Influence of lateral association on forced unfolding of antiparallel spectrin heterodimers. *J Biol Chem*, **279**, 16410-16416.
- Lee, K.K., Starr, D., Cohen, M., Liu, J., Han, M., Wilson, K.L. and Gruenbaum, Y. (2002) Lamin-dependent localization of UNC-84, a protein required for nuclear migration in *Caenorhabditis elegans*. *Mol Biol Cell*, **13**, 892-901.
- Lees-Miller, J.P. and Helfman, D.M. (1991) The molecular basis for tropomyosin isoform diversity. *Bioessays*, **13**, 429-437.
- Lehrach, H., Diamond, D., Wozney, J.M. and Boedtker, H. (1977) RNA molecular weight determinations by gel electrophoresis under denaturing conditions, a critical reexamination. *Biochemistry*, **16**, 4743-4751.
- Leung, C.L., Sun, D. and Liem, R.K. (1999) The intermediate filament protein peripherin is the specific interaction partner of mouse BPAG1-n (dystonin) in neurons. *J Cell Biol*, **144**, 435-446.
- Libotte, T. (2004) Charakterisierung von NUANCE, einem protein der α -aktinin superfamilie. *Mathematics and Natural science Faculty*. University of Cologne, Cologne.
- Lidov, H.G., Byers, T.J., Watkins, S.C. and Kunkel, L.M. (1990) Localization of dystrophin to postsynaptic regions of central nervous system cortical neurons. *Nature*, **348**, 725-728.
- Lin, C.S., Shen, W., Chen, Z.P., Tu, Y.H. and Matsudaira, P. (1994) Identification of I-plastin, a human fimbrin isoform expressed in intestine and kidney. *Mol Cell Biol*, **14**, 2457-2467.
- Lin, F., Blake, D.L., Callebaut, I., Skerjanc, I.S., Holmer, L., McBurney, M.W., Paulin-Levasseur, M. and Worman, H.J. (2000) MAN1, an inner nuclear membrane protein that shares the LEM domain with lamina-associated polypeptide 2 and emerin. *J Biol Chem*, **275**, 4840-4847.
- Maidment, S.L. and Ellis, J.A. (2002) Muscular dystrophies, dilated cardiomyopathy, lipodystrophy and neuropathy: the nuclear connection. *Expert Rev Mol Med*, **2002**, 1-21.
- Mansharamani, M., Hewetson, A. and Chilton, B.S. (2001) Cloning and characterization of an atypical Type IV P-type ATPase that binds to the RING motif of RUSH transcription factors. *J Biol Chem*, **276**, 3641-3649.
- Matsudaira, P. (1994) Actin crosslinking proteins at the leading edge. *Semin Cell Biol*, **5**, 165-174.
- McLean, W.H., Pulkkinen, L., Smith, F.J., Rugg, E.L., Lane, E.B., Bullrich, F., Burgeson, R.E., Amano, S., Hudson, D.L., Owaribe, K., McGrath, J.A., McMillan, J.R., Eady, R.A., Leigh, I.M., Christiano, A.M. and Uitto, J. (1996) Loss of plectin causes epidermolysis bullosa with muscular dystrophy: cDNA cloning and genomic organization. *Genes Dev*, **10**, 1724-1735.
- Meagher, R.B., McKinney, E.C. and Vitale, A.V. (1999) The evolution of new structures: clues from plant cytoskeletal genes. *Trends Genet*, **15**, 278-284.
- Menke, A. and Jockusch, H. (1995) Extent of shock-induced membrane leakage in human and mouse myotubes depends on dystrophin. *J Cell Sci*, **108 (Pt 2)**, 727-733.
- Mislow, J.M., Holaska, J.M., Kim, M.S., Lee, K.K., Segura-Totten, M., Wilson, K.L. and McNally, E.M. (2002) Nesprin-1 α self-associates and binds directly to emerin and lamin A in vitro. *FEBS Lett*, **525**, 135-140.

- Mislow, J.M., Kim, M.S., Davis, D.B. and McNally, E.M. (2002) Myne-1, a spectrin repeat transmembrane protein of the myocyte inner nuclear membrane, interacts with lamin A/C. *J Cell Sci*, **115**, 61-70.
- Moir, R.D., Spann, T.P., Lopez-Soler, R.I., Yoon, M., Goldman, A.E., Khuon, S. and Goldman, R.D. (2000) Review: the dynamics of the nuclear lamins during the cell cycle-- relationship between structure and function. *J Struct Biol*, **129**, 324-334.
- Mosley-Bishop, K.L., Li, Q., Patterson, L. and Fischer, J.A. (1999) Molecular analysis of the klarsicht gene and its role in nuclear migration within differentiating cells of the Drosophila eye. *Curr Biol*, **9**, 1211-1220.
- Mounkes, L., Kozlov, S., Burke, B. and Stewart, C.L. (2003) The laminopathies: nuclear structure meets disease. *Curr Opin Genet Dev*, **13**, 223-230.
- Mounkes, L.C., Burke, B. and Stewart, C.L. (2001) The A-type lamins: nuclear structural proteins as a focus for muscular dystrophy and cardiovascular diseases. *Trends Cardiovasc Med*, **11**, 280-285.
- Mounkes, L.C., Kozlov, S., Hernandez, L., Sullivan, T. and Stewart, C.L. (2003) A progeroid syndrome in mice is caused by defects in A-type lamins. *Nature*, **423**, 298-301.
- Muchir, A., Bonne, G., van der Kooij, A.J., van Meegen, M., Baas, F., Bolhuis, P.A., de Visser, M. and Schwartz, K. (2000) Identification of mutations in the gene encoding lamins A/C in autosomal dominant limb girdle muscular dystrophy with atrioventricular conduction disturbances (LGMD1B). *Hum Mol Genet*, **9**, 1453-1459.
- Muchir, A., van Engelen, B.G., Lammens, M., Mislow, J.M., McNally, E., Schwartz, K. and Bonne, G. (2003) Nuclear envelope alterations in fibroblasts from LGMD1B patients carrying nonsense Y259X heterozygous or homozygous mutation in lamin A/C gene. *Exp Cell Res*, **291**, 352-362.
- Muralikrishna, B., Dhawan, J., Rangaraj, N. and Parnaik, V.K. (2001) Distinct changes in intranuclear lamin A/C organization during myoblast differentiation. *J Cell Sci*, **114**, 4001-4011.
- Nagano, A., Koga, R., Ogawa, M., Kurano, Y., Kawada, J., Okada, R., Hayashi, Y.K., Tsukahara, T. and Arahata, K. (1996) Emerin deficiency at the nuclear membrane in patients with Emery-Dreifuss muscular dystrophy. *Nat Genet*, **12**, 254-259.
- Nedivi, E., Fieldust, S., Theill, L.E. and Hevron, D. (1996) A set of genes expressed in response to light in the adult cerebral cortex and regulated during development. *Proc Natl Acad Sci U S A*, **93**, 2048-2053.
- Nikolova, V., Leimena, C., McMahan, A.C., Tan, J.C., Chandar, S., Jogia, D., Kesteven, S.H., Michalicek, J., Otway, R., Verheyen, F., Rainer, S., Stewart, C.L., Martin, D., Feneley, M.P. and Fatkin, D. (2004) Defects in nuclear structure and function promote dilated cardiomyopathy in lamin A/C-deficient mice. *J Clin Invest*, **113**, 357-369.
- Noegel, A.A., Rapp, S., Lottspeich, F., Schleicher, M. and Stewart, M. (1989) The Dictyostelium gelation factor shares a putative actin binding site with alpha-actinins and dystrophin and also has a rod domain containing six 100-residue motifs that appear to have a cross-beta conformation. *J Cell Biol*, **109**, 607-618.
- Norwood, F.L., Sutherland-Smith, A.J., Keep, N.H. and Kendrick-Jones, J. (2000) The structure of the N-terminal actin-binding domain of human dystrophin and how mutations in this domain may cause Duchenne or Becker muscular dystrophy. *Structure Fold Des*, **8**, 481-491.
- Novelli, G., Muchir, A., Sangiulio, F., Helbling-Leclerc, A., D'Apice, M.R., Massart, C., Capon, F., Sbraccia, P., Federici, M., Lauro, R., Tudisco, C., Pallotta, R., Scarano, G., Dallapiccola, B., Merlini, L. and Bonne, G. (2002) Mandibuloacral dysplasia is caused by a mutation in LMNA-encoding lamin A/C. *Am J Hum Genet*, **71**, 426-431.
- Olave, I.A., Reck-Peterson, S.L. and Crabtree, G.R. (2002) Nuclear actin and actin-related proteins in chromatin remodeling. *Annu Rev Biochem*, **71**, 755-781.

- Ostlund, C., Bonne, G., Schwartz, K. and Worman, H.J. (2001) Properties of lamin A mutants found in Emery-Dreifuss muscular dystrophy, cardiomyopathy and Dunnigan-type partial lipodystrophy. *J Cell Sci*, **114**, 4435-4445.
- Ostlund, C. and Worman, H.J. (2003) Nuclear envelope proteins and neuromuscular diseases. *Muscle Nerve*, **27**, 393-406.
- Padmakumar, V.C. (2004) Characterisation of Enaptin and Sun-1, two novel mammalian nuclear envelope proteins. *Mathematics and Natural science Faculty*. University of Cologne, Cologne.
- Padmakumar, V.C., Abraham, S., Braune, S., Noegel, A.A., Tunggal, B., Karakesisoglou, I. and Korenbaum, E. (2004) Enaptin, a giant actin-binding protein, is an element of the nuclear membrane and the actin cytoskeleton. *Exp Cell Res*, **295**, 330-339.
- Patterson, K., Molofsky, A.B., Robinson, C., Acosta, S., Cater, C. and Fischer, J.A. (2004) The functions of Klarsicht and nuclear lamin in developmentally regulated nuclear migrations of photoreceptor cells in the Drosophila eye. *Mol Biol Cell*, **15**, 600-610.
- Pederson, T. and Aebi, U. (2002) Actin in the nucleus: what form and what for? *J Struct Biol*, **140**, 3-9.
- Pollard, T.D. and Cooper, J.A. (1986) Actin and actin-binding proteins. A critical evaluation of mechanisms and functions. *Annu Rev Biochem*, **55**, 987-1035.
- Pringault, E., Arpin, M., Garcia, A., Finidori, J. and Louvard, D. (1986) A human villin cDNA clone to investigate the differentiation of intestinal and kidney cells in vivo and in culture. *Embo J*, **5**, 3119-3124.
- Puius, Y.A., Mahoney, N.M. and Almo, S.C. (1998) The modular structure of actin-regulatory proteins. *Curr Opin Cell Biol*, **10**, 23-34.
- Raharjo, W.H., Enarson, P., Sullivan, T., Stewart, C.L. and Burke, B. (2001) Nuclear envelope defects associated with LMNA mutations cause dilated cardiomyopathy and Emery-Dreifuss muscular dystrophy. *J Cell Sci*, **114**, 4447-4457.
- Reinsch, S. and Gonczy, P. (1998) Mechanisms of nuclear positioning. *J Cell Sci*, **111** (Pt 16), 2283-2295.
- Rezniczek, G.A., de Pereda, J.M., Reipert, S. and Wiche, G. (1998) Linking integrin alpha6beta4-based cell adhesion to the intermediate filament cytoskeleton: direct interaction between the beta4 subunit and plectin at multiple molecular sites. *J Cell Biol*, **141**, 209-225.
- Rivero, F., Kuspa, A., Brokamp, R., Matzner, M. and Noegel, A.A. (1998) Interaptin, an actin-binding protein of the alpha-actinin superfamily in Dictyostelium discoideum, is developmentally and cAMP-regulated and associates with intracellular membrane compartments. *J Cell Biol*, **142**, 735-750.
- Rolls, M.M., Stein, P.A., Taylor, S.S., Ha, E., McKeon, F. and Rapoport, T.A. (1999) A visual screen of a GFP-fusion library identifies a new type of nuclear envelope membrane protein. *J Cell Biol*, **146**, 29-44.
- Roper, K., Gregory, S.L. and Brown, N.H. (2002) The 'spectraplakins': cytoskeletal giants with characteristics of both spectrin and plakin families. *J Cell Sci*, **115**, 4215-4225.
- Rosenberg-Hasson, Y., Renert-Pasca, M. and Volk, T. (1996) A Drosophila dystrophin-related protein, MSP-300, is required for embryonic muscle morphogenesis. *Mech Dev*, **60**, 83-94.
- Ryan, T.A., Li, L., Chin, L.S., Greengard, P. and Smith, S.J. (1996) Synaptic vesicle recycling in synapsin I knock-out mice. *J Cell Biol*, **134**, 1219-1227.
- Sambrook, J. and Russell, D.w. (2001) *Molecular Cloning A Laboratory Manual*. Cold spring Harbor Laboratory Press, New York.
- Samejima, K., Svingen, P.A., Basi, G.S., Kottke, T., Mesner, P.W., Jr., Stewart, L., Durrieu, F., Poirier, G.G., Alnemri, E.S., Champoux, J.J., Kaufmann, S.H. and Earnshaw, W.C. (1999) Caspase-mediated cleavage of DNA topoisomerase I at unconventional sites

- during apoptosis. *J Biol Chem*, **274**, 4335-4340.
- Schafer, D.A. and Cooper, J.A. (1995) Control of actin assembly at filament ends. *Annu Rev Cell Dev Biol*, **11**, 497-518.
- Smith, E.A. and Fuchs, E. (1998) Defining the interactions between intermediate filaments and desmosomes. *J Cell Biol*, **141**, 1229-1241.
- Stanley, J.R., Tanaka, T., Mueller, S., Klaus-Kovtun, V. and Roop, D. (1988) Isolation of complementary DNA for bullous pemphigoid antigen by use of patients' autoantibodies. *J Clin Invest*, **82**, 1864-1870.
- Starr, D.A. and Han, M. (2002) Role of ANC-1 in tethering nuclei to the actin cytoskeleton. *Science*, **298**, 406-409.
- Starr, D.A. and Han, M. (2003) ANChors away: an actin based mechanism of nuclear positioning. *J Cell Sci*, **116**, 211-216.
- Stossel, T.P. (1993) On the crawling of animal cells. *Science*, **260**, 1086-1094.
- Strasser, P., Gimona, M., Moessler, H., Herzog, M. and Small, J.V. (1993) Mammalian calponin. Identification and expression of genetic variants. *FEBS Lett*, **330**, 13-18.
- Stuurman, N., Heins, S. and Aebi, U. (1998) Nuclear lamins: their structure, assembly, and interactions. *J Struct Biol*, **122**, 42-66.
- Sudhof, T.C. (1990) The structure of the human synapsin I gene and protein. *J Biol Chem*, **265**, 7849-7852.
- Sullivan, T., Escalante-Alcalde, D., Bhatt, H., Anver, M., Bhat, N., Nagashima, K., Stewart, C.L. and Burke, B. (1999) Loss of A-type lamin expression compromises nuclear envelope integrity leading to muscular dystrophy. *J Cell Biol*, **147**, 913-920.
- Sunada, Y. and Campbell, K.P. (1995) Dystrophin-glycoprotein complex: molecular organization and critical roles in skeletal muscle. *Curr Opin Neurol*, **8**, 379-384.
- Takaishi, M., Ishisaki, Z., Yoshida, T., Takata, Y. and Huh, N.H. (2003) Expression of calmin, a novel developmentally regulated brain protein with calponin-homology domains. *Brain Res Mol Brain Res*, **112**, 146-152.
- Theriot, J.A. and Mitchison, T.J. (1993) The three faces of profilin. *Cell*, **75**, 835-838.
- Valenzuela, D.M., Stitt, T.N., DiStefano, P.S., Rojas, E., Mattsson, K., Compton, D.L., Nunez, L., Park, J.S., Stark, J.L., Gies, D.R. and et al. (1995) Receptor tyrosine kinase specific for the skeletal muscle lineage: expression in embryonic muscle, at the neuromuscular junction, and after injury. *Neuron*, **15**, 573-584.
- van den Ent, F., Amos, L.A. and Lowe, J. (2001) Prokaryotic origin of the actin cytoskeleton. *Nature*, **413**, 39-44.
- Vaughan, A., Alvarez-Reyes, M., Bridger, J.M., Broers, J.L., Ramaekers, F.C., Wehnert, M., Morris, G.E., Whitfield, W.G.F. and Hutchison, C.J. (2001) Both emerin and lamin C depend on lamin A for localization at the nuclear envelope. *J Cell Sci*, **114**, 2577-2590.
- Venables, R.S., McLean, S., Luny, D., Moteleb, E., Morley, S., Quinlan, R.A., Lane, E.B. and Hutchison, C.J. (2001) Expression of individual lamins in basal cell carcinomas of the skin. *Br J Cancer*, **84**, 512-519.
- Viel, A. (1999) Alpha-actinin and spectrin structures: an unfolding family story. *FEBS Lett*, **460**, 391-394.
- Vigouroux, C., Auclair, M., Dubosclard, E., Pouchelet, M., Capeau, J., Courvalin, J.C. and Buendia, B. (2001) Nuclear envelope disorganization in fibroblasts from lipodystrophic patients with heterozygous R482Q/W mutations in the lamin A/C gene. *J Cell Sci*, **114**, 4459-4468.
- Volk, T. (1992) A new member of the spectrin superfamily may participate in the formation of embryonic muscle attachments in *Drosophila*. *Development*, **116**, 721-730.
- Wakatsuki, T., Schwab, B., Thompson, N.C. and Elson, E.L. (2001) Effects of cytochalasin D and latrunculin B on mechanical properties of cells. *J Cell Sci*, **114**, 1025-1036.

- Wehrle-Haller, B. and Imhof, B. (2002) The inner lives of focal adhesions. *Trends Cell Biol*, **12**, 382-389.
- Welch, M.D., Mallavarapu, A., Rosenblatt, J. and Mitchison, T.J. (1997) Actin dynamics in vivo. *Curr Opin Cell Biol*, **9**, 54-61.
- Winkelman, J.C. and Forget, B.G. (1993) Erythroid and nonerythroid spectrins. *Blood*, **81**, 3173-3185.
- Winsor, B. and Schiebel, E. (1997) Review: an overview of the *Saccharomyces cerevisiae* microtubule and microfilament cytoskeleton. *Yeast*, **13**, 399-434.
- Worman, H.J. and Courvalin, J.C. (2002) The nuclear lamina and inherited disease. *Trends Cell Biol*, **12**, 591-598.
- Worman, H.J. and Courvalin, J.C. (2004) How do mutations in lamins A and C cause disease? *J Clin Invest*, **113**, 349-351.
- Worman, H.J., Evans, C.D. and Blobel, G. (1990) The lamin B receptor of the nuclear envelope inner membrane: a polytopic protein with eight potential transmembrane domains. *J Cell Biol*, **111**, 1535-1542.
- Yamada, K.M. and Geiger, B. (1997) Molecular interactions in cell adhesion complexes. *Curr Opin Cell Biol*, **9**, 76-85.
- Yan, Y., Winograd, E., Viel, A., Cronin, T., Harrison, S.C. and Branton, D. (1993) Crystal structure of the repetitive segments of spectrin. *Science*, **262**, 2027-2030.
- Yang, Y., Dowling, J., Yu, Q.C., Kouklis, P., Cleveland, D.W. and Fuchs, E. (1996) An essential cytoskeletal linker protein connecting actin microfilaments to intermediate filaments. *Cell*, **86**, 655-665.
- Youssoufian, H., McAfee, M. and Kwiatkowski, D.J. (1990) Cloning and chromosomal localization of the human cytoskeletal alpha-actinin gene reveals linkage to the beta-spectrin gene. *Am J Hum Genet*, **47**, 62-71.
- Zastrow, M.S., Vlcek, S. and Wilson, K.L. (2004) Proteins that bind A-type lamins: integrating isolated clues. *J Cell Sci*, **117**, 979-987.
- Zhang, Q., Ragnauth, C., Greener, M.J., Shanahan, C.M. and Roberts, R.G. (2002) The nesprins are giant actin-binding proteins, orthologous to *Drosophila melanogaster* muscle protein MSP-300. *Genomics*, **80**, 473-481.
- Zhang, Q., Skepper, J.N., Yang, F., Davies, J.D., Hegyi, L., Roberts, R.G., Weissberg, P.L., Ellis, J.A. and Shanahan, C.M. (2001) Nesprins: a novel family of spectrin-repeat-containing proteins that localize to the nuclear membrane in multiple tissues. *J Cell Sci*, **114**, 4485-4498.
- Zhen, Y.Y., Libotte, T., Munck, M., Noegel, A.A. and Korenbaum, E. (2002) NUANCE, a giant protein connecting the nucleus and actin cytoskeleton. *J Cell Sci*, **115**, 3207-3222.

ABBREVIATIONS

ABD	Actin-Binding Domain
AP	Alkaline phosphatase
APS	Ammonium persulphate
BSA	Bovine serum albumin
CH	Calponin homology
CNBr	Cyanogen Bromide
DAPI	4',6-Diamidino-2-phenylindole
DEPC	Diethylpyrocarbonate
DMSO	Dimethylsulfoxide
DNTP	Deoxyribonucleotide triphosphate
DTT	1,4-dithiothreitol
EDTA	Ethylenediaminetetraacetic acid
EGTA	Ethyleneglycol-bis (2-amino-ethylene) N,N,N,N-tetraacetic acid
FITC	Fluorescein-5-isothiocyanate
GFP	Green Fluorescence Protein
GST	Glutathione S-transferase
HRP	Horse radish peroxidase
HEPES	N-(2-hydroxyethyl) piperazine-N-2-ethanesulphonic acid
IPTG	Iso-propylthio-galactopyranoside
IgG	Immunoglobulin G
Kb	Kilobase pairs
kDa	KiloDalton
MOPS	Morpholinopropanesulphonic acid
Neo	Neomycin cassette
mRNA	messenger ribonucleic acid
mAb	Monoclonal Antibody
NP-40	Nonylphenylpolyethyleneglycol
OD	Optical density
PFA	Paraformaldehyde
PIPES	Piperazine-N,N.-bis(2-ethanesulphonic acid)
PMSF	Phenylmethylsulphonyl fluoride
PAGE	Polyacrylamide gel electrophoresis

PVDF	Polyvinylidene fluoride
rpm	Rotations per minute
SDS	Sodium dodecyl sulphate
TRITC	Tetramethylrhodamine β isothiocyanate
TAE	Tris borate EDTA
WT	Wild type allele
X-gal	5-bromo-4-chloro-3-indolyl-D-galactopyranoside

Erklärung

Ich versichere, dass ich die von mir vorgelegte Dissertation selbständig angefertigt, die benutzten Quellen und Hilfsmittel vollständig angegeben und die Stellen der Arbeit - einschließlich Tabellen und Abbildungen -, die anderen Werke im Wortlaut oder dem Sinn nach entnommen sind, in jedem Einzelfall als Entlehnung kenntlich gemacht habe; dass diese Dissertation noch keiner anderen Fakultät oder Universität zur Prüfung vorgelegen hat; dass sie - abgesehen von unten angegebenen beantragten Teilpublikationen- noch nicht veröffentlicht ist, sowie, dass ich eine Veröffentlichung vor Abschluss des Promotionsverfahrens nicht vornehmen werde. Die Bestimmungen dieser Promotionsordnung sind mir bekannt. Die von mir vorgelegte Dissertation ist von Frau Prof. Dr. Angelika A. Noegel betreut worden.

Köln, den

13-05-2004

Sabu Abraham

Teilpublikation:

Padmakumar, V.C.* , **Abraham, S.***, Braune, S.* , Noegel, A.A., Tunggal, B., Karakesisoglou, I. and Korenbaum, E. (2004) Enaptin, a giant actin-binding protein, is an element of the nuclear membrane and the actin cytoskeleton. *Exp. Cell. Res.*, **295**, 330-339.

*equal contribution

CURRICULUM VITAE

Name: Sabu Abraham
Address Bitburger Str 7
50935, Cologne
Germany.
Permanent Address 'Chenakottu'
Thiruvaniyoor PO
Kochi-682308
Kerala, India
E.mail sabuchenakottu@yahoo.com
Date of birth 30.05.1976
Place of Birth Thiruvaniyoor, India
Nationality: Indian

Education

Primary school: Govt. LP School, Attinikkara
(1981-1985)
High School: St Philominas High School, Thiruvaniyoor
(1985-1991)
Pre-degree Maharajas College, Ernakulam.
(1991-1993)
Bachelors Degree B.Sc. Chemistry major with Physics and Mathematics as subsidiaries
(1993-1996) Mahatma Gandhi University, Kottayam, India
Masters Degree M.Sc. (Medical Biochemistry)
(1996-1999) Mahatma Gandhi University, Kottayam, India
1999-2001 Project assistant, AIIMS, New Delhi
Ph.D. thesis Mathematics and Natural Science faculty, University of Cologne
(2001-2004) Advisor : Prof. Dr. Angelika A. Noegel
Institute for Biochemistry I, Medical Faculty,
University of Cologne, Germany

LEBENS LAUF

Name: Sabu Abraham
Adresse: Bitburger Str 7
50935, Cologne,
Germany.
Heimatadresse 'Chenakottu'
Thiruvaniyoor PO
Kochi-682308
Kerala, India
E.mail sabuchenakottu@yahoo.com
Geburtsdatum 30.05.1976
Geburtsort Thiruvaniyoor, India
Staatsangehörigkeit Indisch

Ausbildung

Schulbildung:

1981-1985 Govt. LP School, Attinikkara
1985-1991 St Philominas High School, Thiruvaniyoor
vor Diplom Maharajas College, Ernakulam
(1991-1993)
Bachelors Degree B.Sc. Chemistry major with Physics and Mathematics as subsidiaries
(1993-1996) Mahatma Gandhi University, Kottayam, India.
Masters Degree M.Sc. (Medical Biochemistry)
(1996-1999) Mahatma Gandhi University, Kottayam, India.
1999-2001 Mitarbeiter, AIIMS, New Delhi
Promotions studium Mathematisch-Naturwissenschaftliche Fakultät, Universität zu Köln
(2001 -2004) Betreuerin: Prof. Dr. Angelika A. Noegel
Institut für Biochemie I, Medizinische Fakultät der
Universität zu Köln.